NPS-59SL1021A

United States Naval Postgraduate School

FLOW OF DILUTE POLYMER SOLUTIONS ABOUT CIRCULAR CYLINDERS

by

T. SARPKAYA and P. G. RAINEY

26 February 1971

NAVAL POSTGRADUATE SCHOOL

Monterey, California

Rear Admiral R. W. McNitt, USN
Superintendent

M. U. Clauser
Provost

ABSTRACT

Flow of aqueous solutions of Polyox WSR-301, with concentrations of 1.0 to 200 wppm, past circular cylinders was investigated in the drag-transition region of Reynolds numbers. Drag force, pressure distribution, and separation angle were measured on cylinders with diameters from 1/4 to 1-1/2 inch. Lift and drag forces acting on a NACA-0024 hydrofoil-model were also measured.

The polymer additive was found to alter only those force coefficients which have a Reynolds-number transition region. Two distinct types of cylinder drag transition were observed: (1) At high concentrations, transition from sub-critical to a transcritical flow occurred at the same free-stream velocity independent of body diameter; and (2) at low concentrations and/or molecular weights, tripping from a sub-critical to a super-critical flow occurred at a well defined flow condition which was a function of the free-stream velocity, body diameter, and turbulent pipe-flow friction reduction. In all cases, transition occurred earlier than that in the pure solvent. The polymer had a de-stabilizing effect on the boundary-layer flow.

ABSTRACT

Flow of aqueous solutions of Polyox WSR-301, with concentrations of 1.0 to 200 wppm, past circular cylinders was investigated in the drag-transition region of Reynolds numbers. Drag force, pressure distribution, and separation angle were measured on cylinders with diameters from 1/4 to 1-1/2 inch. Lift and drag forces acting on a NACA-0024 hydrofoil-model were also measured.

The polymer additive was found to alter only those force coefficients which have a Reynolds number transition region. Two distinct types of cylinder drag transition were observed: (1) At high concentrations, transition from sub-critical to a transcritical flow occurred at the same free stream velocity independent of body diameter; and (2) at low concentrations and/or molecular weights, tripping from a sub-critical to a super-critical flow occurred at a well defined flow condition which was a function of free stream velocity, body diameter and turbulent pipe-flow friction reduction. In all cases, transition occurred earlier than that in the pure solvent. The polymer had a de-stabilizing effect on the boundary layer flow.

FOREWORD

The work described in this report was sponsored by the Naval Ship Systems Command General Hydromechanics Research Program, administered by the Naval Ship Research and Development Center. The research is part of a comprehensive study of the effect of dilute polymer solutions on the lift and drag characteristics of circular cylinders and hydrofoils. The generous support of the sponsor is gratefully acknowledged.

TABLE OF CONTENTS

LIST OF FIGURES

LIST OF TABLES

NOMENCLATURE

c^*	critical shear wave velocity
C_d	drag coefficient
C_p	pressure coefficient
d	diameter of circular cylinder
D	drag force
h	test section height
L	length of circular cylinder
M.W.	molecular weight
P_s	stagnation pressure
P.D.R.	per cent (pipe) drag reduction
Re	Reynolds number
Re_c	critical Reynolds number
T.R.T.	total (pump) running time
U	corrected free stream velocity
V	measured free stream velocity
Wn	Weissenberg number
wppm	weight part of solute per million of solvent
α	hydrofoil angle of attack
ε_t	total velocity correction factor
θ	cylinder angle measured from forward stagnation point
μ	dynamic fluid viscosity
ν	kinematic fluid viscosity
ρ	fluid density
τ_w	wall shear stress

I. INTRODUCTION

There has been considerable interest in fluid dynamic studies of the flow of dilute polymer solutions in water during the years since 1965 for the purpose of optimizing the speed and endurance characteristics of submerged or partly submerged bodies. The motivations for this optimization through the reduction of resistance rather than by the increase of the power and efficiency of the propulsion systems and drives came from the "Toms' effect." In 1948, Toms [Ref. 1] demonstrated that a dilute solution of polymer in a Newtonian solvent drastically reduced frictional drag under turbulent flow conditions. The discovery of Toms' effect did not arouse particular interest until the 1960's. Since then, an increasing number of experiments in chemistry, physics and fluid dynamics have been carried out. Some of the reports of these investigations contained empirical correlations, theoretical analyses based on viscoelastic models, and phenomenological descriptions of various mechanisms to explain the role played by polymer molecules, clusters and/or chains in reducing the wall friction, and in modifying the remainder of the flow field. Excellent surveys of such research have been presented by Hoyt and Fabula (1964) [Ref. 2], Deavors (1966) [Ref. 3], Lumley (1967) [Ref. 4], and A. White (1968) [Ref. 5].

Although extensive theoretical and experimental work has been carried out with internal flows where the drag is due to turbulent skin friction alone, little is known about the effects of polymers

on the flow about bluff bodies where separation plays a major role and the wake contributes significantly to the total drag.

The earliest known experiment with bluff bodies in drag-reducing polymers was carried out by Crawford and Pruitt [Ref. 6] in 1963. They dropped 5/8-inch-diameter rubber and steel spheres in Guar gum solutions and reported that at 2,500 wppm[1] the drag on both the steel and rubber spheres was reduced. But at 5,000 wppm, only the drag on the steel sphere was less than it would be in water. Ruszczycky [Ref. 7] carried out some measurements in 1965 on the fall velocity of steel spheres in polyethylene oxide "Polyox WSR-301," using spheres of diameters from 3/8 inch to one inch in concentrations up to 15,000 wppm. He found that for all spheres with a diameter less than 1/2 inch, as the concentration was increased, the drag at first decreased, reaching a minimum between 2,500 wppm and 7,500 wppm. The largest drag reduction observed was 26% obtained with the one-inch sphere in 7,500 wppm solution. These results, although inconclusive because of their limitations and confinement to polymer solutions of very high concentrations, appear to point out that a mechanism different from that observed for turbulent flow in pipes may be in operation.

A. White [Refs. 8, 9] conducted some experiments by dropping concrete and steel spheres with different diameters into a tank which contained a WSR-301 solution. Using high-speed photography, the wake patterns and traces of the spheres were recorded. His experiments

---

[1] Weight part per million

indicated that below the critical Reynolds number, where the boundary layer is laminar, the drag on a sphere is considerably reduced by adding Polyox, although drag reduction in pipe flow occurs only in the turbulent region. White's flow visualization studies showed that delayed boundary layer separation and the small wake size with the polymer solutions are associated with the drag reduction. He further concluded, on the basis of the observations of Brennen and Gadd [Ref. 10], that the delayed laminar separation is caused by viscoelastic effects because the phenomenon seems to occur only with solutions which exhibit normal-stress-difference behavior.

Lang and Patrick [Ref. 11] observed the flow about freely falling spheres, cylinders, disks, and cones in Polyox solutions 200 to 1,000 wppm. They noted that there was drag reduction for only those bluff bodies which had a movable separation point. However, they also reported that there was no significant drag reduction for circular cylinders for $Re < 2 \times 10^4$. They further suggested that the mechanism which causes the polymer molecules to shift the separation point is not apparent and merits further investigation. In Lang and Patrick's experiments, the fall of the objects was not always steady and at times there were sudden shifts in the direction of fall. For reasons yet unknown, the drag of spheres in Polyox solutions did not follow the typical trend of sphere drag in plain water as a function of Reynolds number as far as the characteristic sharp decrease, which is due to sudden transition to turbulent separation is concerned.

Extensive studies on freely falling spheres have been conducted by Hayes [Ref. 12] and Chenard [Ref. 13]. With WSR-301, in a Reynolds

number range of approximately 10^4 to 10^5, Hayes observed that there was no drag reduction at Reynolds numbers below 10^4, drag reduction increased with the Reynolds number, and the maximum drag reduction occurred in a concentration of 100 wppm for Reynolds numbers between 10^4 and 10^5.

James [Ref. 14] investigated the drag reduction of small circular cylinders in laminar flow of WSR-301. The use of small wires and flow speeds limited the Reynolds number range of the experiments to 100. Concentrations were varied from 8 to 220 wppm. An injected dye study was also performed which revealed viscoelastic effects of the polymer on the flow patterns around the cylinder. For the Reynolds number range encountered in this experiment, the drag coefficient increased with increasing polymer concentration when the Reynolds number was greater than a critical value, which itself was a function of concentration.

McClanahan and Ridgely [Ref. 15] towed circular cylinders through WSR-301 in the Reynolds number range of 2×10^3 to 2×10^5. They reported that the drag was increased at Reynolds numbers below 10^4. They supported Hayes' conclusions of drag reduction above 10^4 and maximum drag reduction at a concentration of 100 wppm. Fresh mixtures of the polymer solution were always used for these investigations.

Sanders [Ref. 16], based on the previously mentioned works, proposed that the drag reducing mechanism of dilute polymer solutions was due to a delay in the boundary layer separation caused by the stabilization of the laminar boundary layer. The proposed action reduced the size of the wake, which in turn decreased the drag. He further concluded that only those polymers that produce a dual terminal velocity in high concentrations have the ability to reduce drag.

Brennen [Ref. 17] investigated the effect of polymer additive on the position of the separation line on several cavitating headforms. The apparatus consisted of a container tank and a vertical pipe which was connected to the bottom of the tank. Models were supported on a 0.15-inch-diameter sling inside the pipe, and sudden release of a flap valve at the end of the pipe provided gravity-driven flow. Velocity of the flow was controlled with a variable orifice. He used two spheres and a cylinder with respective diameters of 1/4 inch, 1/2 inch and 1/4 inch in a polymer solution of 50 wppm. Pictures taken with a high-speed camera have shown that the separation lines on the bodies in polymer solutions moved further downstream as compared to those of water. Reynolds number range for these experiments was 10^4 to 8×10^4. This study also revealed another interesting phenomenon: After a certain speed (7 fps for 1/2-inch sphere and 8 fps for cylinder) the separation line became gradually distorted into a wavy pattern. These irregularities appeared to have a lateral wave length reflected on the separation line. The wave length decreased sharply with increasing speed. Degradation produced no measurable effect on the magnitude of the spanwise wave length exhibited at a particular speed and slightly increased the critical speeds at which the various types of distortion occurred. But even for the most degraded solution, these threshold speeds were not raised by more than about 3 fps.

Luikov et al. [Ref. 18] carried out experiments with Na-Cmc solutions at high concentrations and found that the separation point moved farther downstream. They conjectured that the decrease of the resistance of the cylinder was partly due to the smaller size of the wake

and partly due to a change in the character of the vortical motion in the aft region of the cylinder. They observed notable changes in the vortex motion with the increase of the concentration of the polymer and a reduction in turbulence. They concluded that the elastic energy stored in the fluid in the polymer particles was redistributed later near the separation point and, as a result of the additional momentum provided by this redistribution, the fluid particles were able to move farther downstream against a positive pressure gradient. Barenblatt et al. [Ref. 19] measured the drag force on a rough cylinder from which highly concentrated solutions of long-chain polymers were injected. Drag reductions of 20% to 34% were achieved. Tests with glycerin injection, which did not reduce drag, showed that contraction of the wake was independent of the type of fluid injected. He therefore concluded that the contraction of the wake and the displacement of the separation point further downstream cannot conclusively explain the drag reduction phenomenon.

It is apparent from the foregoing that the mechanisms proposed for the reduction of the drag of bodies moving through polymer solutions are less coherent and loosely related to the mechanisms for the drag reduction in pipes. This is partly because the drag reduction has been studied more extensively in conduits and additional data provided ways and means of refuting or substantiating the mechanisms proposed, [Ref. 20]. Secondly, in pipe flows, the motion was essentially steady, uniform, had a uniform wall-shear distribution (somewhat affected by the polymer degradation along the length of the pipe), had no separation, no stagnation point, no curvatures and the motion was often beyond the transition point.

In external flows, however, the motion is unsteady due to the vortex shedding in the aft region of the cylinder, has variable shear and is accompanied by separation, stagnation, rapidly varying pressure gradient, wall curvature, and "drag crisis" at or near the transition of the laminar boundary layer to a turbulent state. Obviously, the flow about bodies introduces many complex factors which are not encountered in the experiments conducted with pipes. It therefore seemed appropriate that a comprehensive investigation be initiated to study the characteristics of the flow of dilute polymer solutions about bluff bodies through the measurement of the pressure distribution, drag, separation angle, and the Strouhal number.

Circular cylinders, with diameters from 1/4 to 1-1/2 inch, were chosen as the test objects and Polyox WSR-301 as the polymer additive. In addition, a series of lift and drag measurements were made with a NACA-0024, four-inch chord, hydrofoil at various angles of attack under non-cavitating conditions. The experiments were performed in the low-speed water tunnel of the Department of Mechanical Engineering of the Naval Postgraduate School. No attempt was made to inject the polymer additive into the boundary layer of the cylinders, and all experiments were carried out with homogeneous polymer solutions. The condition of the test solution, i.e., its ability to reduce friction in pipe flow, was monitored at suitable time intervals with a capillary tube rheometer.

Some of the preliminary results have been presented in an earlier report of limited distribution [Ref. 21], and the present report supplements and supersedes this earlier report. Results of a particular phase of the investigation have also been presented at a recent meeting [Ref. 22].

II. EQUIPMENT AND PROCEDURE

A. EQUIPMENT

1. NPS Water Tunnel

The experiments were performed in a recirculating water tunnel (Fig. 1) of approximately 500 gallons capacity fitted with a test section four inches wide, eight inches high, and 16 inches long. A low-rpm, high-capacity, 14-inch-diameter-discharge, centrifugal pump circulated the fluid at test-section velocities of 5 to 25 fps. Grids were specifically not used to minimize polymer degradation. Three flow straighteners were welded into the 14-inch pipe elbow which preceded the 5:1 nozzle section. These proved sufficient to provide a velocity profile which remained uniform within a region 0.5 inches away from the top and bottom of the test section with a standard deviation of 1.8%.

Associated with the tunnel are a 150-gallon stainless steel storage tank, a small recirculating pump and filter system, and a 15-gallon head tank 12 feet above the test-section centerline.

2. Test Specimens

Aluminum cylinders of diameters of 3/4 inch, one inch, and 1-1/2 inch, placed across the width of the test section, were used to evaluate the effect of polymer additives on the drag coefficient of bluff bodies.

Local pressure measurements and flow visualization studies were conducted with a 1/4-inch-diameter brass tube and 1/2-inch, one-inch and 1-1/2-inch-diameter plexiglass cylinders. A small bore hole (three degrees of arc) drilled radially from the cylinder surface, at the

mid-span, served as the total pressure tap. Static pressure was measured at the entrance of the test section with a wall tap.

The end conditions differed between the cylinders used for direct drag measurements and those used for pressure measurements (Fig. 2). All of the aluminum specimens were mounted with one end held by a self-aligning bearing imbedded in one plexiglass window, and one end passing through the other plexiglass window into the cantilever beam system. All of the plexiglass cylinders extended through both tunnel windows. They were fitted with "O" rings which permitted rotation to any desired angle yet sealed the passage through tne tunnel walls.

A series of exploratory measurements of the lift and drag forces acting on an uncambered, streamlined, fully-wetted hydrofoil of four-inch chord length (NACA-0024) was also carried out, (see Fig. 3).

3. Instrumentation

The drag force acting on the cylinders was directly measured with a strain-gage fitted cantilever beam (Fig. 4). The lift and drag forces acting on the hydrofoil were measured with a separate cantilever beam system (Fig. 5). All of the bridges used four active gages and each beam was fitted with a redundant bridge circuit to maximize reliability. Static calibration of the lift-drag system exhibited a 1% interference between the two force components. The lift and drag forces acting on the hydrofoil were not corrected for this balance interaction partly because the interference was, in most cases, negligible and partly because the tests with hydrofoil were made for exploratory purposes only.

Differential pressure measurements were made with a Pace transducer (model KP-15) with a range of 0 to 25 psig.

The outputs of the strain-gage bridges and the pressure transducer were fed into the carrier-preamplifiers of two strip-chart recorders.

4. Turbulent Pipe Rheometer

For the purpose of correlating the effectiveness of the polymer solution in turbulent pipe flow with that in external flows, a turbulent-flow pipe rheometer, identical in principle to that used by W. D. White [Ref. 23], was used. It consisted basically of a 0.073-inch I. D. stainless steel pipe connected at one end to a reservoir and at the other end to a 100 cc graduated syringe. The syringe was driven through a worm-gear box by a variable speed motor. The pressure drop across a six-inch length of the pipe was measured by a Pace transducer and recorded on a strip chart recorder. The duration of the flow was measured with an electric timer.

5. Polymer

The water-soluble polymer, Polyox WSR-301, Blend 8051 F, manufactured by Union Carbide, was the polymer used for all the data reported herein.

B. PROCEDURE

1. Rheometer Operation

First, the temperature of the fluid in the rheometer reservoir was measured. Then the syringe was lowered slowly to the 120 cc level as it was filled from the reservoir. The motor was started at a preselected speed by closing a relay. As the syringe plunger passed the

100 cc mark, the electric timer was manually started. At the 20 cc mark, the relay was released, instantly stopping the timer and shutting off the motor. The pipe friction factor was then calculated from the measured pressure drop, flow rate, and temperature.

The Fanning friction factor for tap water (f_t) was determined for the Reynolds number range from 3,950 to 5,660. This data established the reference values for computing the per cent pipe drag reduction (P. D. R.) relative to laminar flow caused by a polymer solution. The tap water friction factors had a systematic error of approximately 3% below the expected smooth pipe value. The error in repeatability was on the order of ±2%.

The polymer solutions were tested in the Reynolds number range of 4800 ±300. The Reynolds numbers reported herein are based on the viscosity of water at the measured temperature. The value of pipe drag reduction for each sample of polymer solution was calculated from the value of the tap-water friction factor corresponding to the Reynolds number of the test.

$$P.\ D.\ R. = 100 \times (f_t - f)/(f_t - 64/Re)$$

Conversion to absolute pipe drag reduction can be made by multiplying the values of P. D. R. reported herein by 0.65. Ten-liter sample solutions of 10 wppm Polyox WSR-301 were prepared without stirring in order to establish the characteristics of this batch of Polyox in a condition as virgin as possible. The master solution, after aging approximately 20 hours, was used to prepare diluted solutions of concentrations from 10 to 0.1 wppm. The P. D. R. was determined for this range of concentrations. The repeatability of this experiment was then spot checked.

Tunnel samples were tested for fresh solutions as well as for solutions taken every half-hour of pumping. Sufficient sample was withdrawn from the tunnel to allow three flushes of the rheometer prior to two pipe tests.

2. Polymer Mixing in the Tunnel

Preliminary investigations indicated that the most satisfactory mixing technique would be the direct feeding of the polymer powder into the tunnel. For this purpose the water level was set at the middle of the test section and a funnel was installed through a fitting on top of the test section. The weight of the dry Polyox was measured to ±0.01 gm accuracy on a laboratory balance for samples of 10 gm or less. For larger samples a laboratory scale of accuracy ±0.5 gm was used. The powder was then slowly sprinkled into the water as the pump ran at its lowest speed. The total pumping time (TRT) reported for each solution includes this mixing time. All solutions were then aged for approximately 24 hours.

The following procedure was followed unless otherwise noted: All solutions were made fresh (i.e., not made by diluting a previous solution) with the solutions of the highest concentration prepared first for each part of the test program. After each solution was dumped, the tunnel was flushed twice prior to mixing the next lower concentration. Water data was taken after chemically treating the tunnel water with potassium bichromate, allowing 72 hours to degrade any residual polymer, and then flushing three times with water.

For the case when distilled water was used to prepare a 5 wppm solution, the tunnel was flushed with 1,200 gallons of distilled water prior to filling the tunnel and storage tank.

3. Hydrofoil -- Direct Measurement of Lift and Drag Force

The lift and drag forces acting on the NACA 0024 hydrofoil were measured at the nominal angle settings of 0, 3, 6, 9 and 12 degrees. The actual measured angles were .7, 3.7, 6.3, 9.6, and 11.7 respectively.

The apparatus used to measure the force was calibrated by static loading of the hydrofoil with the angle of attack set at zero degrees. Calibration was repeated each time the tunnel was emptied.

The actual, unfiltered output from each strain-gage bridge was observed on the strip chart recorders. The mean force was obtained by switching in the capacitance time-averaging circuit internal to the recorder. In those cases where the oscillations still appeared, the capacitance was switched out and the estimated mean of the actual fluctuating signal was used.

The tunnel velocity was determined from the measured stagnation pressure on a 3/4-inch diameter cylinder which was inserted into the tunnel for this purpose. The cylinder was then retracted and the dynamic forces acting on the test body were measured. This method of determining the free stream velocity was used in preference to a Pitot tube since the Pitot tube used to measure the velocity profile in water broke at the location where it penetrated through the tunnel after only a few hours of pumping. Furthermore, it was expected that the pressure anomaly common to dilute polymer solutions could be avoided with a velocity probe of relatively large radius.

The transducer used to measure the differential pressure between the total stagnation pressure (on the 3/4-inch cylinder) and the

test-section-entrance wall was calibrated with the standard water-manometer technique each time the force apparatus was calibrated.

The test procedure consisted of first measuring in tap water the forces acting on the hydrofoil throughout the tunnel-velocity range for each angle. After each test, the water level was reduced to a sufficiently low level (by gravity feeding 100 gallons of water into a storage tank) to allow the installation of the appropriate angle-setting yoke. The amount of water withdrawn was then pumped back into the tunnel and the test program was continued. Each set of data was obtained in an increasing order of pump speeds, and then repeated in a reverse order. Prior to and after taking each data set, the recorder balance and zero setting were checked. The entire test program was repeated with tap water. This established the reference data with which the forces produced in the flow of polymer solutions could be compared.

A 100 wppm solution was prepared in which the hydrofoil was tested in the following order of angle settings: 9, 12, 6, 3, 0, 12, 9. The hydrofoil lift and drag forces were then measured in a 25 wppm solution in the following order of angle settings: 0, 9, 3, 12. Another 25 wppm solution was prepared in which data were taken with an angle setting of six degrees.

A nut-and-bolt locking device was added to the angle-setting yoke in order to eliminate the possibility of an undesirable oscillatory force or an apparent increased oscillatory-lift force on the hydrofoil. The lift force was then measured in tap water with the angle set at six degrees nominal, 4.5 measured. This was repeated at the same angle in

a 200 wppm solution. After two hours of pumping, the solution was diluted 4:1 (producing 21 P. D. R.) and the lift force measurements were repeated. Again the solution was diluted 4:1 (producing 7 P. D. R.) and the test procedure was repeated. Finally, the tunnel was flushed and filled with tap water and the test procedure was repeated. This concluded the hydrofoil test program.

4. Cylinder -- Direct Measurement of Drag Force

The procedure followed for the direct measurement of the drag experienced by the cylinders was similar to that followed for measurements on the hydrofoil. The test program was essentially as follows:

(1) Each cylinder was tested in water;

(2) Each cylinder was tested in separate 100 wppm solutions;

(3) The one-inch diameter cylinder was tested in a 25 wppm solution;

(4) Each cylinder was tested in separate 5 wppm solutions;

(5) The one-inch cylinder was tested in a 5 wppm solution prepared with distilled water;

(6) The one-inch cylinder was tested in a 2.5 wppm solution; and finally,

(7) The one-inch cylinder was tested in a 1 wppm solution.

5. Cylinder -- Measurement of Pressure Distribution

The pressure distribution was measured on the one-inch-diameter cylinder in solutions of 100, 25, and 5 wppm. The local dynamic pressure on the cylinder surface was measured at five-degree intervals around the mid-circumference. The angle setting was measured on a two-inch radius circle which allowed the measurement of the angle to an accuracy of ±0.5 degrees. The pressure drag coefficient was calculated

from the pressure distribution for comparison with that obtained from the direct drag measurement.

6. Separation Angle Measurements

Concurrent with the determination of pressure distributions, the angle of separation at the mid-section of the cylinder was observed by dye injection from the cylinder surface. The reported angle is the minimum angle at which separation occurred. The location of separation was measured by injecting dye aft of the separation point and then rotating the cylinder forward while reducing the injection rate until two degrees aft of the apparent separation point. The dye injection rate was then reduced to a minimum and the actual separation point observed. The reported separation angle is considered to be accurate to within ±1 degree in those cases where separation was steady. In the case of the unsteady separation (to be discussed later) caused by the flow of degraded solutions, the reported minimum separation angle is considered to be reliable to within ±3 degrees.

7. Tunnel Correction Factors

Tunnel correction factors were not applied to the data obtained with the hydrofoil. The standard correction factors for wake and solid blockage have been uniformly applied to all cylinder drag coefficients. The total correction factor (e_t), the sum of the solid and wake-blockage correction factors, was calculated from

$$e_t = \frac{\pi^2}{12} \left(\frac{d}{h}\right)^2 + \frac{1}{2} \left(\frac{d}{h}\right) C_d \quad ,$$

where $\frac{d}{h}$ is the ratio of cylinder diameter to test section height (eight inches) and C_d is the corrected drag coefficient defined by

$$C_d = 2D/(\rho U^2 Ld) \quad ,$$

where D is the drag force acting on the cylinder, L is the cylinder length (four inches), and U is the corrected free-stream velocity given by

$$U = V(1 + e_t) \quad ,$$

where V is the velocity determined from the measured stagnation pressure P_s.

The drag coefficients are plotted as a function of the corrected Reynolds number

$$Re = Ud/\nu \quad ,$$

where ν is the kinematic viscosity of water at the measured fluid temperature. The actual solution viscosities were not measured and theoretical corrections based on polymer concentrations and estimated molecular weight were not applied. The common practice of reporting the drag coefficients obtained in dilute polymer solutions as a function of water Reynolds number has been followed in the presentation of the data.

The pressure distributions are plotted in terms of corrected pressure coefficients C_p. Since the free stream velocity was determined from the stagnation pressure, the reported values of C_p are the ratio of the local dynamic pressure to the front stagnation point dynamic pressure. The total tunnel correction factor was applied to obtain the corrected pressure coefficient [Ref. 24].

$$\text{(corrected)} \qquad C_p = 1 - \frac{1 - C_p}{(1 + e_t)^2}$$

III. PRESENTATION OF DATA

A. PIPE FRICTION REDUCTION

The data obtained with the master solutions #1 through #5 are tabulated in Table I. Apparently, the pipe-friction reduction capability of the polymer solution at low concentrations reduces with age and that the P. D. R. is proportional to concentration for concentrations equal to and less than 1 wppm (Fig. 6). For concentrations above 5 wppm, the P. D. R. is approximately constant at 80. Preliminary investigations revealed that above approximately 25 wppm, the P. D. R. decreases with increasing concentration.

The pipe friction reduction of the solutions mixed in the tunnel and aged 24 hours is compared in Fig. 7 with that of standard master solutions. It is apparent that in the range where P. D. R. is sensitive to concentration, the solutions mixed in the tunnel are somewhat degraded relative to standard samples. The degradation curves, P. D. R. versus total running time, are shown in Figs. 8, 9, and 10 for 100, 25, and 5-wppm solutions.

B. DRAG FORCE ACTING ON CYLINDERS IN TAP WATER AND THE CRITICAL REYNOLDS NUMBER REGIME

The drag force acting on 3/4-inch, one-inch, and 1-1/2-inch diameter cylinders in tap water was measured for tunnel velocities ranging from approximately 7 to 25 fps and the data have been corrected for tunnel effects. Drag coefficient versus Reynolds number is presented in Fig. 11 and compared with the data previously obtained [Ref. 21] with the same

water tunnel. These data will now be compared with those obtained by others under various conditions following a brief review of the critical drag-transition region characteristics.

A recent review of lift, drag, and vortex-shedding frequency data for rigid circular cylinders (in Newtonian fluid flow) has been made by Lienhard [Ref. 25]. As noted by him, the drag coefficients differ from experiment to experiment, the scatter within one set of data can be appreciable, and the Eiffel effect occurs over a range of Reynolds numbers depending upon the characteristics of the water tunnel used.

A plot of drag coefficient versus Reynolds number is presented in Fig. 12, for the Eiffel effect region. Data are obtained from the reports of Fage [Refs. 26, 27, 28], Delany and Sorensen [Ref. 29], and Humphreys [Ref. 30]; and include results from Göttingen open jet tunnel, various NPL (National Physical Laboratory) tunnels, Ames 7 x 10-foot, and Harvard one-meter tunnels. As seen from the data in Fig. 12, the critical Reynolds number for smooth circular cylinders depends upon the tunnel characteristics. Furthermore, as Fage and Warsap [Ref. 28], in 1929, have demonstrated (Figs. 13 - 15), by rope netting of 0.25-inch diameter and a mesh of 1.5 inches, the effect of upstream turbulence is to shift the transition curve to lower Reynolds numbers while maintaining the same transition characteristics (shape of curve). However, the effects of surface roughness and tripping wires alter the transition characteristics. In other words, the earlier the Eiffel effect occurs, the higher the value of the drag coefficient in the supercritical flow regime. It is apparent from a comparison of the NPS data shown in Fig. 11 with those in Fig. 12 that the NPS data lie between the results obtained on the NPL tunnel and the Göttingen tunnel.

The water data reported herein will be used as reference and the additional characteristics of flow in the subcritical, critical, supercritical, and the transcritical regimes will be discussed later in connection with the discussion of pressure distribution.

C. DRAG FORCE ACTING ON CYLINDERS IN DILUTE POLYMER SOLUTIONS

Preliminary investigations indicated that at relatively high concentrations of fresh Polyox WSR-301, the characteristics of the C_d versus Re curve are similar to those obtained in sphere drop tests and cylinder tow tank tests. However, very dilute solutions (i.e., 5 to 1.0 wppm) were found to be much more effective in reducing the drag coefficient than the higher concentrations (i.e., 25 to 100 wppm). It was observed that for all concentrations, sufficient pumping time (degradation) decreased the drag coefficient for Reynolds numbers above a certain value which depended upon the cylinder size. *With sufficient pumping, a new flow behavior was observed which resulted in a low drag coefficient above a critical Re, a drag coefficient approximately equal to that of water below the critical Re, and a large unsteady secondary flow near the separation line at the critical Re.*

The results of flow about the 3/4-inch, one-inch and 1-1/2-inch cylinders at a concentration of 100 wppm Polyox WSR-301 are presented in Figs. 16 - 20. Apparently, the value of C_d decreases as velocity increases, approaching a minimum value of approximately 0.7, independent of the cylinder size.

Data were obtained with the 3/4-inch and 1-1/2-inch cylinders as the solution degraded during a four-hour period of pumping. This amount

of degradation significantly reduced the drag coefficient at the lower test velocities on all three cylinders. At higher velocities, the difference between the fresh solutions which produced 70 P. D. R. in the rheometer and the degraded solution which produced 40 P. D. R. in the rheometer was insignificant.

The test was continued on the one-inch cylinder for a total of 14 hours of pumping time. As degradation increased, measured by decreasing per cent drag reduction in the rheometer, the value of C_d increased toward 1.2 when Re was less than 10^5 and decreased toward 0.6 for Re greater than 10^5 as shown in Fig. 21. The critical region formed at a total running time (TRT) of 819 minutes.

The critical region and the critical Reynolds number are identified here by the occurrence of two phenomena:

(1) The Reynolds number at which the drag force jumps back and forth from a high to a low value;

(2) For a small increase in velocity the drag force becomes steady at the low value.

Once the critical region forms, the behavior of the flow about the cylinder is quite distinctive. As the solution degrades, however, the critical region occurs at higher Reynolds numbers and eventually approaches that of the pure solvent.

A solution of 25 wppm was tested with the one-inch cylinder. As seen in Figs. 22 and 23, the behavior of this solution is approximately identical to that of the 100 wppm solution at equal per cent drag reduction in the rheometer down to 40 P. D. R. This solution degraded faster than the one more concentrated. With continued degradation, this solution produced a lower value of C_d than the 100 wppm

solution for Re greater than 10^5. The critical region formed when the solution produced 7.5 ±1 P. D. R. in the rheometer. Drag oscillations were large below Re_c and small above Re_c as seen in Fig. 24.

An extensive series of tests was conducted with solutions of 5 wppm Polyox WSR-301. The fresh solutions displayed a drag coefficient which monotonically decreased from 1.2 to 0.5 as the velocity increased from 7 to 25 fps for all three sizes of cylinders. The 5 wppm solutions degraded faster than the more concentrated solutions producing the critical region with less pumping time.

The critical region existed on the 1-1/2-inch cylinder at $Re = 13 \times 10^4$ when the solution displayed a 13 P. D. R. in the rheometer. As shown in Fig. 25, the graphs of max C_d'/C_d (the relative maximum amplitude of oscillation of C_d) versus Re indicate that the critical region had initially formed in the Reynolds number range of 11 to 13×10^4.

The one-inch cylinder was tested in solutions prepared with tap water and also with distilled water (Figs. 26 - 28). The only significant difference between the behavior of the solutions prepared with tap water and the solutions prepared with distilled water was that the distilled water reduced the rate of degradation.

At equal P. D. R. in the rheometer, both solutions produced drag forces at any given velocity which differed by less than the expected experimental error.

The gradual transition to the dual value drag-coefficient region is graphically displayed in Figs. 26 and 27. The critical region initially formed on the one-inch cylinder at $Re = 10.5 \times 10^4$ when the

solution produced approximately 11 P. D. R. in the rheometer. Once the critical region formed, C_d remained approximately constant at 0.43 and independent of the amount of degradation for Re greater than Re_c. Increased pumping produced less P. D. R. in the rheometer and raised the critical Reynolds number.

The 3/4-inch cylinder was tested in a 5 wppm Polyox WSR-301 tap water solution which rapidly degraded (Fig. 29). The critical region formed after 78 minutes of pumping, at Re = 9.9×10^4 in a solution which produced 12.5 P. D. R. in the rheometer.

The one-inch cylinder was tested in very dilute solutions of 2.5 and 1.0 wppm Polyox to further investigate the increase in critical Reynolds number with pumping time, and to determine if the critical Reynolds number was also relatively independent of concentration at these very low concentrations. As seen in Figs. 30 and 31, the behavior is the same as with the 5 wppm solution at equal P. D. R. in the rheometer. The critical Reynolds number was 10.5×10^4 and occurred in 2.5 and 1.0 wppm solutions which produced 13.5 and 10.2 P. D. R. respectively.

Both solutions were pumped until they produced essentially no drag reduction in the rheometer. The critical Reynolds number increased to 18×10^4 *(when the test was terminated), the values of* C_d *increased toward the water curve for Re less than* Re_c *and remained approximately constant at* $C_d = 0.4 \pm .05$ *for Re greater than* Re_c.

Lower concentrations were not tested due to the increase in degradation rate with decrease in concentration. In the first data run (10 minutes), the 1.0 wppm solution exhibited from 17.5 to 10 P. D. R. in the rheometer.

The characteristics of the drag oscillations are shown in Fig. 32. The relative maximum oscillation of drag coefficient attained its largest value at the critical Reynolds number. The oscillation greatly attenuated at a slightly higher Re, (See also Fig. 24). After falling to a minimum just above Re_c, the magnitude of oscillation increased with Reynolds number probably due to increased turbulence level in the test section.

Figure 33 is an assemblage of all the data obtained in the critical region. The critical Reynolds number is plotted as a function of P. D. R. in the rheometer for all the previously mentioned data. In addition, two data points for a 1/2-inch cylinder, which were obtained from the pressure measurements, are also included. A 1/4-inch cylinder was tested up to Re = 0.6×10^5 in the same solution, but no critical region was found even though the same solution produced a critical region for a 1-1/2-inch cylinder.

It is to be noted that the expected error in the values of P. D. R. is ±2 while the values of Re_c are reliable to within $\pm 0.1 \times 10^5$. The dashed line through the 1-1/2-inch cylinder data indicates the probable trend as evidenced by Fig. 33.

Figure 34 indicates the relative importance of concentration in determining the drag force on a one-inch cylinder for solutions which produced approximately the same P. D. R. in the rheometer, prior to the formation of the critical region. The data fell into two groups: The higher concentrations, 25 and 100 wppm, yielded one curve and the lower concentrations, 2.5 and 5 wppm, yielded another curve. Apparently, the lower concentrations produce a steeper transition to a lower C_d.

Figure 35 indicates the relative importance of concentration on the characteristics of the critical region. The main effect of concentration is to set the value of C_d at an Re greater than Re_c, the highest concentration producing the largest drag coefficient. The value of the first observed critical Reynolds number for the one-inch cylinder varied only from 10.3×10^4 to 11.4×10^4 while the concentration varied by a factor of 100 and the total pumping time by a factor of 82. The only difference between the tap and distilled water was that the distilled water required twice as much pumping time to form a solution which produced approximately 14 P. D. R. in the rheometer.

D. HYDROFOIL LIFT AND DRAG FORCES

The dilute Polyox solutions had no discernible effect upon the mean forces produced on the hydrofoil (Figs. 36 to 46). The apparent slight increase in lift at a six-degree angle of attack in the 200-wppm solution is most probably due to the pressure anomaly commonly encountered in dilute polymer solutions. The apparent decrease in lift and corresponding 20% increase in drag at a nine-degree angle of attack in a relatively fresh 100-wppm solution was not repeatable.

The only significant difference between the forces on the hydrofoil in water and in polymer solutions was the presence of a larger amplitude of oscillations in lift in polymer solutions. In order to conclusively determine that this increase was due to the flow of polymer solution rather than just to the loosening of the angle-setting clamp in the force-measuring apparatus, the angle was set at six degrees and a 200-wppm solution was prepared. After the data were obtained at 200 wppm, the solution was diluted 4:1 with the result of noticeable

reduction in the amplitude of lift oscillation. The solution was further diluted 4:1 which further reduced the amplitude of lift oscillation. Then the tunnel was flushed and filled with water. The strip chart recordings of the first set of data (200-wppm fresh) are compared with that obtained last (water) in Fig. 47. If the oscillations were due to the loosening of the angle-setting clamp, the last set of data should have shown larger oscillations than the first set of data. This was not the case as seen from the figure cited above.

E. PRESSURE DISTRIBUTION ON A CYLINDER IN THE FLOW OF DILUTE POLYMER SOLUTIONS

Preliminary investigations revealed that the pressure distribution about a cylinder in the flow of a dilute polymer solution is quite distinct from that in a Newtonian fluid.

Figure 48 shows the (corrected) pressure distribution measured on a one-inch diameter cylinder in the flow of fresh 100 wppm Polyox WSR-301 solution at slow and fast speeds. At $Re = 7.2 \times 10^4$, the pressure distribution is typical of that found in the subcritical region in Newtonian fluids. The pressure distribution at $Re = 2.1 \times 10^5$ is typical of that corresponding to the low-drag region in relatively high (25 to 100) concentrations of Polyox. As the Reynolds number increased from 7.2×10^4 to 2.1×10^5, the magnitude of back pressure decreased, the magnitude of minimum C_p increased and its location on the cylinder moved only slightly rearward from 70 to 80 degrees. The value of back pressure, for a given Reynolds number in the test range, was essentially constant from 110 to 180 degrees. In the low drag region of Reynolds numbers, this pressure distribution is markedly different from that

produced by plain tap water both at the same Reynolds number and at the Reynolds number in the transition region which would produce the same drag coefficient.

With fresh high-concentration solutions, as the pressure recovery improved (back pressure magnitude decreased) with increasing Re, the separation angle moved gradually rearward and the measured drag coefficient decreased.

The change of pressure distribution at a constant Reynolds number above the critical Reynolds number was studied with a one-inch cylinder in 25 wppm Polyox solution at Re = 1.3×10^5. As shown in Fig. 49, the back pressure coefficient changed from -0.67 to -0.30, significantly reducing C_d, while the value and location of minimum C_p were only slightly affected by degradation. The separation angle was measured at intervals between data sets and was found to increase only from 82 to 86 degrees. With increased pumping time, the critical Reynolds number approached 1.3×10^5. The resulting pressure distribution (uncorrected for tunnel effects) is plotted in Fig. 50. It indicates large pressure oscillations in the region of unsteady separation and smaller oscillations in the front and rear of the cylinder. Oscillograph tracings indicated the relatively low frequency (and large amplitude) of these oscillations as compared to the Strouhal frequency in tap water at the same Reynolds number.

Figures 51 through 53 illustrate the local pressure oscillations, at Re = 1.3×10^5, caused by the flow of solutions which produced 37, 20 and 4 P. D. R. The chart speed used for these tracings was 1 mm/sec. The pressure oscillations which occurred at 75, 90 and

110 degrees from the forward stagnation point at the critical Re are presented in Fig. 54. These tracings were recorded at a chart speed of 5 mm/sec.

After a solution has degraded sufficiently to produce a dual-value drag coefficient region, two distinct pressure distributions developed, one at Re less than critical and the other for Re greater than critical. Figure 55 illustrates these two types of pressure distributions on a one-inch cylinder in a 5 wppm Polyox solution.

The pressure distributions presented are typical of the pressure distributions measured on 1/2-inch, 3/4-inch, one-inch, and 1-1/2-inch cylinders at comparable velocities, concentrations, and degradations during preliminary investigations. The one-inch cylinder was chosen for the presentation and discussion of the data since the use of this particular size of cylinder maximized the accuracy of separation-angle measurement for cylinders which displayed an approximately constant drag coefficient in tap water throughout the range of velocities tested.

F. OBSERVATIONS OF THE SEPARATION OF FLOW OF DILUTE POLYMER SOLUTIONS ABOUT CYLINDERS

The technique for measuring the separation angle was described in the section dealing with experimental procedure. It must, however, be noted that the separation angle plotted herein is the most forward angle at which separation was observed in the mid-circumferential plane by dye injection at minimum possible injection velocity.

The measurements (Figs. 56 and 57) have shown that fresh solutions with relatively higher concentrations yield greater separation angles in the range of velocities tested and that the effect of degradation

is to move the separation line forward at Re less than Re_c and rearward at Re greater than Re_c.

At the critical velocity, observations made by injecting air at a point 10 degrees forward (nearer the front stagnation point) revealed wavy separation patterns similar to those first reported by Brennen [Ref. 17]. The injection of dye alone, at minimum injection velocity, revealed an even more interesting, three-dimensional, unsteady, separated flow pattern. At first it was thought that a switching from forward (laminar) to rearward (turbulent) separation was being observed. Further observation revealed a three-dimensional unsteady flow which displayed the following characteristics (Fig. 58): (1) The locus at which the boundary layer detached oscillated over a small range of angles (approximately 74 to 82 degrees); (2) The separated flow fluctuated with low frequency and high amplitude both in the plane normal to the main flow and in the plane parallel to the main flow; (3) Dye streaks which remained close to the cylinder surface actually curved from their plane and became almost perpendicular to the ambient flow at a cylinder angle of approximately 100 degrees; (4) Streams of dye which did not remain close to the cylinder indicated a strong vorticity the vector of which was <u>parallel</u> to the direction of the main flow; and (5) In addition, to further complicate the subject, fine lines of dye were observed approximately perpendicular to the main stream of dye which resembled the effects produced in sonic compressible fluid flow when a shock line interacts with the boundary layer.

At a slightly (approximately 0.3 fps) higher velocity, the separation line (no longer a wave) switched rearward and remained steady.

The dye became blurred a few degrees forward of the separation line indicating a transition from a laminar to a purely turbulent flow in the boundary layer at or just prior to separation. Because of the high tunnel-velocities, low dye-injection velocities, and solubility of the dye, it was not possible to observe the flow systematically more than 1/2 inch aft of the cylinder. Observations made with air bubbles, with the tunnel head reduced to a minimum, indicated a contraction of the wake followed by alternating expansion and contraction for fresh 100 wppm Polyox solutions.

Pressure measurements were made on a flat plate (one inch wide) placed normal to the flow of fresh dilute polymer solutions with relatively high concentrations (100 wppm) for the purpose of exploring the effect of the additive on the flow in the near-wake region of a body with fixed separation points. The amplitude of the pressure oscillations, which increased with pumping time, is presented in Fig. 59. When the solution had been pumped for two hours, the oscillograph tracings of the back pressure became identical to those obtained in tap water, although the sample solution still produced 80 P. D. R. in the rheometer. These measurements, however exploratory, revealed that the polymer additive has a profound effect on the wake-vortex structure of bluff bodies with or without fixed separation points. A detailed investigation of the variation of the Strouhal number and the characteristics of the near-wake of various types of bluff bodies immersed in dilute Polyox solutions are currently underway and will be reported separately.

IV. DISCUSSION OF RESULTS

A. GENERAL DISCUSSION OF THE DATA

The data presented in the previous sections have shown that dilute aqueous polymer (Polyox WSR-301) solutions flowing about a bluff body alter the pressure distribution and the force coefficients relative to pure water only in the flow regime where there is a transition or drag-crisis.

The mean lift coefficient of the NACA-0024 hydrofoil, immersed in dilute Polyox solution of moderate concentrations, did not significantly differ from that for the pure solvent. However, the amplitude of the oscillatory component of the lift force increased significantly in solutions of higher concentrations (200 wppm).

The variation of the mean drag coefficient for the cylinders was significantly altered by the presence of the polymer: (1) The Reynolds number at which the transition occurred shifted to lower values; (2) The characteristics of the flow such as the pressure distribution, separation, etc., markedly changed; and (3) the drag-crisis, in fresh polyox solutions, occurred at approximately the same free-stream velocity for all the cylinders tested.

The effect of degradation, i.e., the ability of the polymer solution to reduce pipe friction, was to reduce the width of the transition region. In other words, the transition curve became steeper and shifted to lower velocities (for a given cylinder) or Reynolds numbers as the solution degraded. When the degradation reached a sufficiently high critical value, i.e., when the per cent pipe-drag reduction reached a sufficiently low value, transition became critical with all its attendant features.

Further degradation pushed the critical velocity or the critical Reynolds number to higher values.

When the free-stream velocity was slightly less than the critical value: (1) separation occurred at approximately 74 degrees; (2) a strong secondary flow developed in the separation region; and (3) relatively large amplitude pressure oscillations occurred over the entire cylinder. At the critical Reynolds number, the flow was "tripped" to a turbulent boundary layer which delayed separation and caused a decrease in the drag coefficient. As the solution further degraded, the critical Reynolds number increased, as noted above, toward the Newtonian-fluid drag-crisis region.

B. DEPENDENCE OF THE TRANSITION CHARACTERISTICS UPON THE FREE STREAM VELOCITY

There appears to be a strong correlation between the observations made by Brennen [Ref. 17] and the characteristics of the drag force produced by the flow of dilute polymer solutions about bluff bodies. According to Brennen, the flow of fresh 50 wppm Polyox WSR-301 solution past 1/4-inch and 1/2-inch spheres at a free stream velocity of less than 4 fps produced little visible difference from the flow of plain water and velocities from 4 to 7 fps produced three-dimensional cavity surface irregularities, and finally, velocities above 7 fps caused separation line distortion. The published drag coefficients for spheres falling freely through Polyox solutions of comparable concentrations [Refs. 8, 9, 11, 16, 31] were classified into three groups: (1) At a velocity of less than 4 fps, the drag coefficient was similar to the subcritical value in water; (2) In the range of velocities from

4 to 7 fps, the drag transition occurred; and (3) At velocities above 7 fps, the drag coefficient was approximately constant at 0.25.

Cavity surface irregularities behind a 1/4-inch cylinder were observed by Brennen at all speeds. Separation line distortion occurred above approximately 8 fps. The average velocity at which cylinder drag transition was initiated (U_{tr}) in the flow of fresh dilute Polyox solutions in the NPS water tunnel was also found to be approximately 8 fps.

Figure 60 illustrates the drag transition region for 3/4-inch, one-inch and 1-1/2-inch diameter cylinders in the flow of fresh 100 wppm Polyox solutions. The drag coefficient is determined essentially by the free stream velocity throughout the entire Reynolds number range surveyed. The drag transition range extended from $U/U_{tr} = 1$ to $U/U_{tr} = 2$. At higher values of this ratio, the drag coefficient remained constant at approximately 0.75 even though the drag coefficient of the 1-1/2-inch diameter cylinder at the highest test velocity in plain water was approximately 0.45. The apparent drag increase at the low velocity is probably due to the pressure anomaly previously mentioned. The drag transition region for these cylinders after 70 minutes of total pump-running time is also shown in Fig. 60. In addition, as shown in Figs. 16 through 23, the drag coefficient for the 100 and 25 wppm solutions was relatively independent of further degradation until the per cent pipe drag reduction decreased to approximately 30%.

At much lower polymer concentrations, the drag coefficient was found to be dependent upon the cylinder diameter as seen in Fig. 61. However, for the fresh 5 wppm solutions, $U/U_{tr} = 1$ did indicate the

initiation of transition for all three cylinders tested. The free stream velocity at which transition was initiated for the one-inch and 1-1/2-inch cylinders in the flow of a degraded 5 wppm solution, which displayed 30 per cent pipe drag reduction, could not be determined since it was below the minimum attainable tunnel velocity. *Thus the evidence suggests that when the concentration and/or the molecular weight of the additive are sufficiently reduced, the velocity at which the transition is initiated becomes dependent also on the cylinder size.*

Figures 62 and 63 show that the critical velocity increases as the solution degrades but the transition always occurs at a velocity larger than 8 fps. For similar solutions, equal P. D. R., the critical velocity appeared to be approximately inversely proportional to the square root of the cylinder diameter, i.e., the critical Reynolds number was proportional to the square root of the cylinder diameter.

The drag coefficients obtained with the 5 wppm solutions are plotted in Figs. 64 through 67, as a function of U^2d. The systematic narrowing of the transition range as the polymer degrades is clearly indicated.

C. DEPENDENCE OF THE DRAG COEFFICIENT UPON POLYMER CONCENTRATION

The minimum value of the drag coefficient was found to be determined by the polymer concentration. Without exception, as the solution degraded, the drag coefficient beyond the point of inception of transition decreased until it attained a minimum. The minimum value of the drag coefficient for very low concentrations was the same as

that attained with the Newtonian solvent in the drag-crisis region. As seen in Fig. 68, for concentrations above 10 wppm, the minimum C_d increased with concentration. It was not determined whether the minimum drag coefficient for 100 and 25 wppm solutions would have continued to decrease as the P. D. R. further decreased. Since, for these solutions the rate of degradation was very low, the test was terminated soon after the critical transition was first observed.

D. DEPENDENCE OF THE DRAG COEFFICIENT ON PER CENT (PIPE) DRAG REDUCTION

As the per cent drag reduction displayed by a Polyox solution in the turbulent pipe rheometer decreased, the transition range narrowed. At 12 ±3 P. D. R., the critical transition occurred independently of the initial value of the concentration (1 to 100 wppm) on the 1/2-inch, 3/4-inch, one-inch and 1-1/2-inch diameter cylinders. A critical velocity was not observed on the 1/4-inch cylinder. However, it is predicted that it will occur at a velocity greater than the maximum attainable test-section velocity.

For concentrations of 5 wppm and less, the minimum drag coefficient depended only on the P. D. R. Thus, for a given size of cylinder immersed in the flow of Polyox solutions of relatively low concentration, identical transition characteristics were observed in solutions which produced identical P. D. R. in the rheometer.

For concentrations of 25 to 100 wppm, the minimum drag coefficient, although higher than that for lower concentrations, was constant for solutions of the same P. D. R. when the P. D. R. was greater than approximately 40. Thus, for these conditions, the transition curve was also observed to be dependent upon the P. D. R. irrespective of the actual concentration.

E. DEPENDENCE OF THE DRAG COEFFICIENT UPON SEPARATION ANGLE

The drag coefficient is not uniquely determined by the separation angle in the flow of dilute Polyox solutions about cylinders. In the transition region, as shown in Fig. 69, the separation angle shifted rearward as the drag coefficient decreased. At critical transition, the separation point jumped rearward. At higher Reynolds numbers, it continued to shift further rearward although the drag coefficient remained practically constant.

For a Newtonian fluid, the flow regime in the drag transition region can be characterized by the angle of minimum pressure, i.e., 70 degrees for subcritical and 90 degrees for supercritical. The separation angle is approximately 10 degrees past the minimum pressure angle; and therefore, the separation angle correlates with the drag coefficient. In the flow of Polyox solutions, however, the difference between the angle of minimum pressure and the separation angle is dependent upon concentration, degradation, free stream velocity and the cylinder size. As seen in Fig. 70, the polymer destabilizes the boundary layer under certain conditions and in turn causes early separation. Under other conditions, however, it can delay the boundary-layer separation to a point well beyond the point of minimum pressure.

The location of minimum pressure on the cylinder immersed in Polyox solutions, which cause greater than 15 P. D. R., moved from 70 degrees to only 80 degrees as the Reynolds number was increased through the drag transition range. Figure 71 compares the pressure distribution on a one-inch cylinder immersed in the flow of a 100 wppm

solution beyond the transition region (Re = 2.1 x 10^5), with that of a 1-1/2-inch cylinder in tap water at a comparable drag coefficient. Also shown in Fig. 71 is the pressure distribution obtained by Roshko [Ref. 32] in the transcritical regime at Re = 8.4 x 10^6 in air to illustrate its similarity to that obtained in the polymer solution. The strong similarity between the two pressure distributions suggests that at relatively high concentrations the transition takes place from a subcritical regime directly to a transcritical regime and that the transition is, as discussed earlier, independent of the body diameter and uniquely determined by a constant free-stream velocity. Furthermore, observations of the dye filament at velocities and concentrations cited above, regarding transition from a laminar to a purely turbulent one, appear to be in conformity with Roshko's suggestion [Ref. 32] that in the transcritical regime there are no laminar separation bubbles and that separation is purely turbulent.

F. RELATIVE INFLUENCE OF VELOCITY, DIAMETER, POLYMER CONCENTRATION AND PIPE-FRICTION REDUCTION ON THE DRAG COEFFICIENT

The dependence of the drag coefficient on various parameters is schematically illustrated in Fig. 72. In region-I, the drag coefficient was found to be principally dependent upon the free-stream velocity. In region-IIb, the drag coefficient varied with the cylinder size, velocity, concentration and P. D. R., velocity and P. D. R. being the dominant factors. In regions-IIa and IIIa, the minimum drag coefficient and thus the transition characteristics were found to be independent of concentration. In regions-IIIa and IIIb, the critical transition occurred. The drag coefficients in regions-IIa, IIIa and IIIb were principally a function of U^2d and P. D. R.

Region-IV signifies the Newtonian-fluid transition characteristics. It should be noted that even when a polymer solution does not produce any pipe-friction reduction, the critical transition can still occur on the cylinder. The wall-shear stress and velocity in the pipe were 280 dynes/cm^2 and 250 cm/sec respectively. For the cylinders tested, maximum wall-shear stress and maximum local velocity were in the order of 1,000 dynes/cm^2 and 1,000 cm/sec respectively. Therefore, it is not unexpected that degradation past the point of zero pipe-drag reduction is necessary before Newtonian transition characteristics are re-established.

G. COMPARISON WITH PREVIOUS WORKS

The only previously reported work on direct drag measurements on smooth cylinders of comparable size is that of McClanahan and Ridgely [Ref. 15]. They tested cylinders of length-to-diameter ratios of 5:1 and 10:1 by towing them, in a circular tank, through fresh solutions of Polyox WSR-301. The major difference between their results (for fresh solutions) and those obtained in the NPS tunnel is that the drag transition occurred at a velocity of approximately 4 fps in their experiments. In two cases (solutions of 50 and 200 wppm), the one-inch diameter cylinder of L/d ratio of 5:1 experienced drag transition at a lower velocity than the longer cylinder of identical diameter. End conditions are known to influence the drag force acting on a cylinder in the flow of a Newtonian fluid. In addition, it is reasonable to assume that the end conditions also influence the wavy separation pattern observed on cylinders in the flow of polymer solutions.

Therefore, the higher transition velocity observed in the NPS tunnel may be primarily due to the absence of undesirable end conditions.

The only previously reported work regarding the determination of the drag coefficient for bluff bodies of comparable size in degraded solutions was the work of A. White [Ref. 9]. He found that the drag coefficient on a 1/2-inch sphere at a free-fall velocity of 4.8 fps increased toward the water value as the solution aged over a six-day period. This is consistent with the results obtained on cylinders at velocities less than the critical velocity.

Brennen [Ref. 17] observed that the velocity at which separation - line distortion (on a 1/4-inch cylinder) occurred increased 3 fps by degradation in a 50 wppm Polyox solution. However, he did not observe the tripping to a Newtonian supercritical separation. In the experiments reported herein, such a stripping action was observed in solutions which produced less than 15 P. D. R. Brennen's degraded solution produced a turbulent drag of approximately 92% of that of water in a rotating-wheel rig. The details of that device and the per cent drag-reduction versus concentration-curve were not given. It is speculated that Brennen's dilute solution would have produced more than 15 P. D. R. in the 0.073-inch rheometer for the following reasons: Firstly, fifteen per cent drag reduction relative to laminar flow corresponds to a turbulent friction of 90% of that of water. Secondly, as Hoyt and Fabula [Ref. 2] found, a concentration of 5 wppm of Polyox of molecular weight 4×10^6 produces maximum friction reduction in a 0.109 cm pipe whereas a tenfold increase in concentration, 50 wppm, is necessary to achieve maximum drag reduction in a wheel rig.

No other experiments have been reported in the literature with bluff bodies in either severely degraded or in very low concentration (i.e., 1 wppm) Polyox solutions at velocities near critical. In the NPS water tunnel, however, practically the entire critical-range of velocities was covered for the sizes of cylinders tested.

V. POSSIBLE FLOW MECHANISM(S) FOR BLUFF-BODY DRAG REDUCTION

The previous explanations of the observed reduction of the drag of bluff bodies were based on the limited observations of the rearward shift of the separation line, relative to water, of spheres dropped into polymer solutions of relatively high concentrations. It was conjectured that the polymer stabilizes the laminar boundary layer or causes a reattachment rearward of the expected separation point. The data reported herein have shown clearly that there is no correlation between the separation angle and the drag coefficient in dilute polymer solutions.

In order to attempt to explain the phenomenon, it seems necessary to re-examine the basic question of the drag alteration by additives: The question is not why does the polymer additive cause drag reduction on bluff bodies, for in many cases it does not (e.g., 1-1/2 in. diameter cylinder in a 100 wppm solution at $Re = 2 \times 10^5$), but rather why does the dilute-polymer solution alter the characteristics of the drag-crisis region of bodies for which such a crisis occurs in Newtonian fluids. This question will now be explored in as much detail as possible.

It is a well-known fact that the turbulence-intensity of the ambient flow, surface roughness and threads, and the modified pressure gradients materially affect the range of the Reynolds number in the Eiffel-effect region. Although the tunnel-turbulence levels were not measured in the present study, it may be inferred from the location of the transition region in tap water that the turbulence level was in the order of 2%. At this turbulence level, smooth bluff-body drag transition is relatively

unaffected by slight increases in turbulence level. Based on the works of Fabula [Ref. 33] and Friehe and Schwarz [Ref. 34], it is difficult to conceive that a concentration of 1 wppm Polyox WSR-301, aged 24 hours, could increase the free stream turbulence to the level necessary to cause a 50% decrease in the drag-crisis Reynolds number. If the cause of the "early" drag transition had been principally an increase of the intensity of the free stream turbulence, then the drag coefficient of the 1-1/2-inch cylinder in a 100 wppm solution would not have remained constant at approximately 0.7 as the tunnel velocity was raised above the velocity at which drag transition occurred in tap water. Similar drag characteristics have been reported for spheres dropped into quiescent tanks of fresh Polyox solutions. Therefore, attempts to explain the observed change in drag crisis on the basis of a change in free-stream turbulence level are not tenable.

On the contrary, an explanation based on the concept of roughness elements or threads in the boundary layer appears to be physically more realistic. Even for a concentration of only 1 wppm, there are approximately 10^{10} large polymer molecules in the cylinder boundary layer. A departure from Reynolds number similarity in the drag-crisis region does occur for roughened cylinders. As seen in Fig. 14, the smaller cylinder (larger ϵ/d) experienced transition at a lower Reynolds number in air flow than the larger cylinders, with the ratio of the transition Reynolds number proportional to the square root of the ratio of cylinder diameters. The drag-crisis Reynolds number in Polyox solutions which were severely degraded and/or of very low concentration was found to be also proportional to the square root of the ratio of the cylinder

diameters. When Humphreys attached threads to the front of a cylinder in air flow at critical Reynolds number, the spanwise cell structure at separation and the transition characteristics markedly changed [Ref. 30]. In a similar manner, the separation cell structure is ordered by the polymer molecules to an extent that Brennen was able to measure their spanwise wave length. In addition, the occurrence of separation-line distortion in polymer solutions is closely and naturally related to the occurrence of drag crisis. However, this analogy cannot be carried too far since, as in turbulent pipe flow, the polymer molecules are many times more effective in altering the flow near a wall than can be justified on the basis of their physical size alone. In addition, this analogy suggests a much greater dependence of the drag-crisis on bluff-body size than has been observed in solutions of higher concentrations. Therefore, it is suggested that there is some other influence of the additive on the boundary-layer flow which affects the transition characteristics.

This other property is usually given the title of viscoelasticity under which the literature abounds with the concepts of normal stresses, fluid relaxation times, and strain field dependent viscosity, each or all of which would certainly modify the boundary layer in the convective flow about a bluff body. However, it is finally conjectured that it is specifically the finite (but not necessarily constant) critical shear-wave speed (c^*) which is the fundamental polymer property which imparts a significant change in the characteristics of the flow [Refs. 35, 36, 37].

It is significant to note that all mathematical models do not exhibit a finite shear wave speed. Even a model such as the Oldroyd type visco-elastic-fluid model [Ref. 37] has a number of different definitions of stress flux, etc., the choice of which alters the predicted boundary layer flow. Thus, the following discussion will deal not so much with the particular characteristics of models that display a finite shear wave speed but rather with the behavior of fluids such as dilute polymer solutions used in the present investigation.

The behavior of the dilute polymer flow is governed by the interaction of the viscous boundary layer and a "hydro-polymeric" boundary layer in a manner similar to the interaction of hydrodynamic and thermal boundary layers in convective heat transfer. Above the hydro-polymeric boundary layer, shear waves can propagate and standing waves exist on the characteristic surface similar to the propagation of sound and shock waves in a compressible fluid. When the hydro-polymeric boundary layer is much less than the viscous boundary layer thickness, the viscous boundary layer flow is insensitive to the wall shear stress. This is analogous to the case when the thermal boundary layer thickness is much less than the viscous boundary layer thickness, i.e., the viscous boundary-layer flow is insensitive to the wall temperature.

When the wall shear stress exceeds the critical shear stress (ρc^{*2}), the hydro-polymeric boundary layer thickness becomes principally a function of fluid properties, i.e., independent of body size.

When the wall shear stress is much less than the critical shear stress, the locus of the hydro-polymeric boundary layer can be shown to be at $u = c^*$, and thus dependent upon the body size.

An exact solution of the equations of motion for the stagnation point flow of a second-order viscoelastic fluid have shown [Ref. 38] that the boundary layer velocity profile and the wall-shear stress are drastically altered when the Weissenberg number Wn (the ratio of the first normal-stress difference to the shear stress) is greater than zero. In fact, as the Weissenberg number increases, critical shear stress decreases, the wall stress increases and inflections occur in the velocity profile. Furthermore, the velocity-over-shoot occurs closer to the wall and increases in magnitude as the Weissenberg number increases.

Based on previous discussions, the following conjectures for the observed anomalous behavior of the flow of dilute polymer solutions about bluff bodies may be offered:

(1) The polymer molecules cause the solution to have a finite critical shear wave speed (c*);

(2) As a result of this finite shear wave speed, a hydro-polymeric boundary layer results;

(3) The entire boundary layer flow is strongly influenced by the hydro-polymeric boundary layer thickness;

(4) The mechanics of the drag crisis are principally unaltered; however, transition characteristics are controlled by the hydro-polymeric boundary layer thickness;

(5) Above the hydro-polymeric boundary layer, shear waves propagate and can have a secondary influence on the transition characteristics;

(6) When the wall shear stress is expected to exceed the critical shear stress, the hydro-polymeric boundary layer thickness is

principally determined by the fluid properties (density, dynamic viscosity and critical shear wave speed), independent of the body size;

(7) When the wall shear stress is less than the critical shear stress, the hydro-polymeric boundary layer thickness is principally determined by the distance from the wall at which the streamwise velocity equals the critical shear wave speed;

(8) The ratio of inertial forces to viscous shear forces in the viscous boundary layer, above the hydro-polymeric boundary layer, is altered. This ratio, a generalized Reynolds number, is a function of $\rho U^2/\rho c^{*2}$ when the critical shear stress is exceeded; and finally,

(9) When the wall shear stress is less than critical and the free stream velocity is greater than the shear wave speed, the shear stress at the interface of the viscous and hydro-polymeric boundary layers ($u = c^*$) is a function of $\mu c^*/d$. Therefore, the generalized Reynolds number is a function of $\rho U^2/(\mu c^*/d)$, i.e., $(U/c^*)Re$. In both cases, the generalized Reynolds number is larger than Re.

F. White [Ref. 39] stated that the local-friction coefficient (C_f) in (flat plate) turbulent dilute-polymer-flow at a given Rex is equal to the Newtonian C_f evaluated at an effective Reynolds number, Ren, given by*

---

*It is interesting to note that for laminar boundary-layer flow τ_w is proportional to $\rho U^2 Re^{-1/2}$, with ka=4, and Ren is proportional to $(U/c^*)^4$.

$$Ren = Rex\ (v^*/c^*)^{ka} \text{ for } v^* > c^*$$

where $v^* = (\tau_w/\rho)^{1/2}$, k is equal to 0.4, c* is equal to .08 ±.02 fps for Polyox WSR-301 and "a" is dependent upon concentration. For concentrations greater than 20 wppm "a" is approximately constant at 10. For lower concentrations, both "a" and the shear-wave speed depend upon concentration. However, the above stated value of the critical shear-wave speed correlates, for concentrations greater than 20 wppm, with that cited in other works to be discussed in the following.

Ultman and Denn [Ref. 35] analyzed James' data based on a simple Oldroyd type fluid model and stated that the onset of anomalous heat- and momentum-transfer at low Reynolds numbers (10^{-3} inch diameter wires) in dilute polymer solutions occurs when the free stream velocity is equal to the critical shear wave velocity. The onset for anomalous heat transfer occurred at a free stream velocity of .08 ±.02 fps for a 52.4 wppm Polyox WSR-301 solution, independent of wire size (1×10^{-3} to 6×10^{-3} inch diameter).

The data for the onset of the Toms effect in turbulent pipe flow, from the work of Pruitt and Crawford as reported by Walsh [Ref. 40], clearly show that for Polyox, the critical shear stress increases with decreasing concentration and molecular weight:

M. W. x 10^6	Conc. wppm	Onset Stress dynes/cm^2	c* fps
0.5	2	600	.8
0.5	10	120	.36
0.5	50	24	.16
1.6	2	60	.25
1.6	10	15	.125

As a comparison, the maximum shear stress on a 1-1/2-inch diameter cylinder in water flowing at 10 fps is approximately 300 dynes/cm^2, whereas the local free stream velocity at 60 degrees is approximately 17 fps.

For the case of the flow of fresh Polyox WSR-301 solutions with concentrations greater than 10 wppm, the expected wall-shear stress exceeds the critical value over a large portion of the cylinder surface. Thus, the drag coefficient is dependent upon the ratio of the free-stream velocity to the critical shear wave speed. As the concentration or molecular weight is decreased, the region where the wall-shear stress exceeds the critical value is also decreased. However, the region where the local free stream velocity exceeds the critical shear wave velocity is practically unaffected.

As noted earlier, the critical transition occurred in solutions which produced, at the particular state of degradation, approximately 15 P. D. R. Identical P. D. R. could have been obtained with a fresh solution had it a concentration of 1/3 wppm. Walsh's hypothesis (concentration x onset stress=constant, for a given M. W.) predicts that the 1/3 wppm Polyox WSR-301 solution should have a critical shear stress on the order of 360 dynes/cm^2 and, thus, a critical shear wave speed of 0.6 fps. Therefore, the critical transition occurs not when the shear exceeds the critical shear stress but when the free stream velocity is an order of magnitude larger than the critical shear-wave speed. Thus the drag coefficient is a function of the product of velocity ratio (U/c^*) and the Reynolds number.

This, obviously, does not predict the exact velocity at which drag crisis would occur but *it does indicate that the drag crisis occurs at a free-stream velocity greater than the shear-wave speed and less than the free-stream velocity at which the drag crisis would occur on the same body in pure solvent.*

The experimental evidence indicates that the drag transition in fresh solutions of Polyox WSR-301 with concentrations of 25 and 100 wppm is similar to the drag transition in a Newtonian fluid. However, the flow changes from subcritical directly to the transcritical flow observed by Roshko with an 18-foot cylinder in air flow at $Re > 3.5 \times 10^6$.

It is speculated that the critical type drag transition, which occurred in solutions of relatively smaller concentrations and/or in solutions of drastically reduced molecular weight, is a manifestation of an apparently new type of instability for steady shearing flows of viscoelastic fluids [Ref. 36]: A breakdown of the steady flow by the rapid growth of a disturbance involving a jump in the acceleration.

Since the bluff bodies were tested in homogeneous solutions, it is not possible to discriminate the effect of the polymer molecules on the boundary-layer flow from their effect on the free-shear layer and wake flow. However, since both free-shear layer and wake flows are dependent upon the boundary-layer flow in a Newtonian fluid, it is conjectured that the direct interaction between free shear layer vortices and wake vortices and the polymer molecules are of secondary importance. The primary effects produced by the polymer molecules in dilute solutions occur near the wall.

Obviously, much of the foregoing is speculative and a complete explanation of the critical transition and the shift of the transition region must await a detailed exploration of the exact nature of the disturbances, their formation and growth.

VI. SUMMARY OF RESULTS AND CONCLUSIONS

The preceding discussion shows that the effect of polymer molecules on the flow past bluff bodies cannot be considered as drag reduction per se for a given Reynolds number. Small amounts of Polyox WSR-301 in water flowing about a bluff body significantly alter the pressure distribution only in the flow regime where there is a transition region.

The results further indicate that the shift in separation point and the change in back pressure on cylinders, caused by the additive, are not directly related. On the contrary, each depends upon the concentration, degradation, free stream velocity and the cylinder size. Furthermore, the drag coefficient is not uniquely determined by the separation angle.

Two distinct types of drag transition occur: The first is a continuous transition for fresh solutions, the characteristics of which resemble the drag transition on roughened cylinders. The second is an actual drag "crisis" or "tripping" of the boundary layer at a well defined flow condition for degraded solutions which produce approximately the same friction reduction, in the turbulent-flow pipe rheometer, independent of the initial concentration.

The details of the dependence of cylinder drag coefficient upon the free stream velocity, cylinder diameter, per cent pipe-drag reduction and concentration have previously been discussed. In general, it was found that the drag coefficient predominantly depends upon the free stream velocity and per cent pipe-drag reduction. There are two

significant conclusions which can be drawn from this result: (1) The Reynolds number similarity does not hold true for flows of dilute polymer solutions past bluff bodies, and (2) there is a relationship between the effect of polymer molecules on fully developed turbulent pipe flow and their effect on convective "laminar" external boundary layer flow. No definitive causal mechanism to explain this relationship and the anomalies produced in the transition flow regime can be offered. Even though conjectures based on viscoelastic phenomenon have been presented, so little data concerning the rheology of dilute Polyox solutions are available that it is not possible to attach specific significance to the predictions of either the Oldroyd or second-order fluid models.

The recirculating water tunnel has been demonstrated to be a vital and economical tool for the investigation of external flows of dilute polymer solutions, providing the properties of the solution are monitored. It is vital because the Reynolds number similarity does not apply and the flow velocity must be varied independently of the body size. It is economical because the body is fixed; thus instrumentation is greatly simplified. In addition, with the recirculating tunnel, observation time is neither limited by space nor fluid storage capacity. The implicit assumption is, of course, made that the results obtained in homogeneous solutions can be extrapolated to the case of polymer injection from the wall. It has previously been shown by others that this assumption is fairly valid for turbulent flow over a flat plate. Furthermore, a little reflection shows that whether the polymer solution is injected into the boundary layer or into the entire flow, all of the hydrodynamic effects take place within the boundary layer and thus

the presence of polymer in the shear-free flow region does not play, for all intents and purposes, any role on the boundary layer. It is, therefore, justifiable to conclude that the results of the present investigation, attained through the use of a homogeneous solution, should be applicable to cases where polymer solutions of the same molecular weight, type and boundary layer concentration are directly introduced into the flow by injection.

The results of the on-going investigation on Strouhal frequency in the critical regime, the growth and formation of disturbances in the critical region, the detailed observations of the hairpin vortices in the vicinity of the separation line, and finally the results of the investigation on drag-transition for cylinders where the degraded polymer solution is injected into the boundary layer formed by an otherwise additive-free ambient flow will be separately reported.

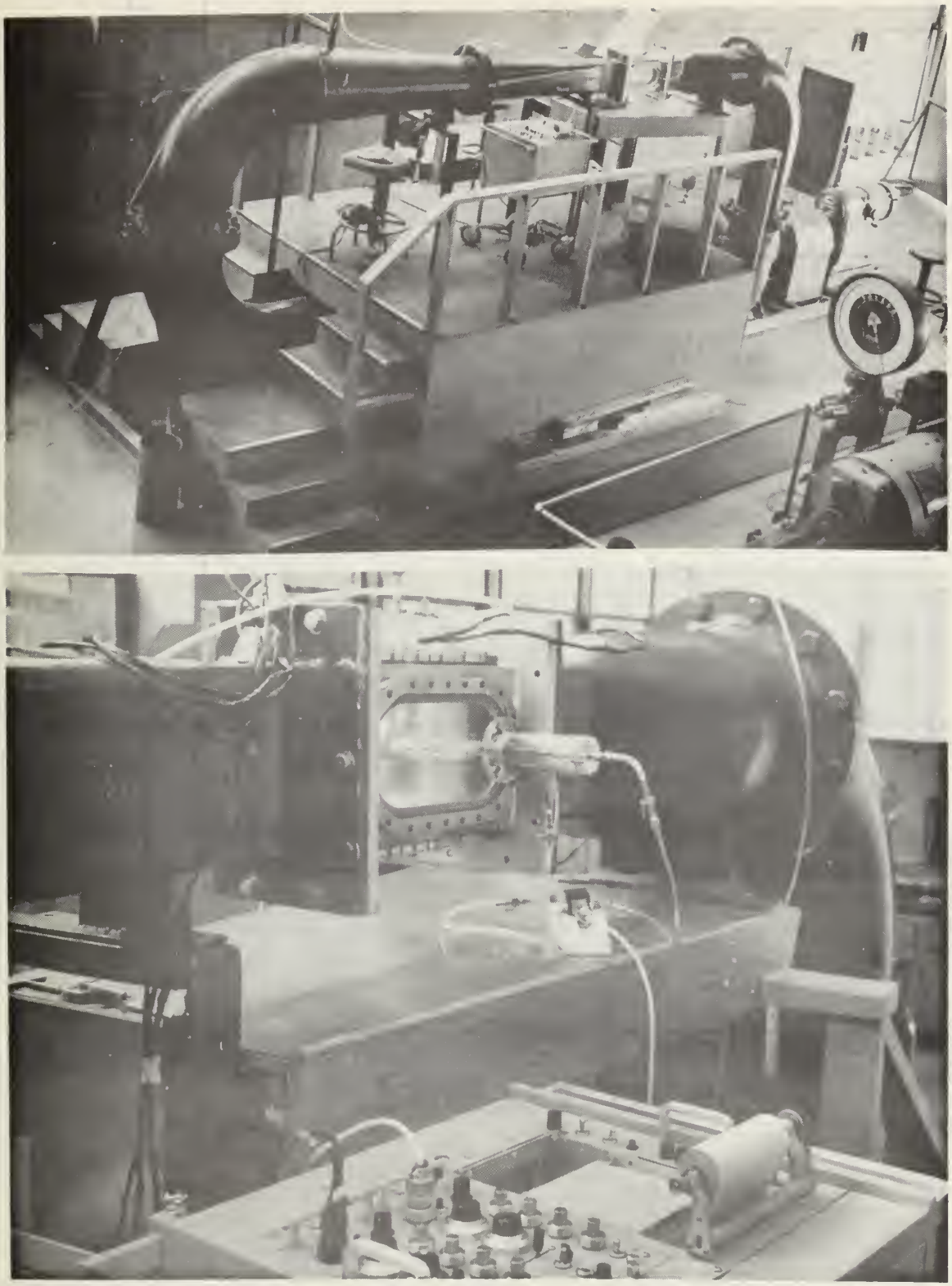

FIG. 1 NPS WATER TUNNEL

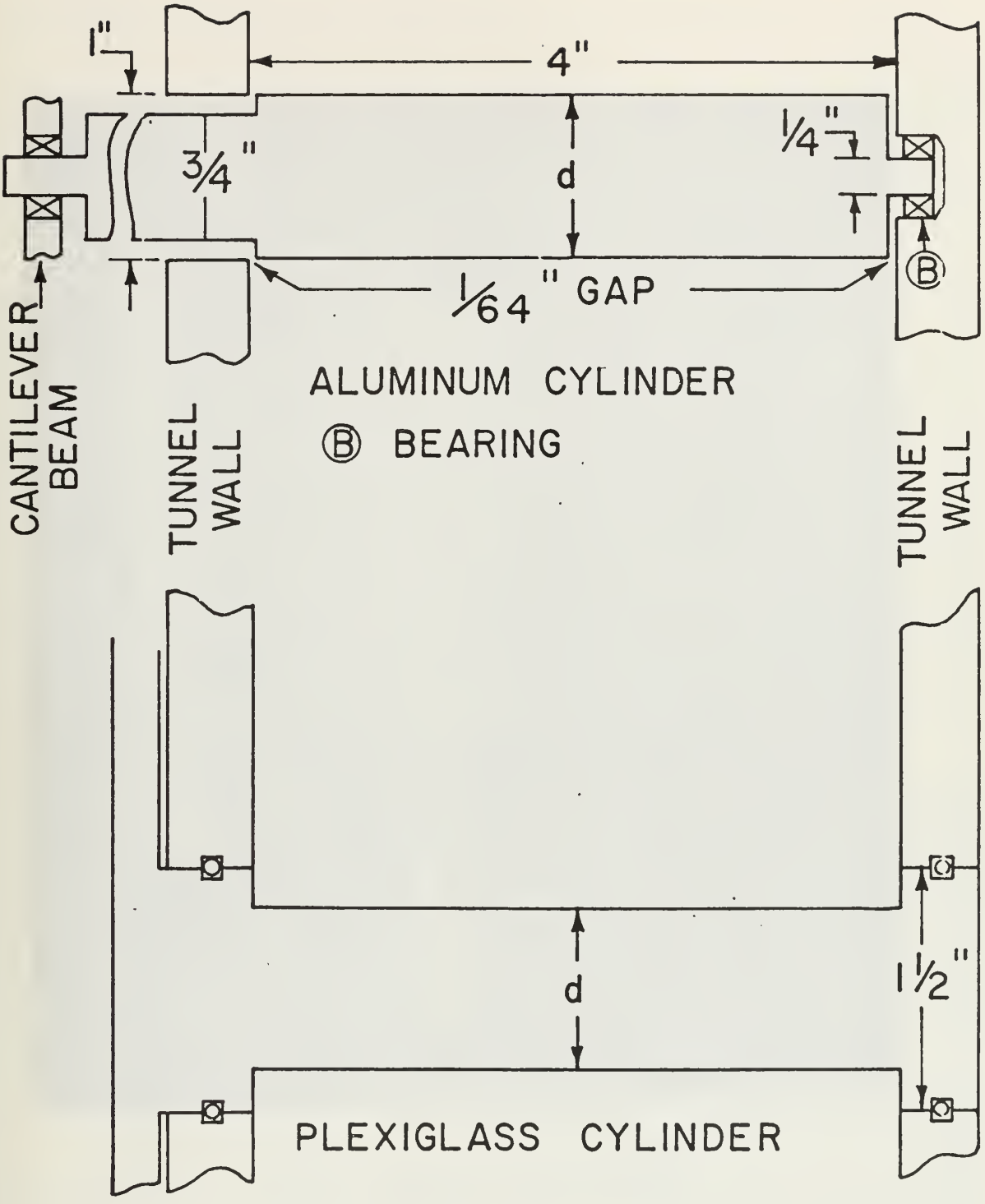

FIG. 2 COMPARISON OF
CYLINDER END CONDITIONS

FIG. 3 HYDROFOIL TEST SPECIMEN

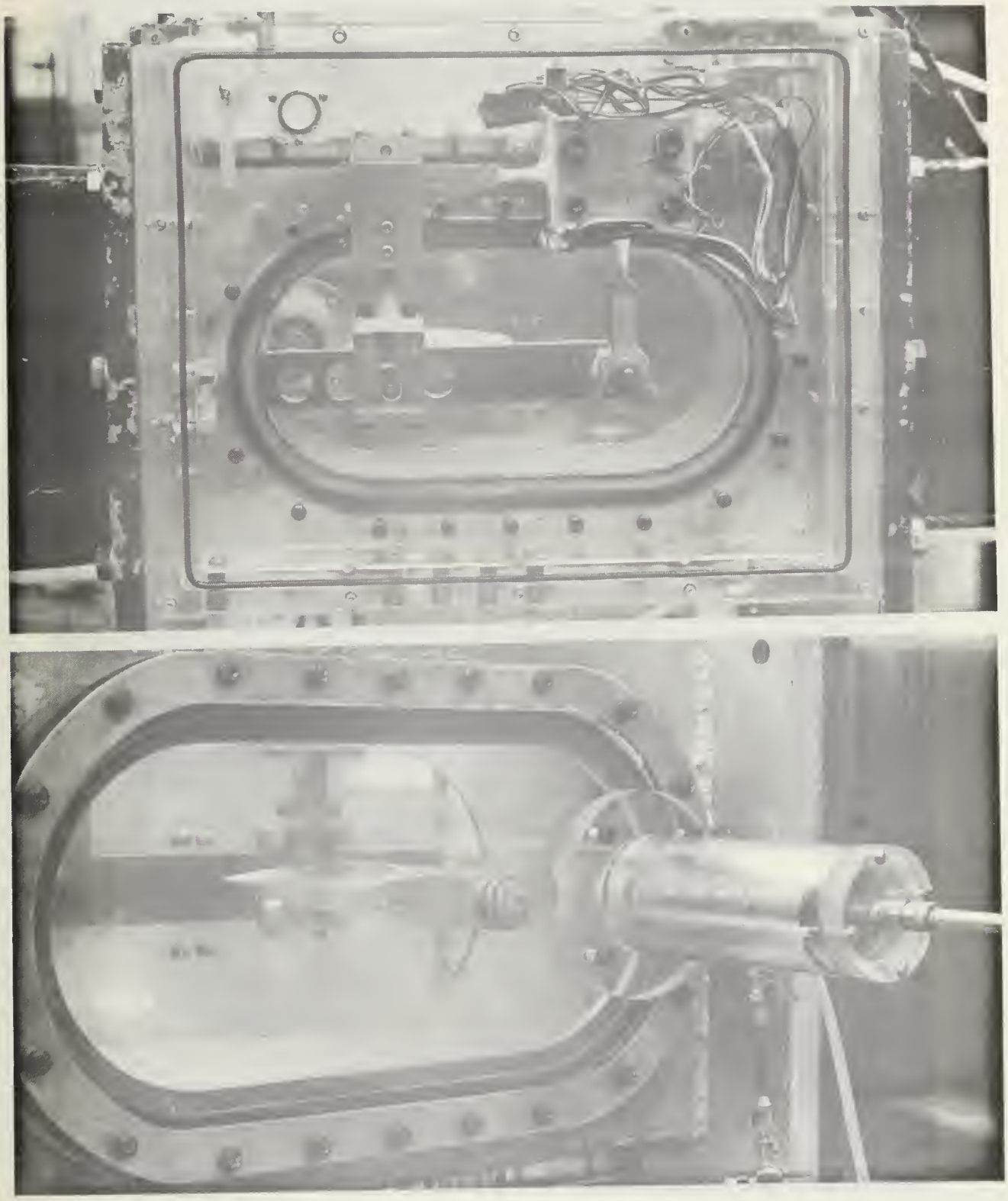

FIG. 4 LIFT AND DRAG MEASURING SYSTEM FOR HYDROFOIL

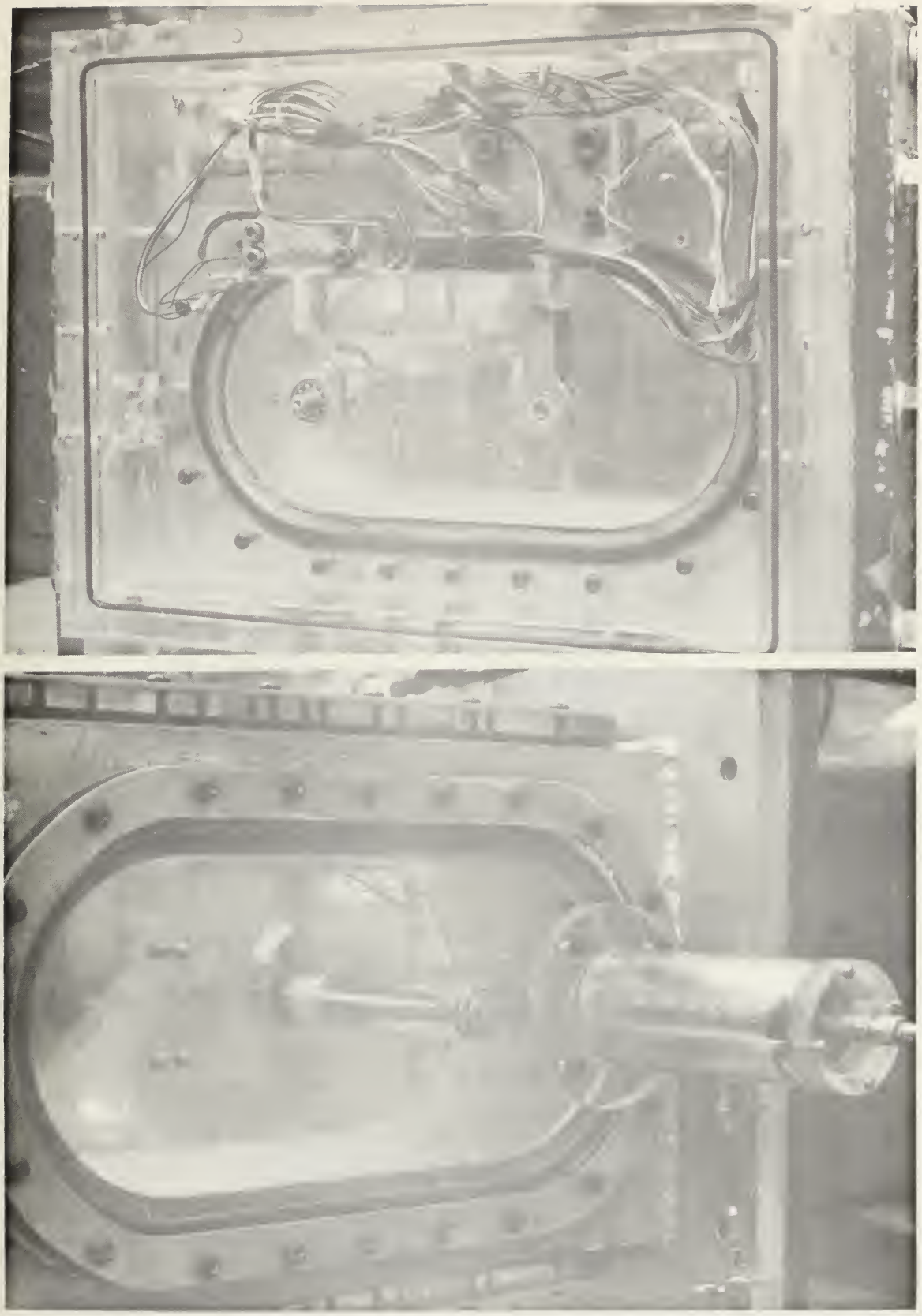

FIG. 5 DRAG MEASURING SYSTEM FOR CYLINDERS

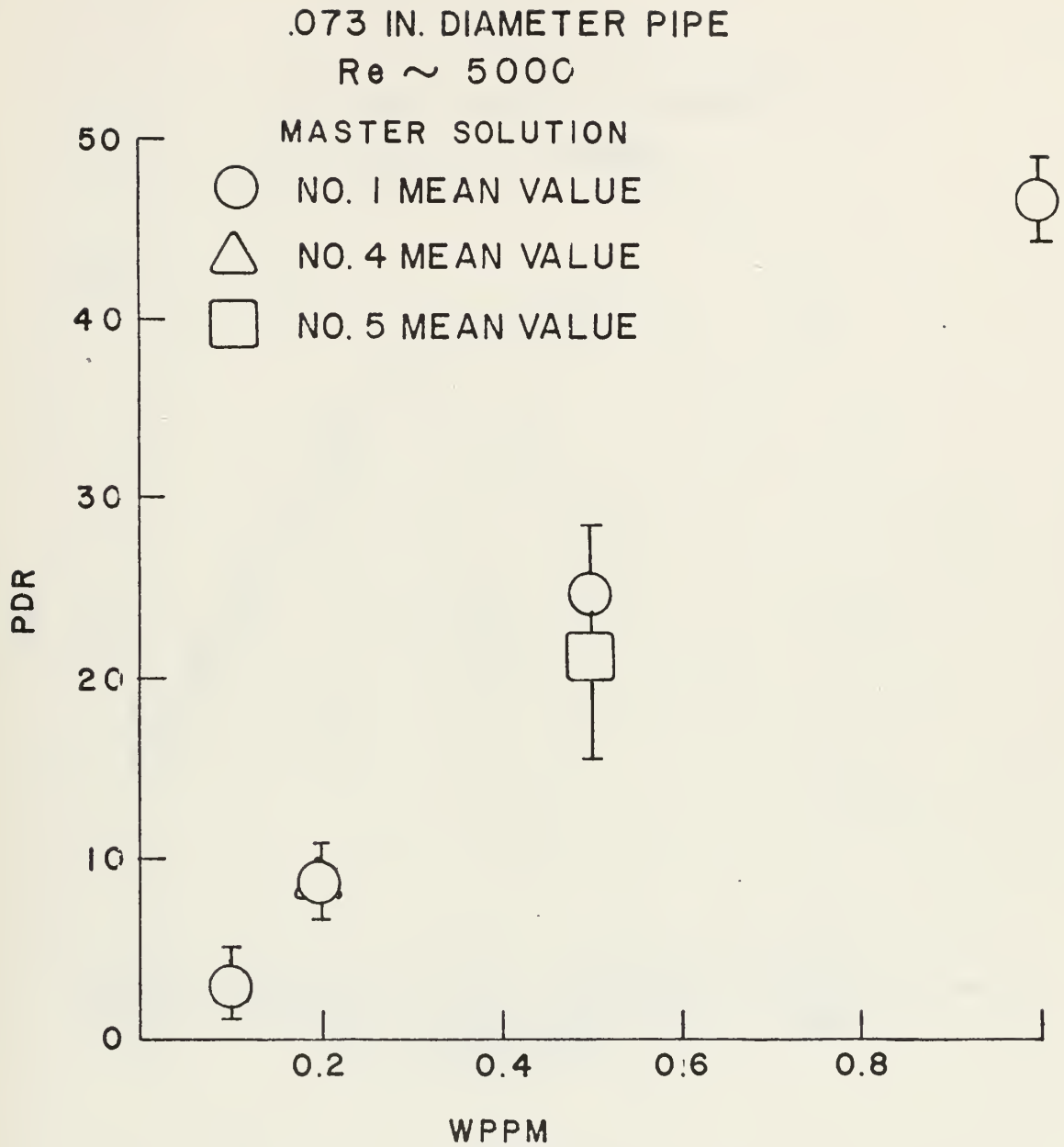

FIG. 6 PDR VERSUS WPPM
POLYOX WSR-301
LABORATORY SOLUTIONS

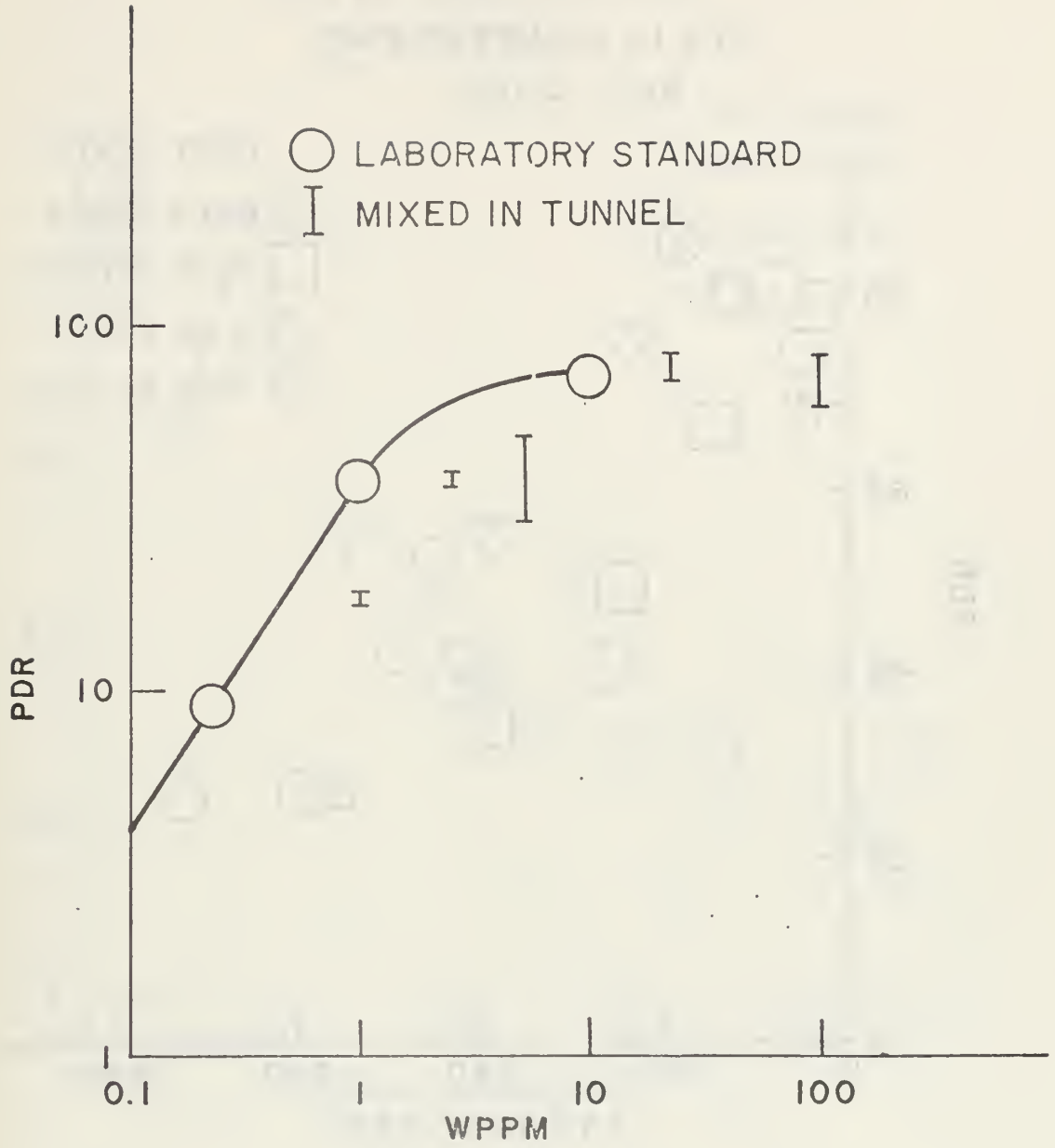

FIG. 7 PDR VERSUS WPPM
FRESH TUNNEL-SOLUTIONS

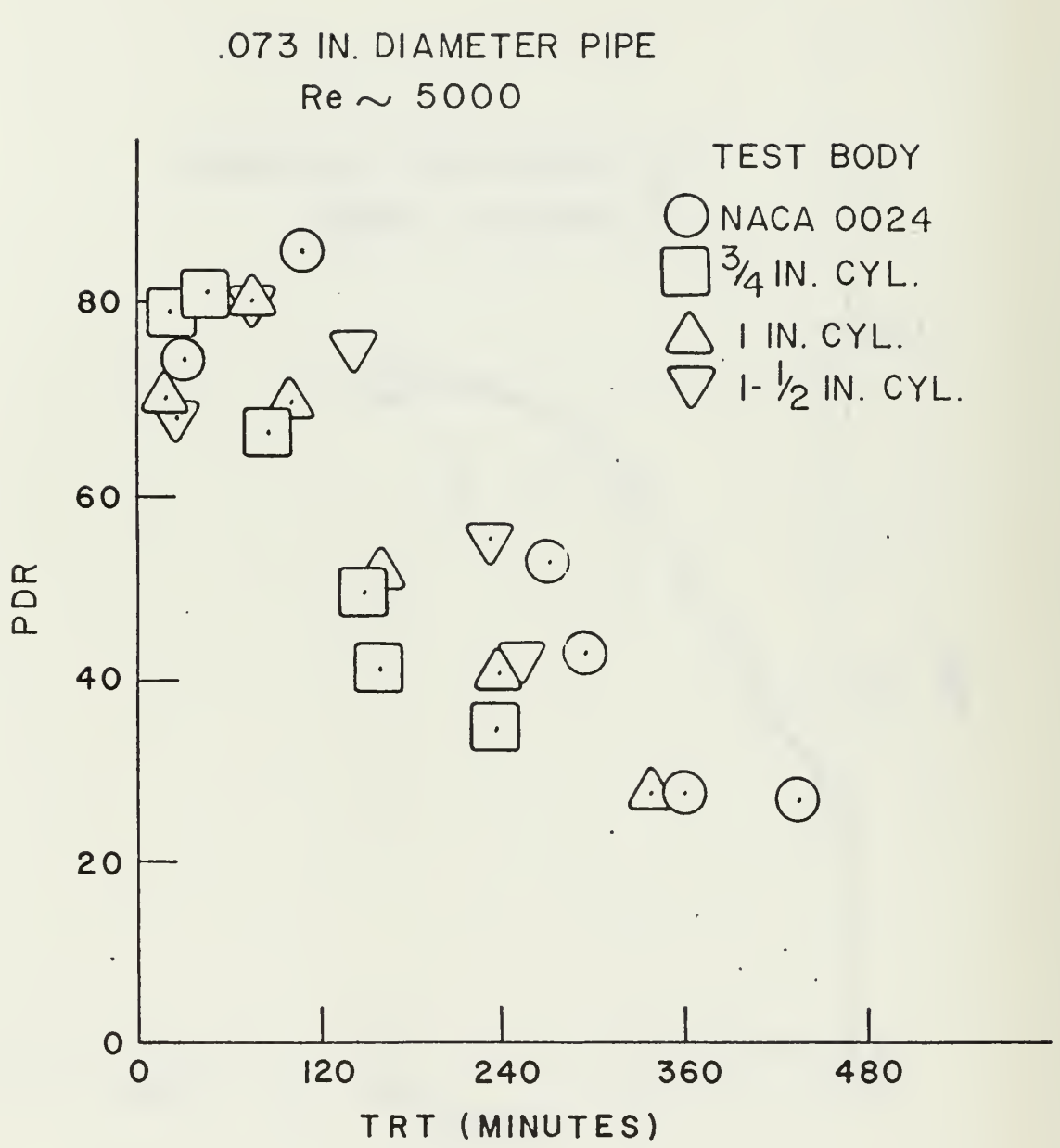

FIG. 8 PDR VERSUS TRT
100 WPPM POLYOX WSR-301

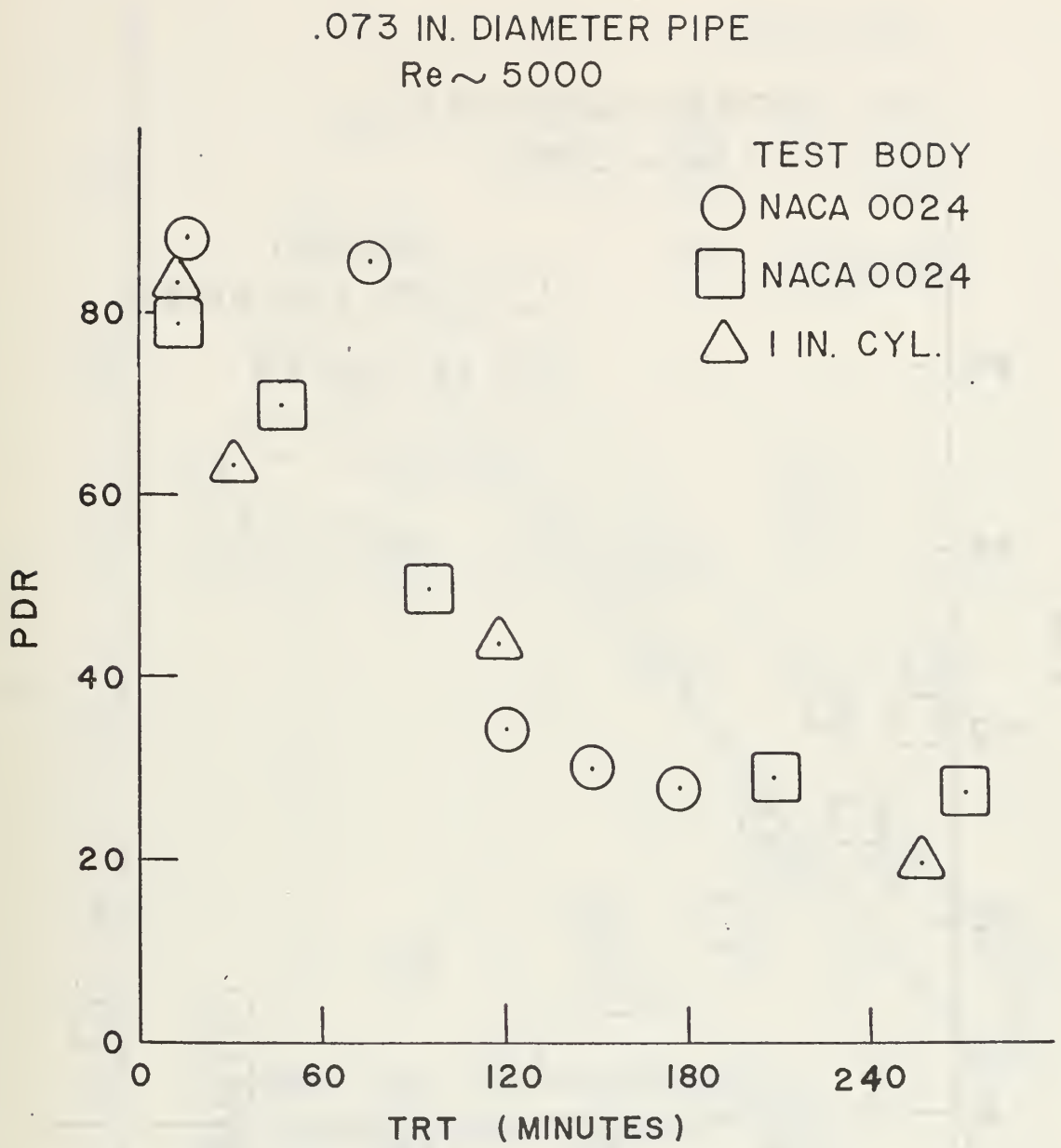

FIG. 9 PDR VERSUS TRT
25 WPPM POLYOX WSR-301

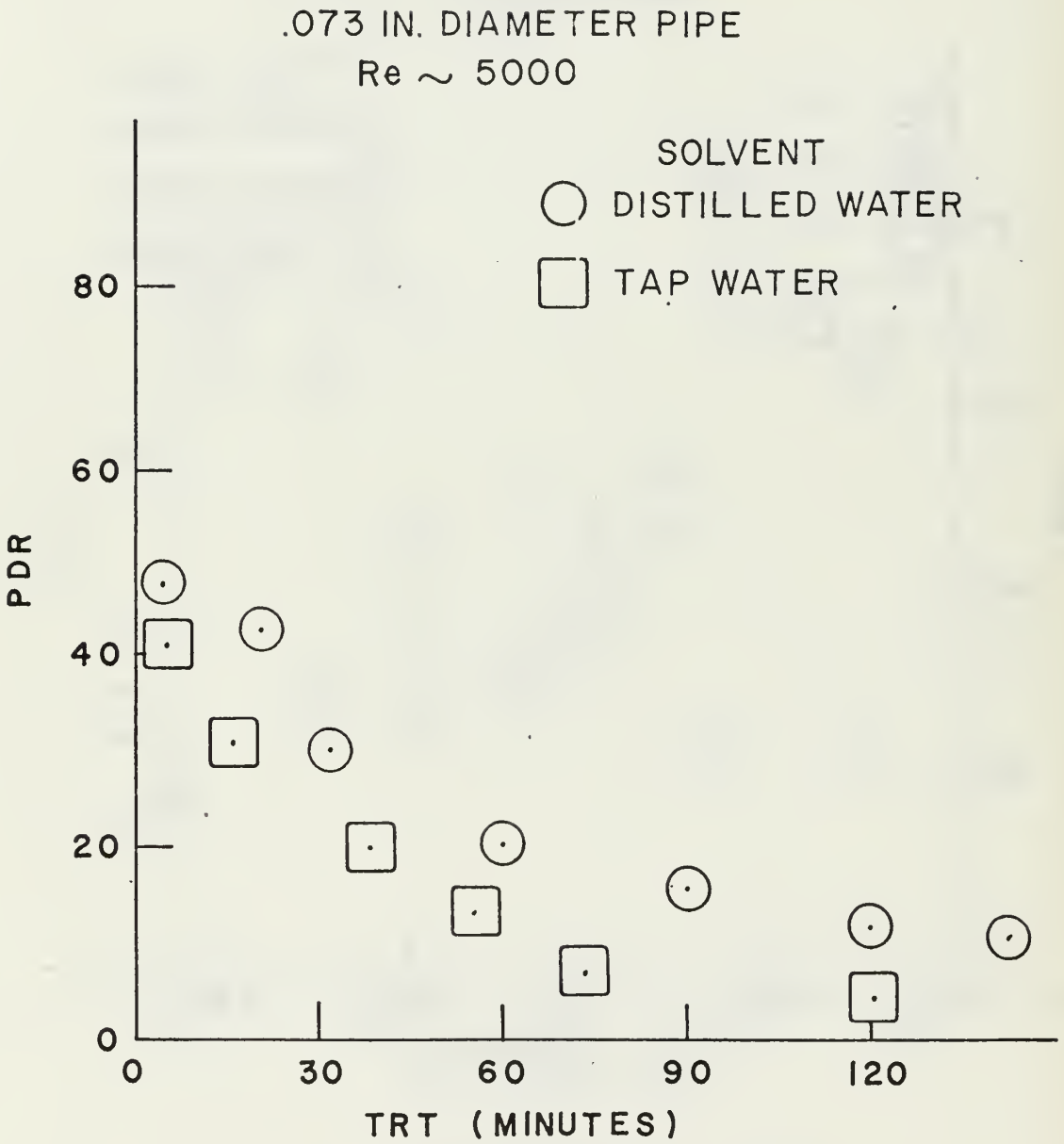

FIG. 10 PDR VERSUS TRT
5 WPPM POLYOX WSR-301

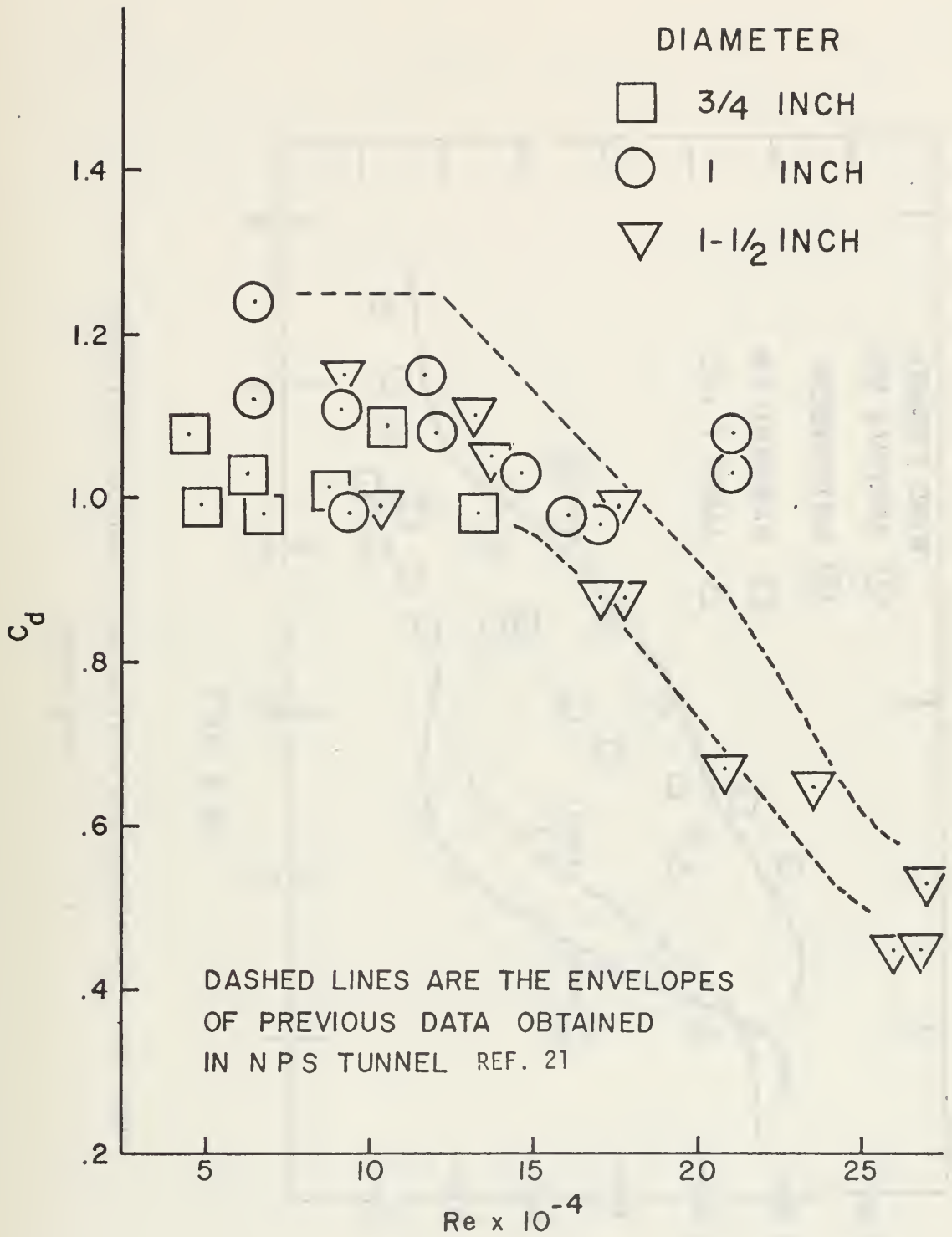

FIG. 11 C_d VERSUS Re
CYLINDERS IN TAP WATER

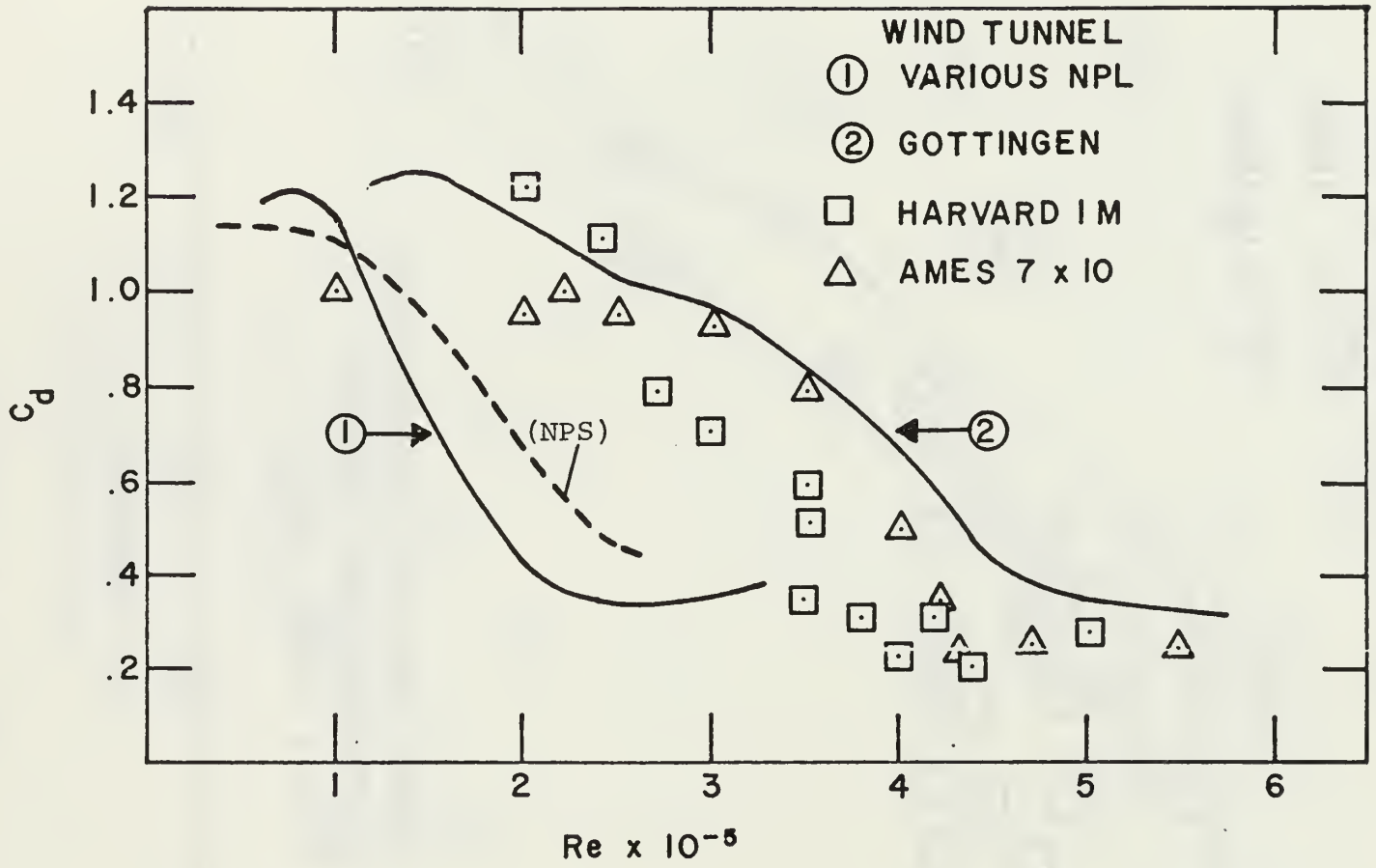

FIG. 12 C_d-TRANSITION REGION FOR CIRCULAR CYLINDERS

(- - - - NPS DATA)

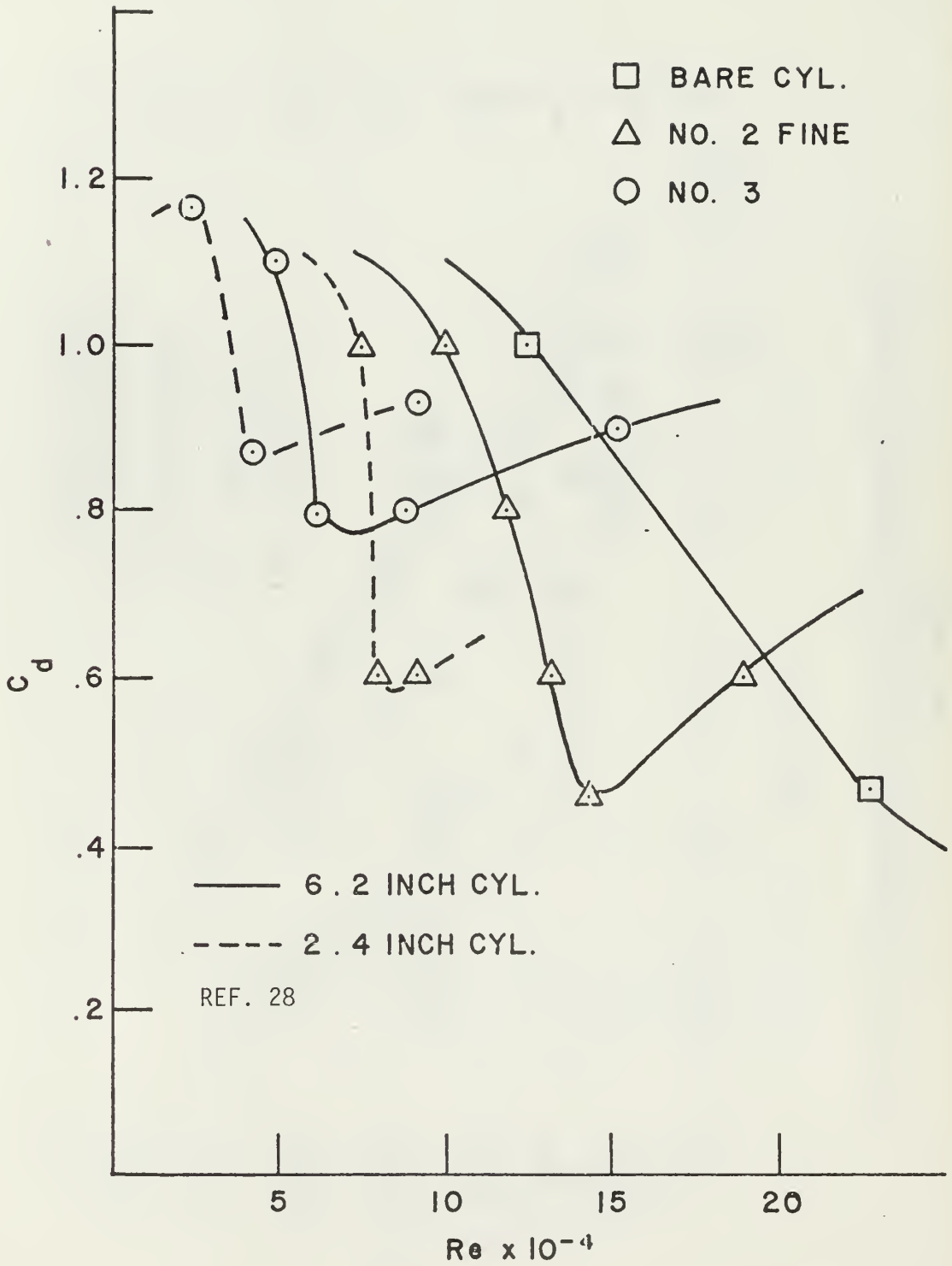

FIG. 14 C_d VERSUS Re SHOWING THE EFFECT OF SURFACE ROUGHNESS

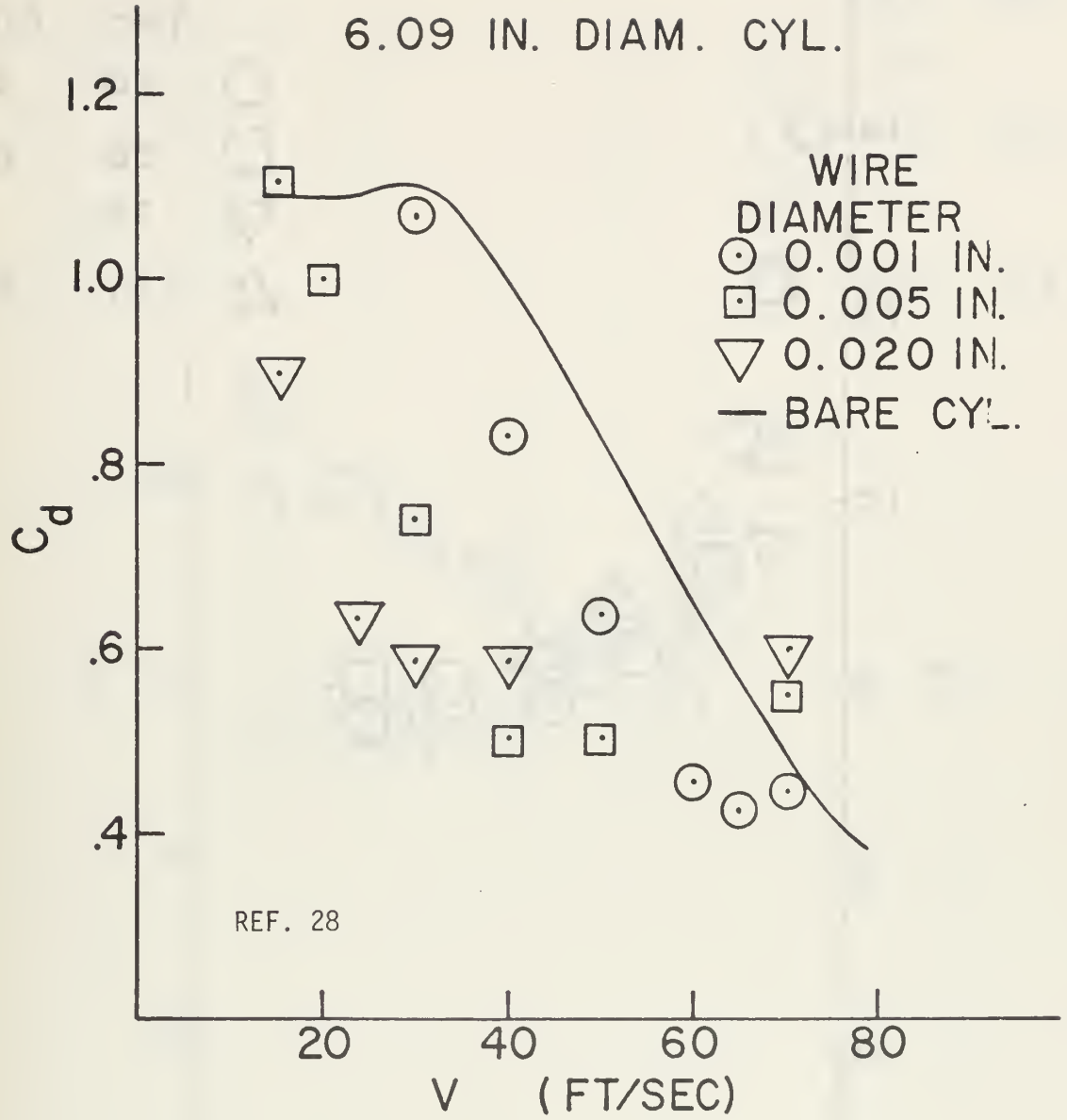

FIG. 15 EFFECT OF TRIPPING WIRE

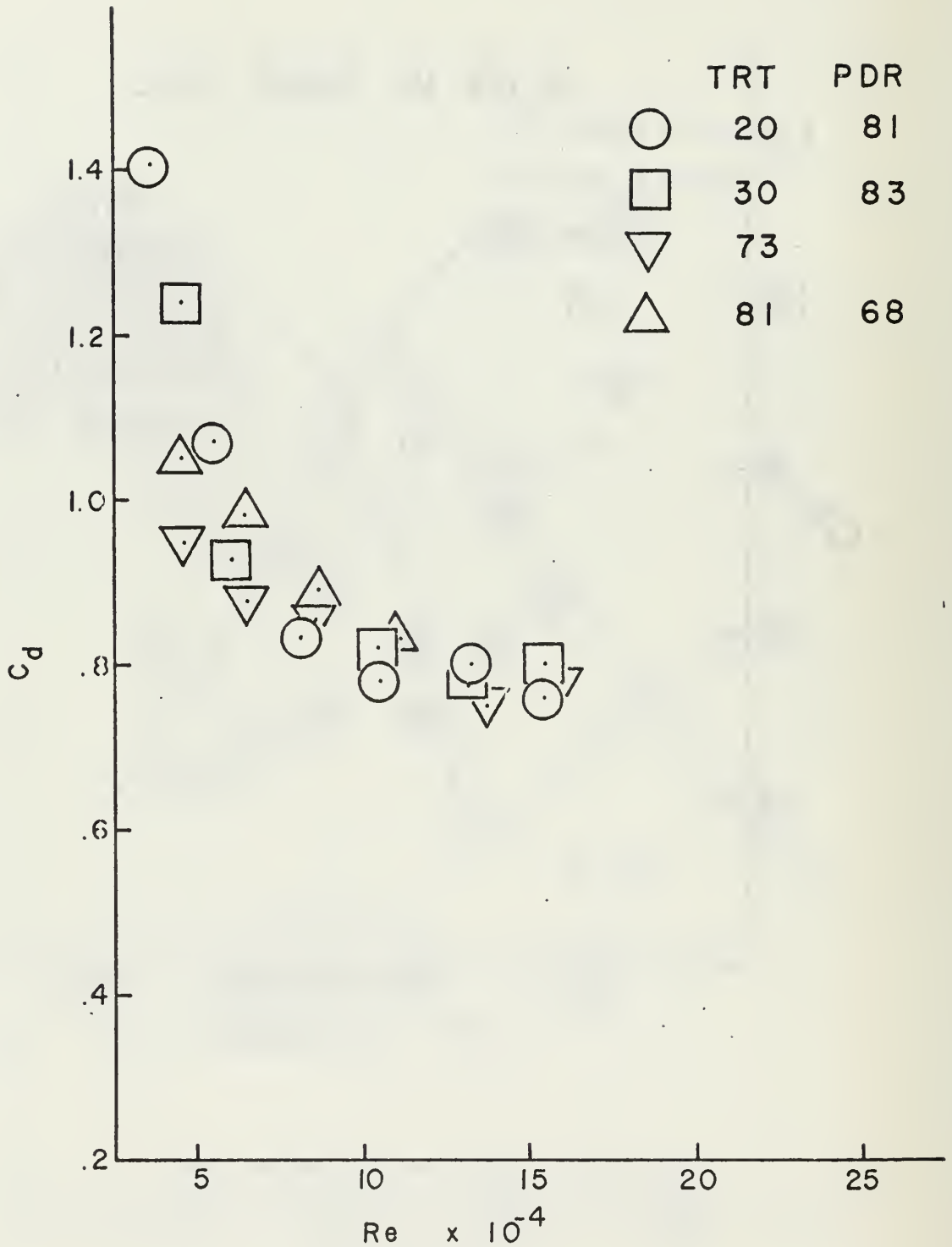

FIG. 16 C_d VERSUS Re
3/4 in. DIAMETER CYLINDER
IN 100 WPPM SOLUTION

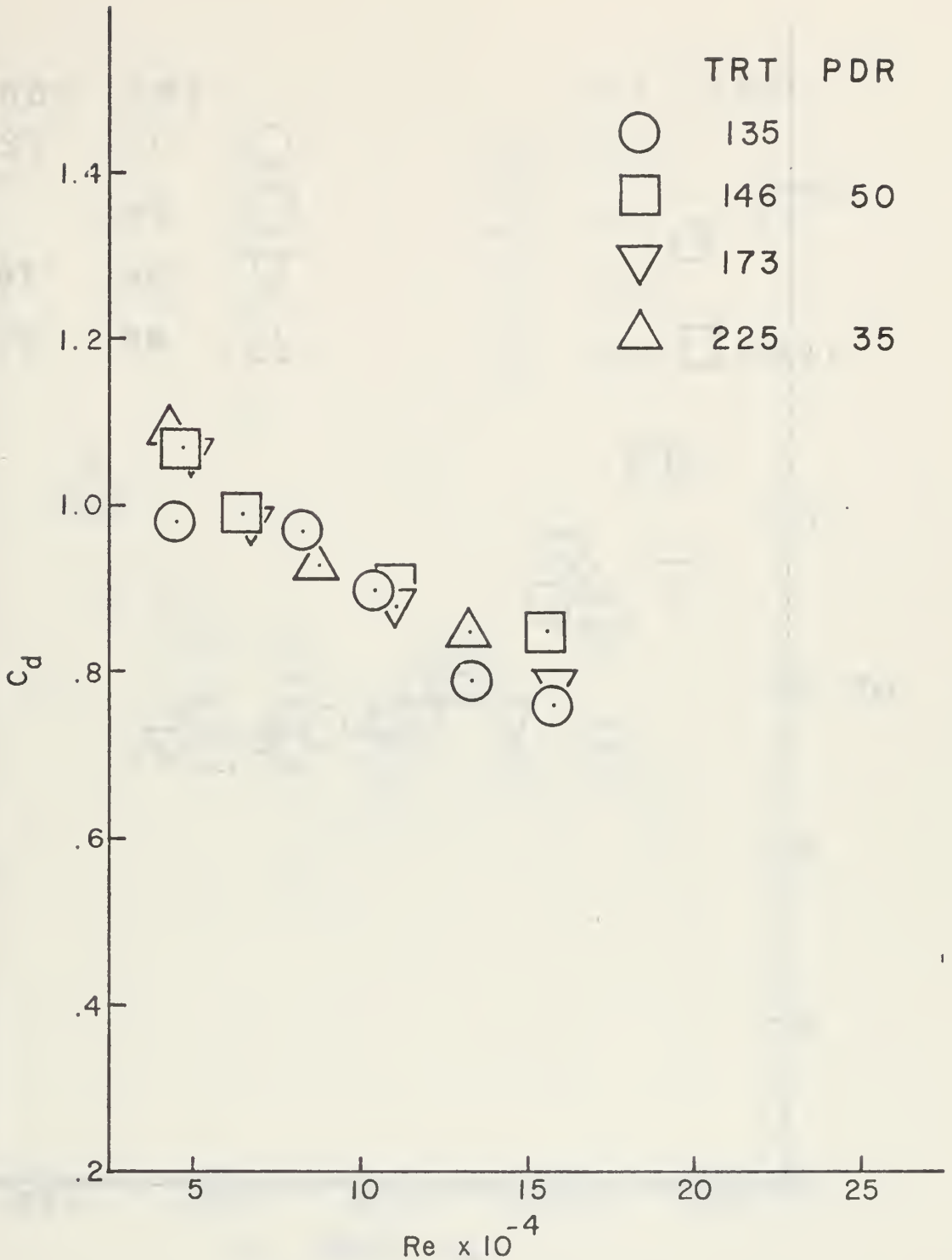

FIG. 17 C_d VERSUS Re

3/4 in. DIAMETER CYLINDER
IN 100 WPPM DILUTE SOLUTION

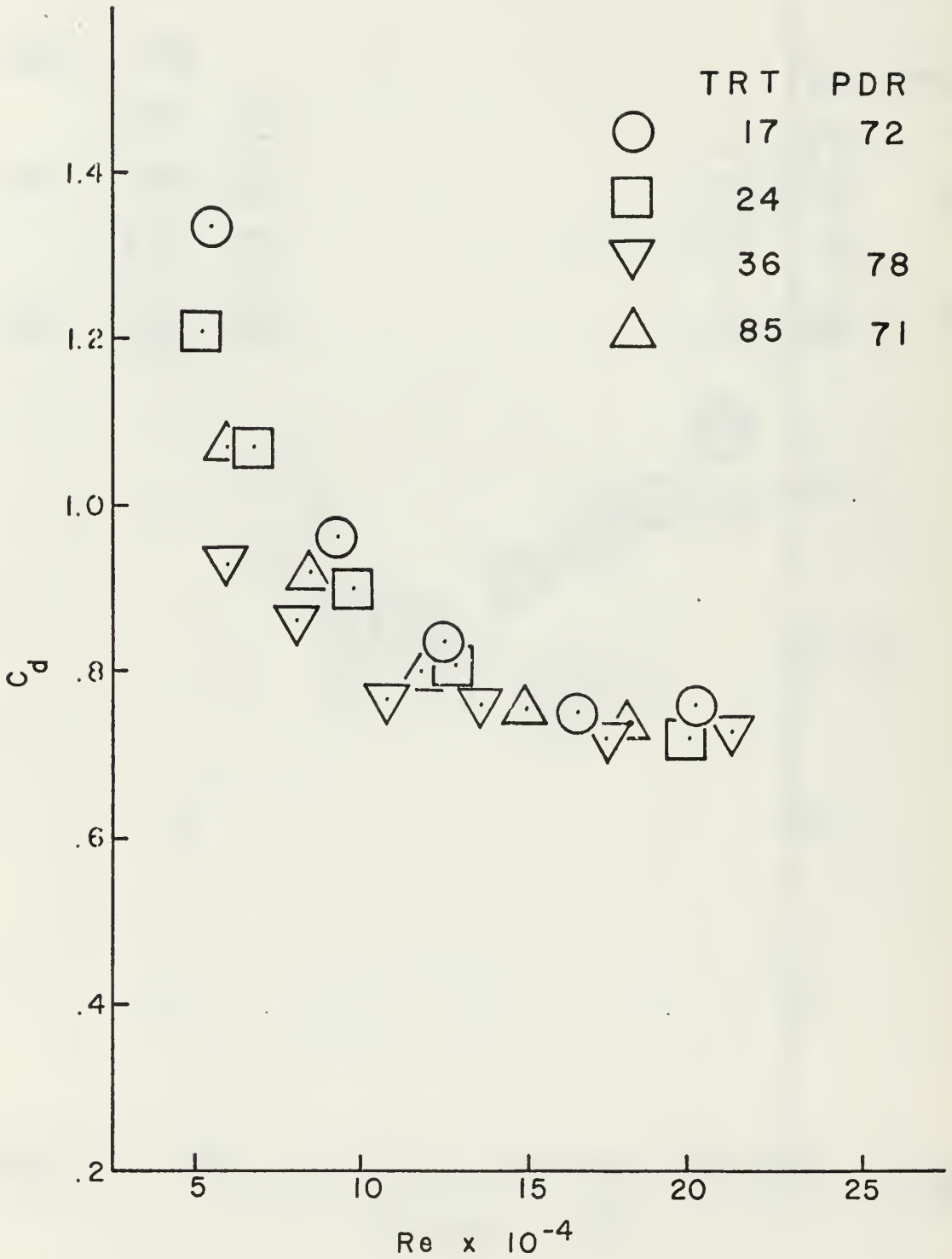

FIG. 18 C_d VERSUS Re
1 in. DIAMETER CYLINDER IN
100 WPPM DILUTE SOLUTION

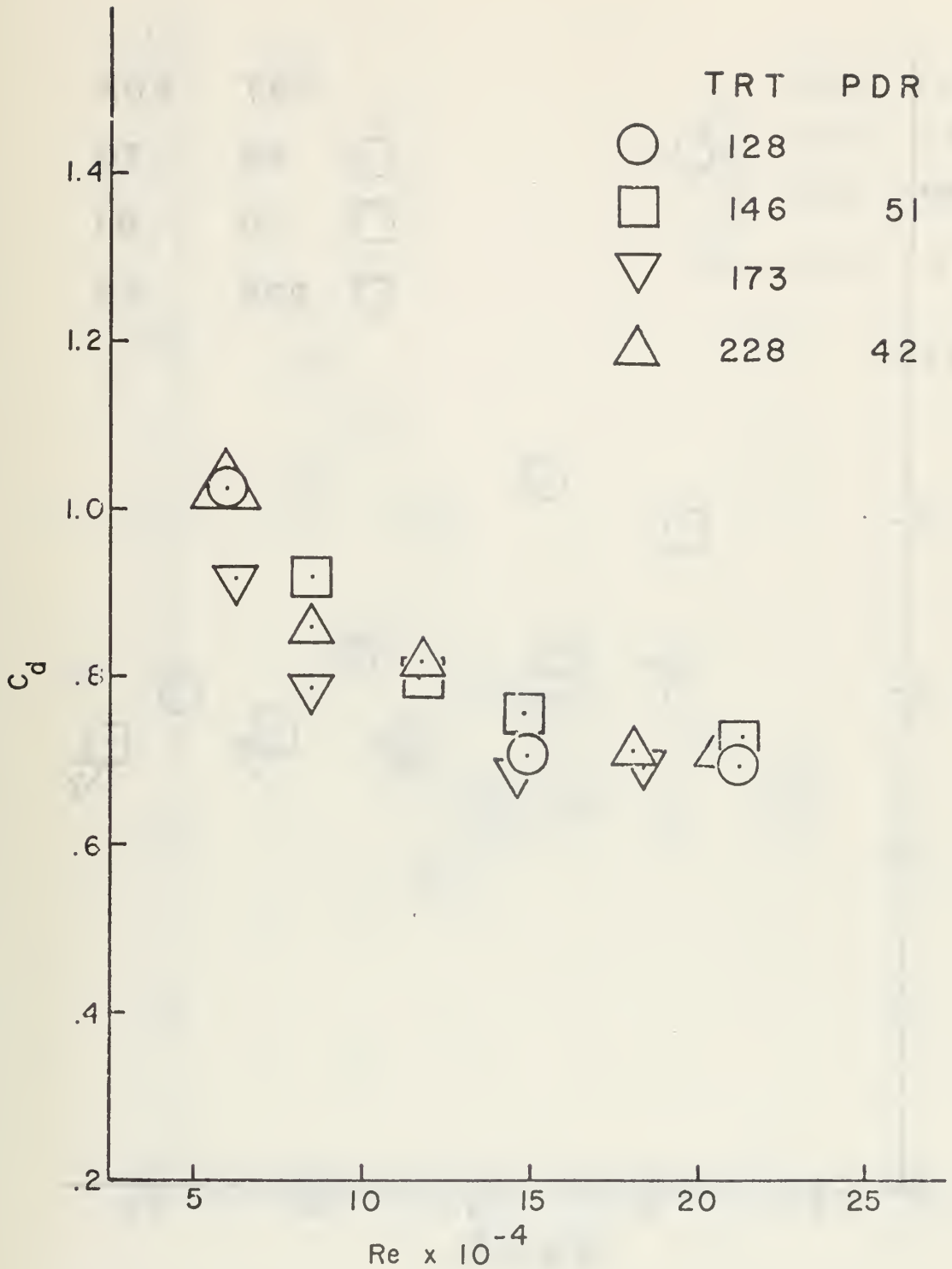

FIG. 19 C_d VERSUS Re
1 in. DIAMETER CYLINDER IN
100 WPPM DILUTE SOLUTION

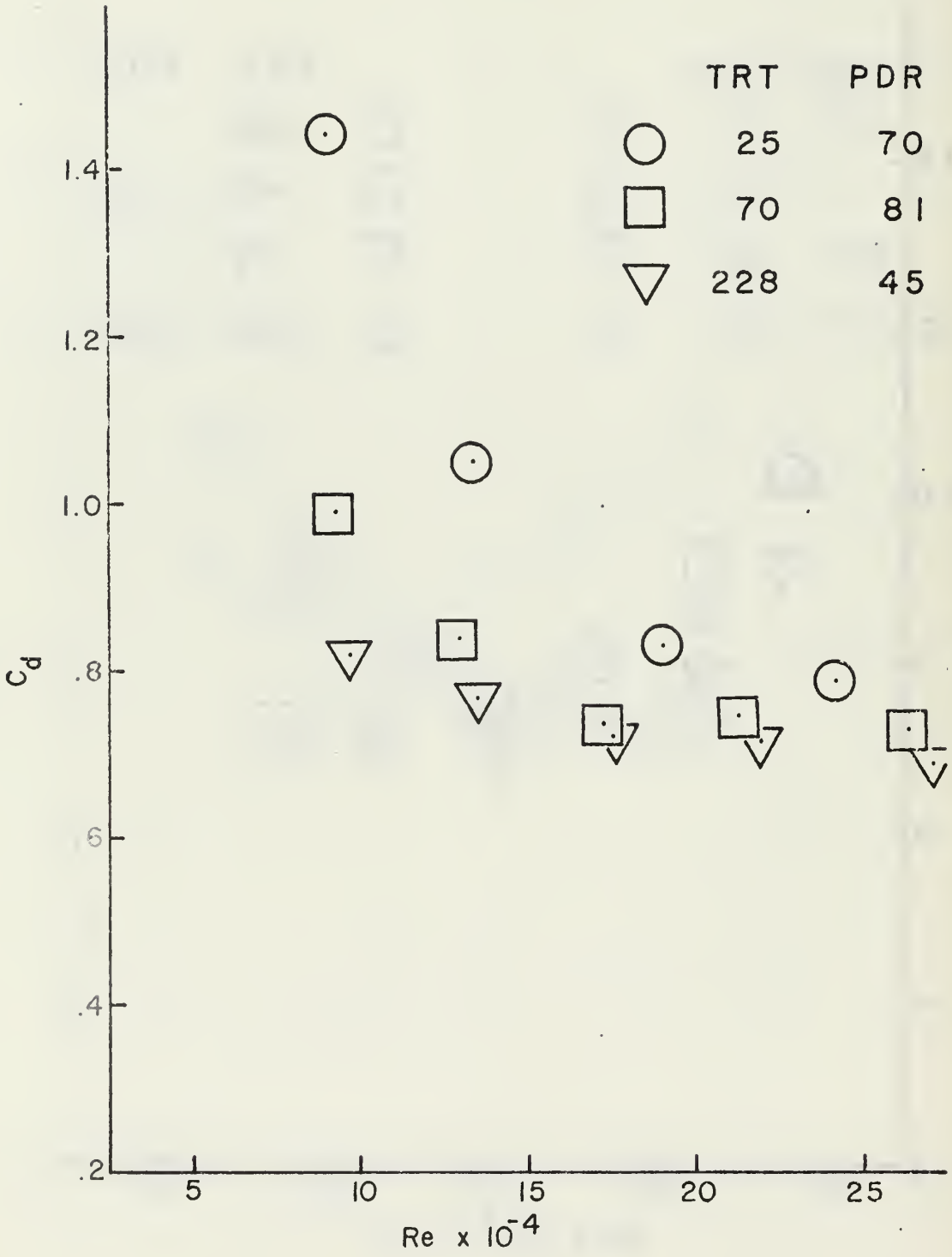

FIG. 20 C_d VERSUS Re
1-1/2 in. DIAMETER CYLINDER
IN 100 WPPM DILUTE SOLUTION

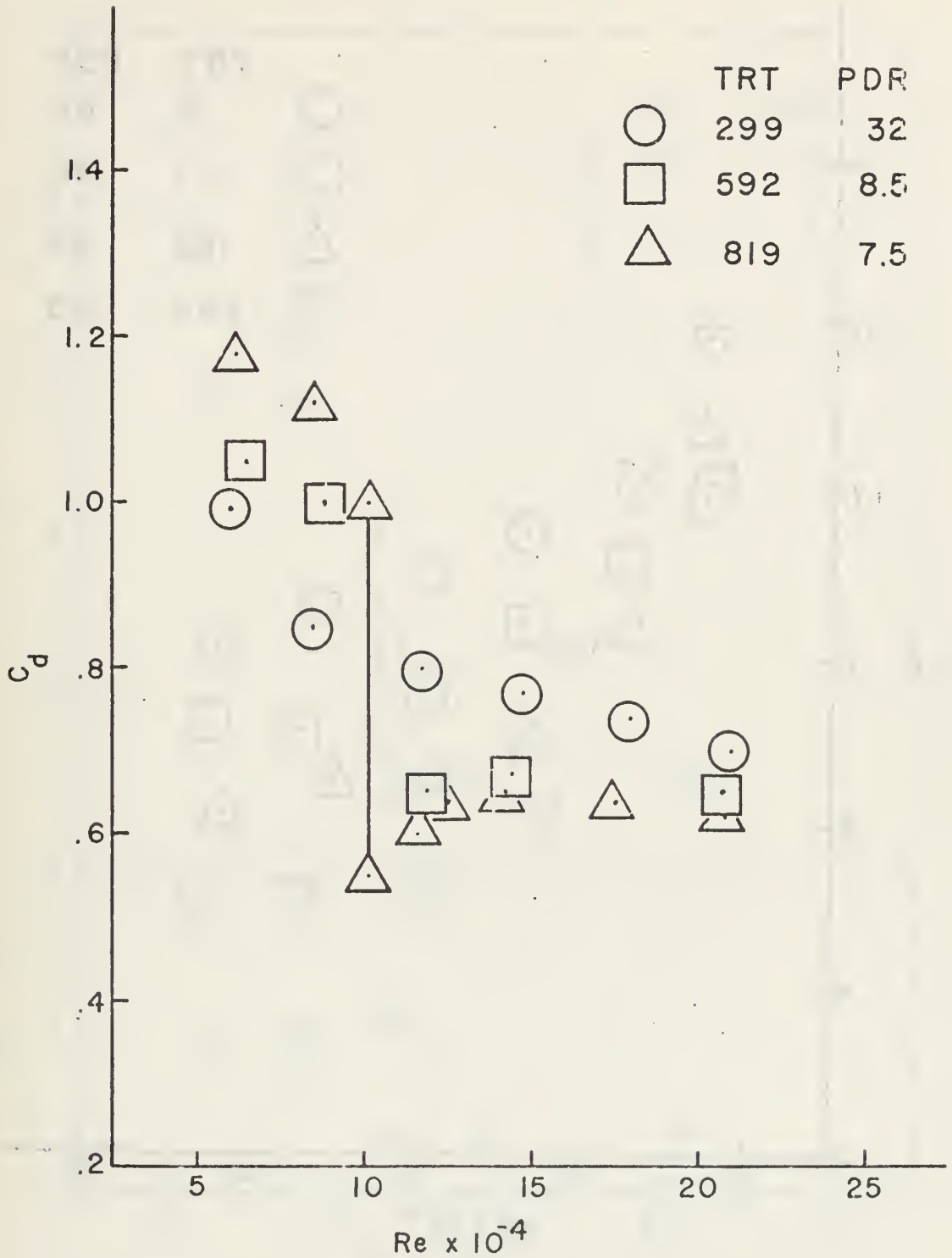

FIG. 21 C_d VERSUS Re
1 in. DIAMETER CYLINDER IN
100 WPPM DILUTE SOLUTIONS

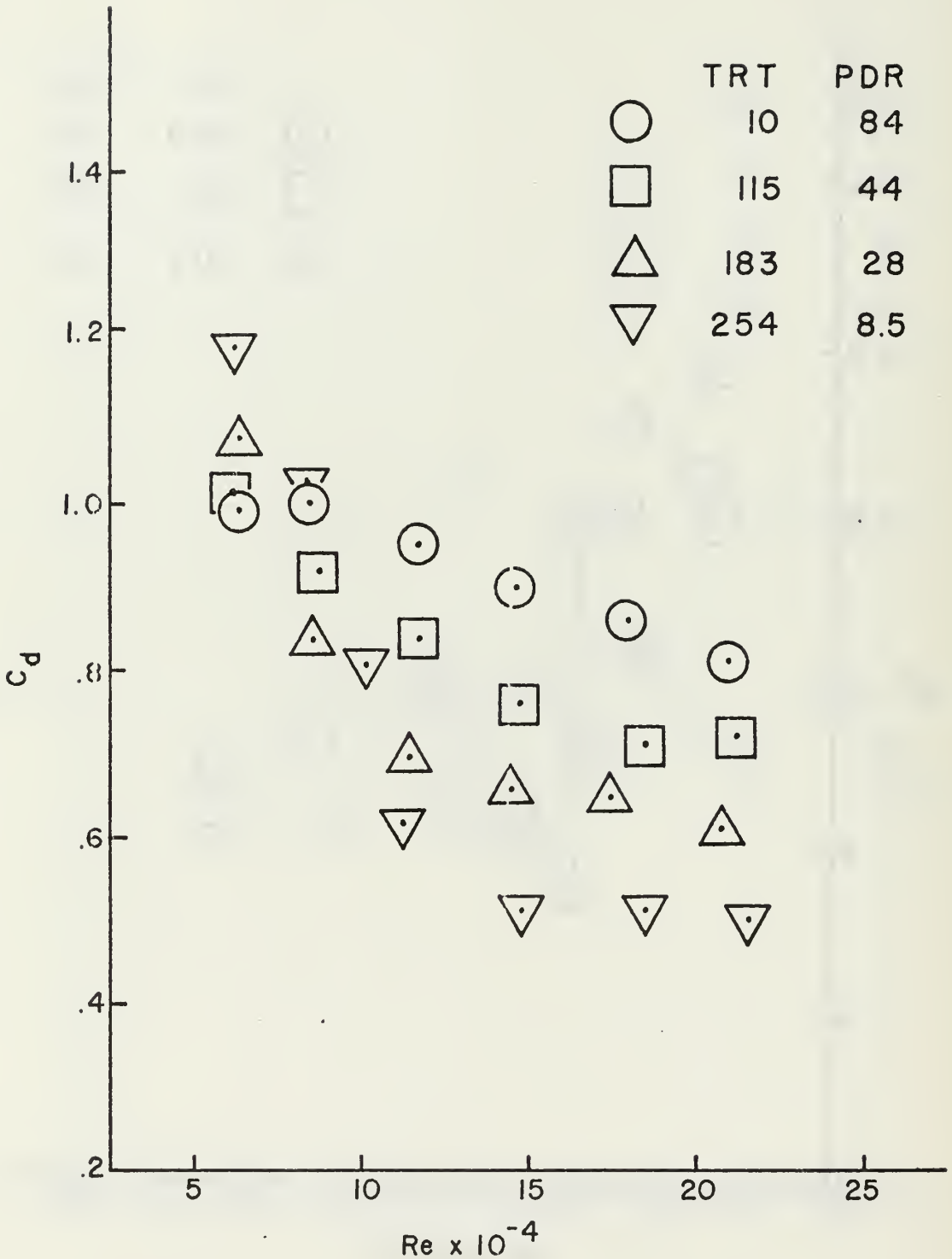

FIG. 22 C_d VERSUS Re
1 in. DIAMETER CYLINDER IN
25 WPPM DILUTE SOLUTIONS

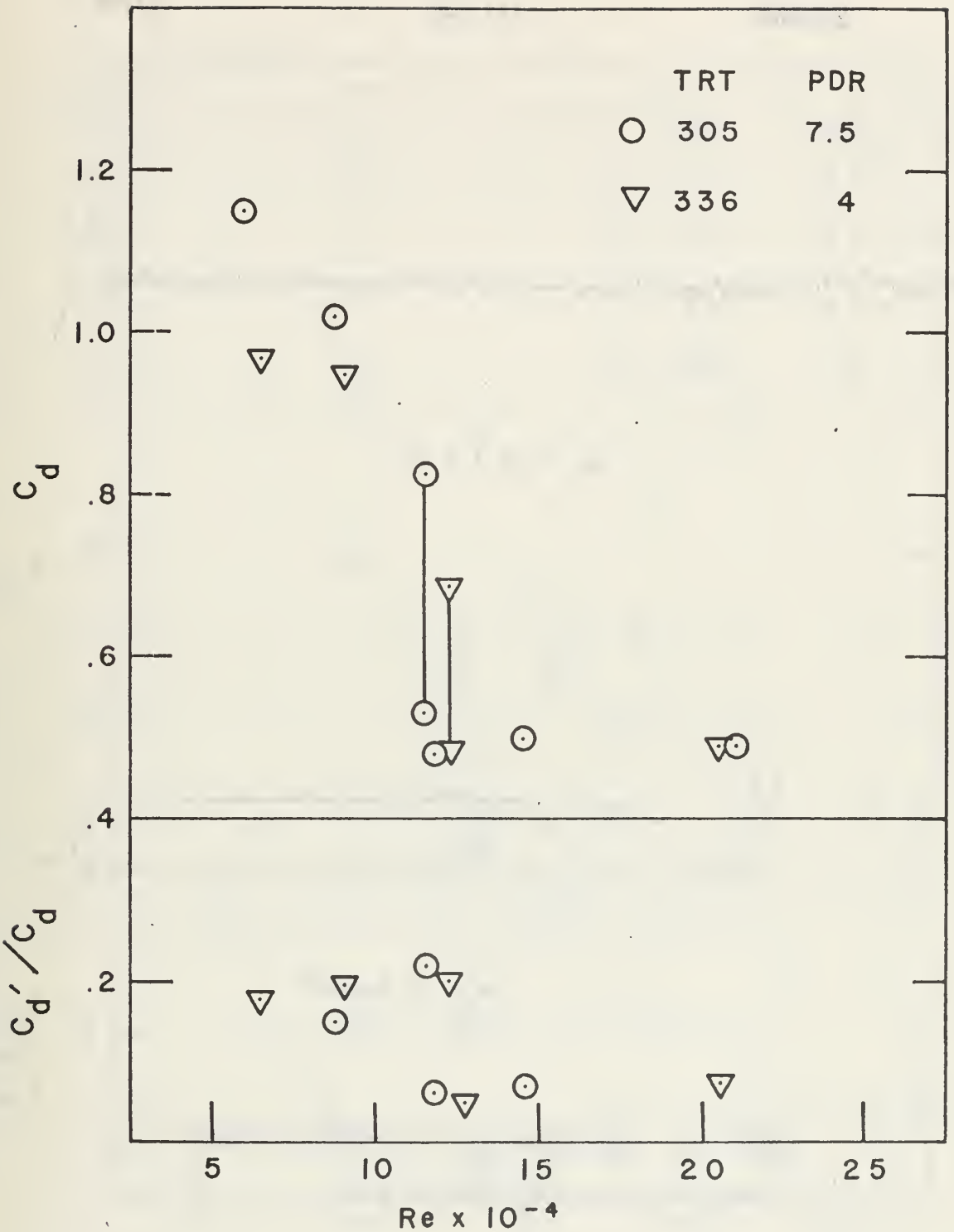

FIG. 23 CRITICAL TRANSITION IN
25 WPPM SOLUTION FOR 1 in. CYLINDER

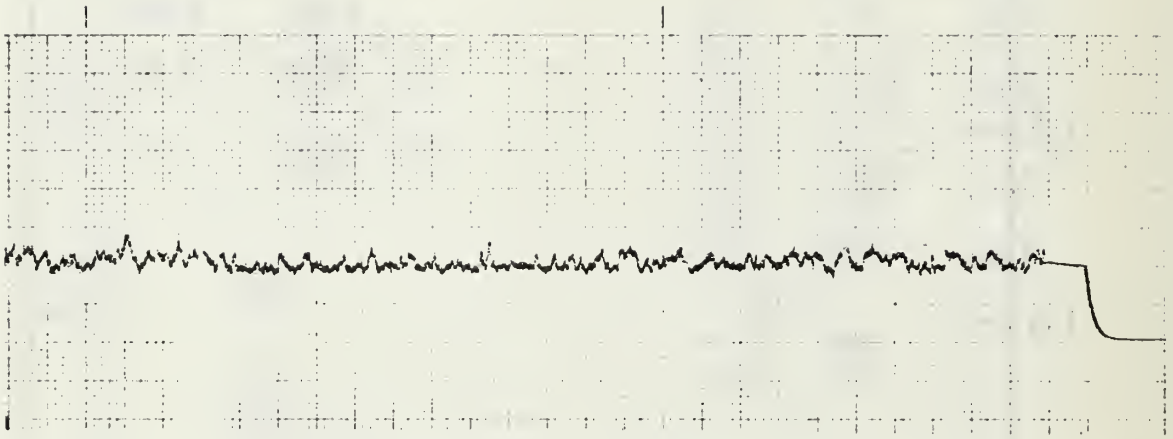

$Re_c = 12.1 \times 10^4$

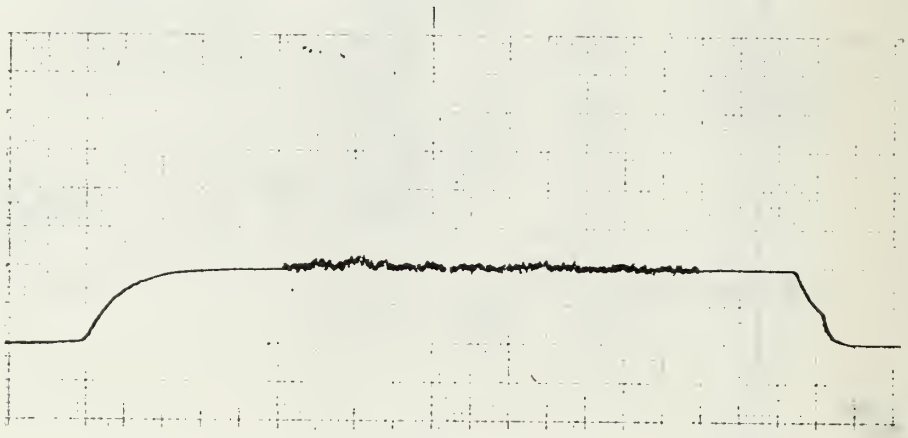

$Re = 12.4 \times 10^4$

FIG. 24 OSCILLOGRAPH TRACINGS OF DRAG FORCE AT $Re = Re_c$ and $Re > Re_c$

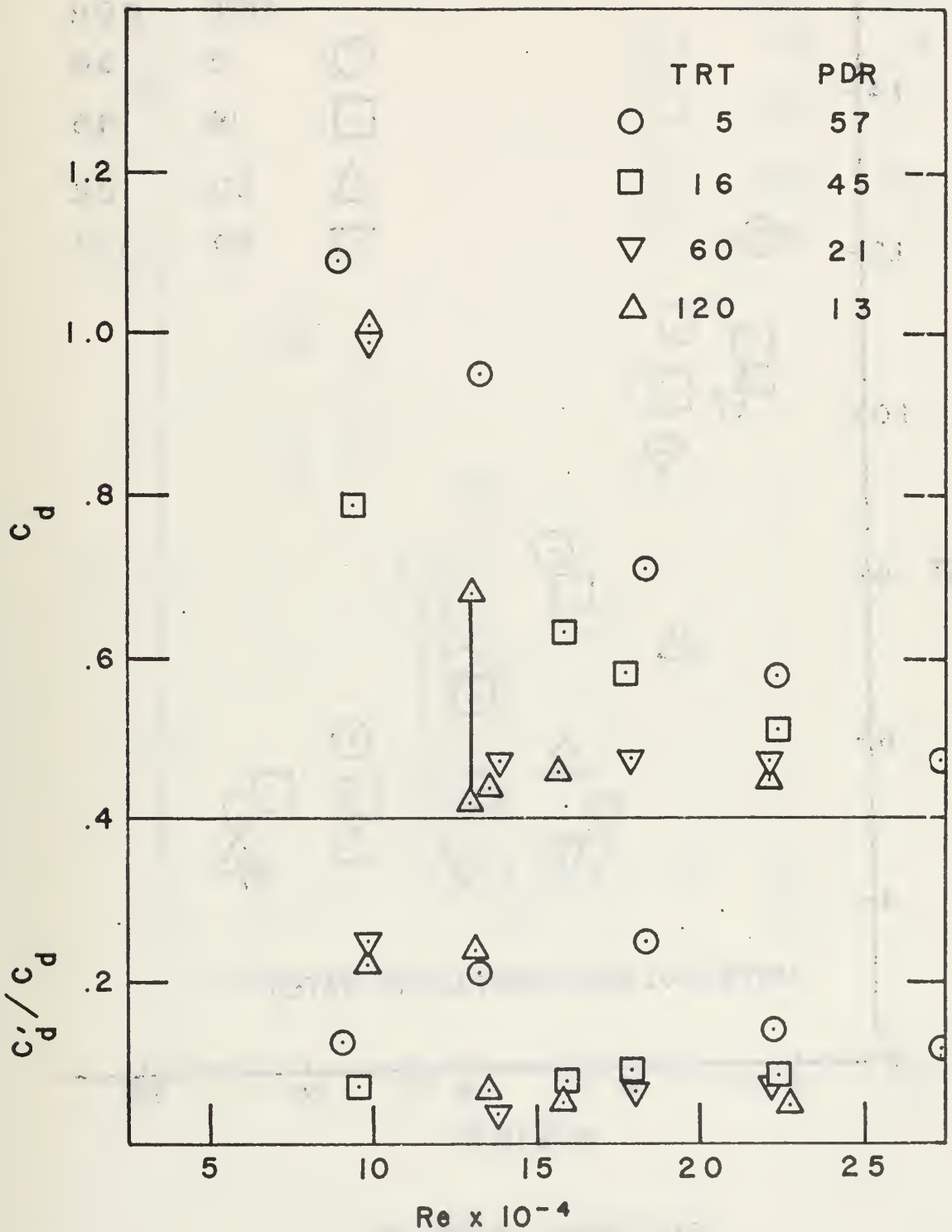

FIG. 25 CRITICAL TRANSITION IN 5 WPPM SOLUTION FOR 1-1/2 in. CYLINDER

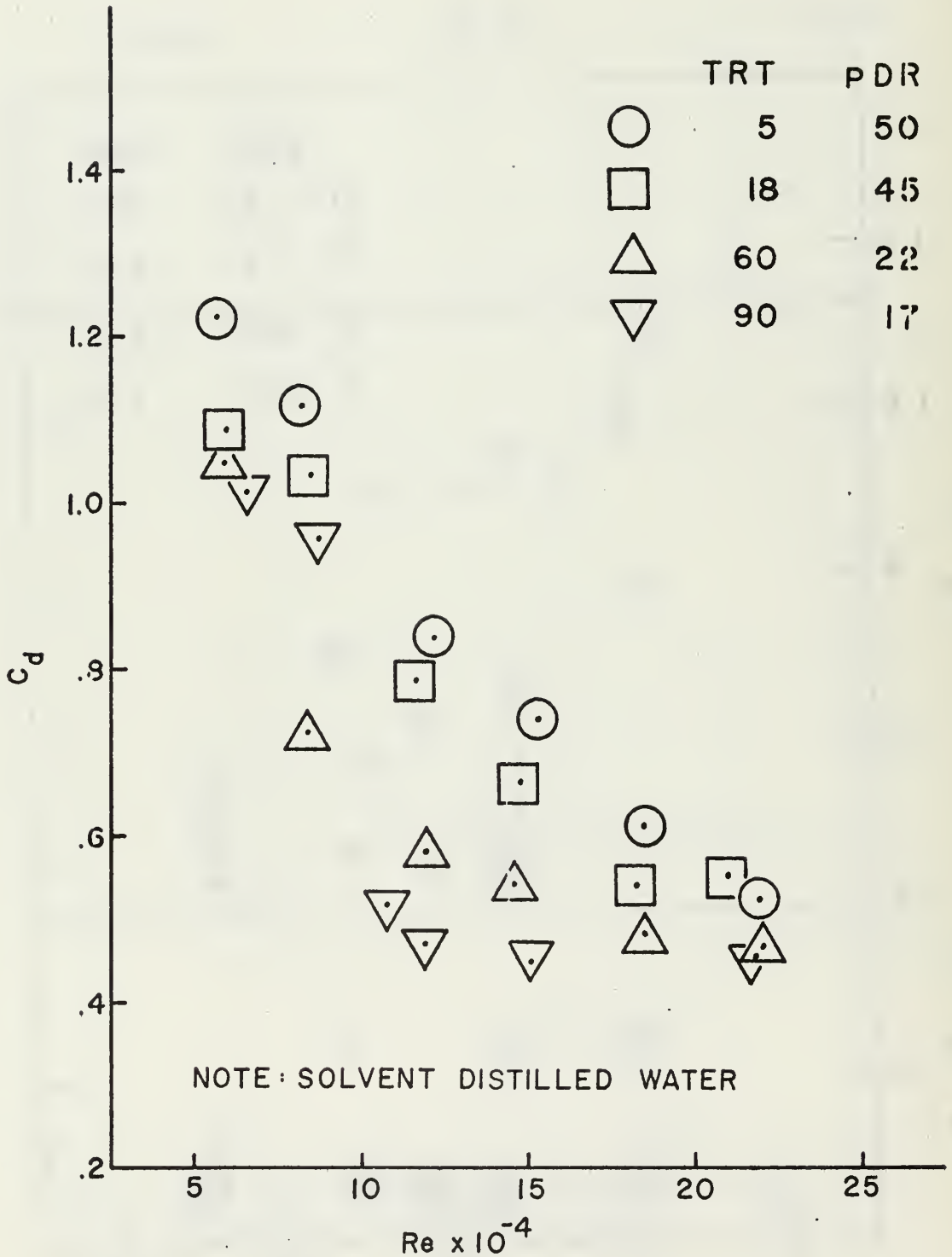

FIG. 26 C_d VERSUS Re

1 in. DIAMETER CYLINDER IN 5 WPPM SOLUTION

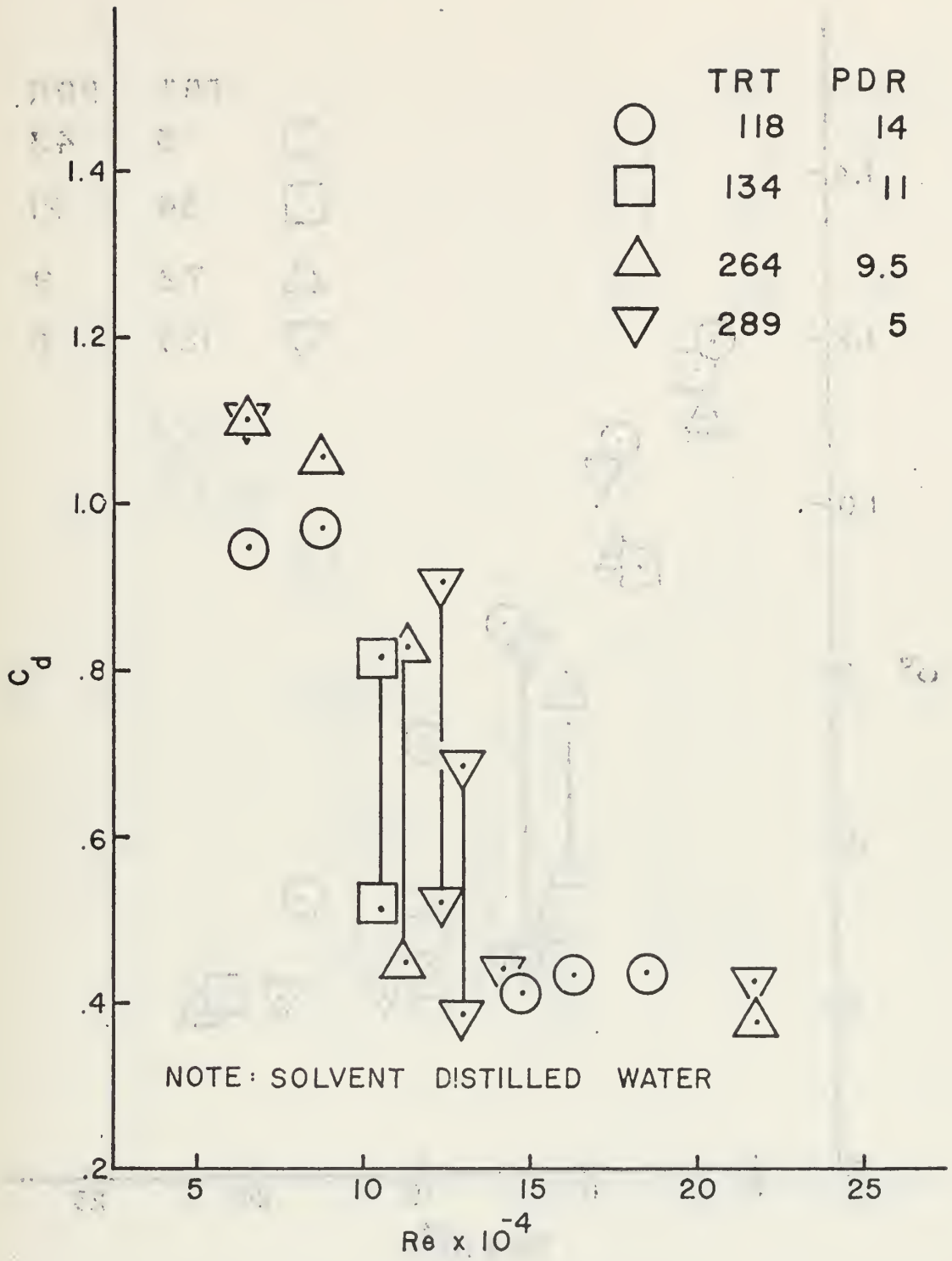

FIG. 27 C_d VERSUS Re
1 in. DIAMETER CYLINDER IN 5 WPPM SOLUTION

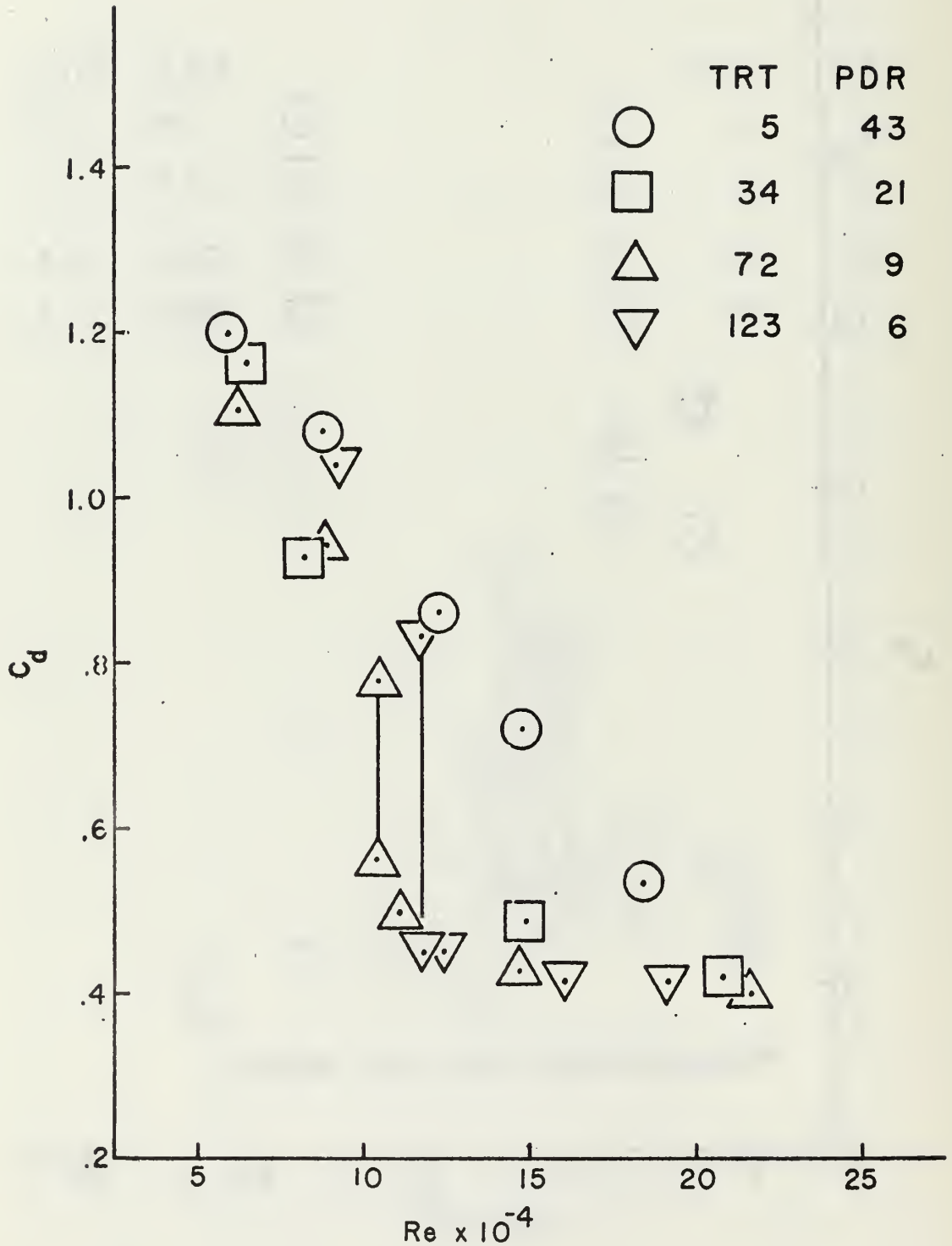

FIG. 28 C_d VERSUS Re

1 in. DIAMETER CYLINDER IN 5 WPPM SOLUTION

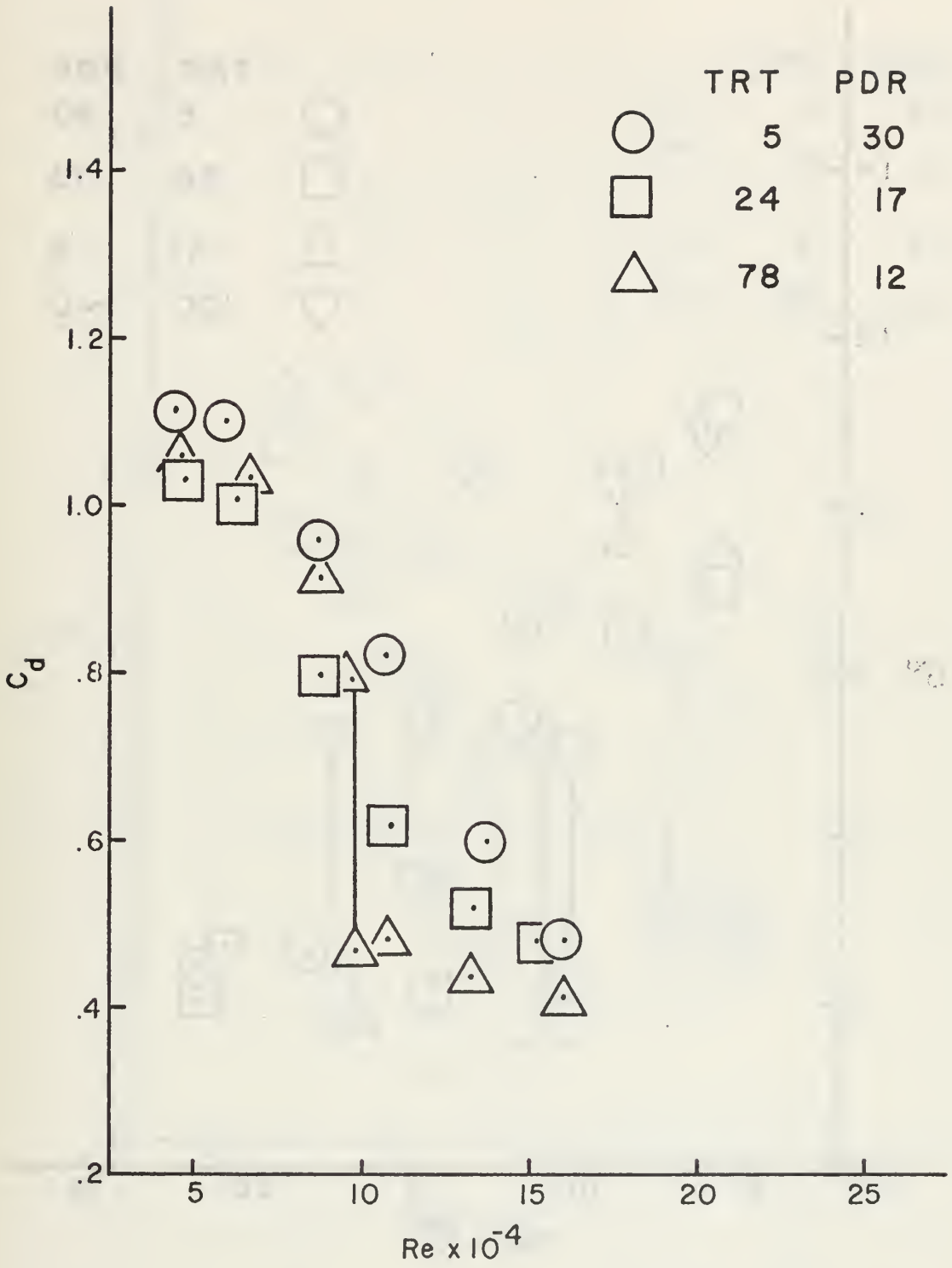

FIG. 29 C_d VERSUS Re
3/4 in. DIAMETER CYLINDER IN 5 WPPM
SOLUTION

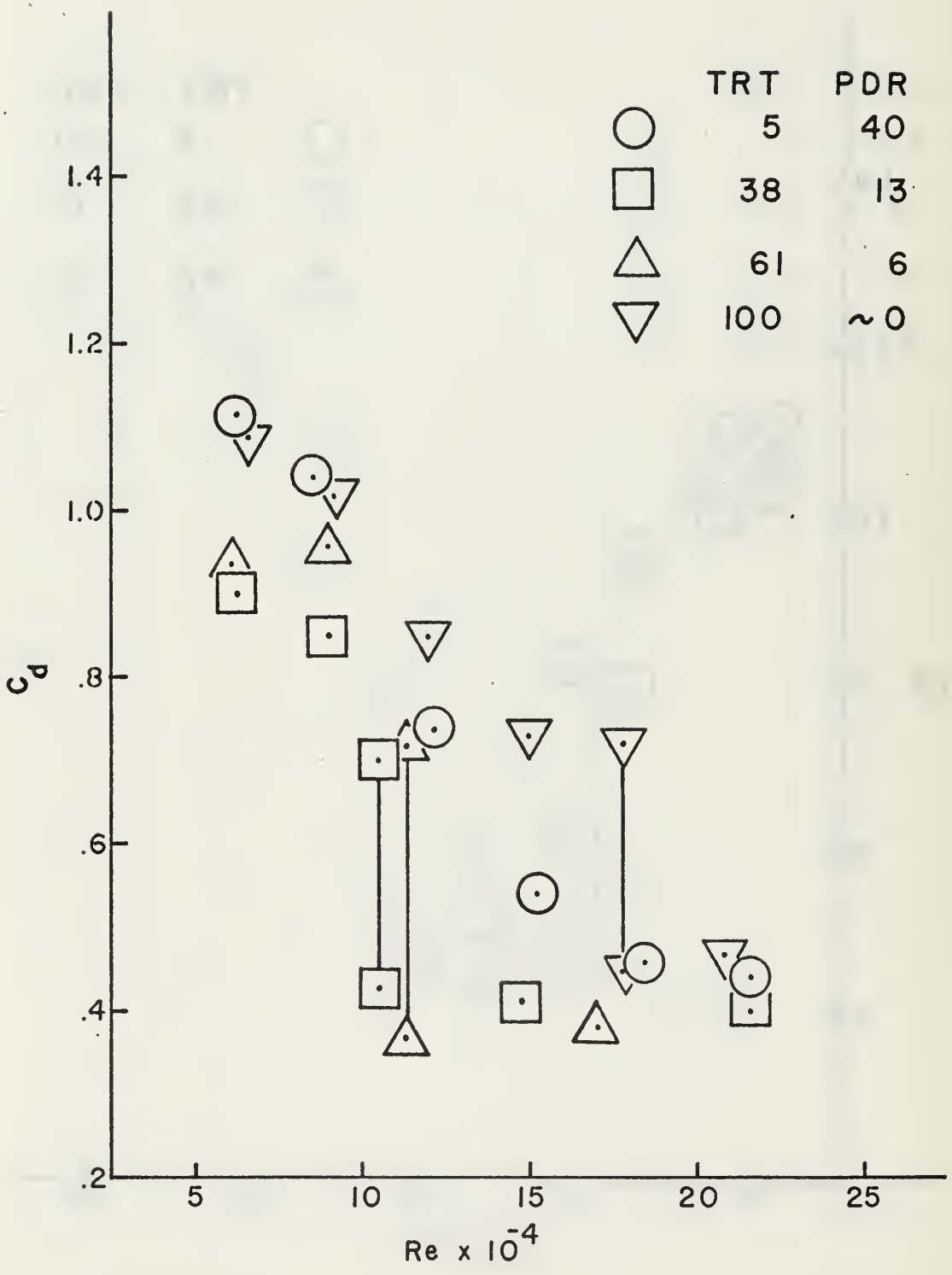

FIG. 30 C_d VERSUS Re

1 in. DIAMETER CYLINDER IN 2.5

WPPM SOLUTION

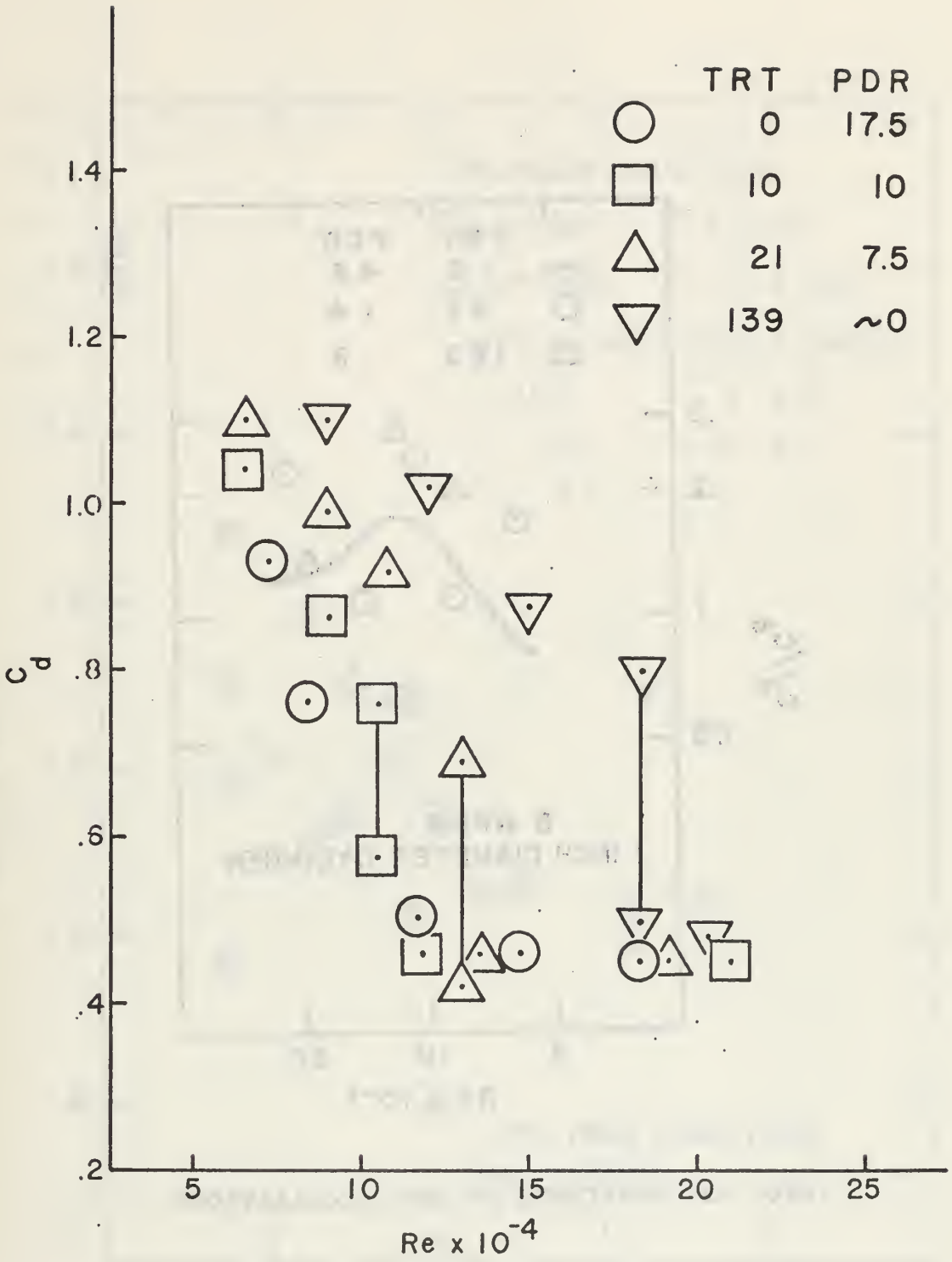

FIG. 31 C_d VERSUS Re

1 in. DIAMETER CYLINDER IN 1.0 WPPM SOLUTION

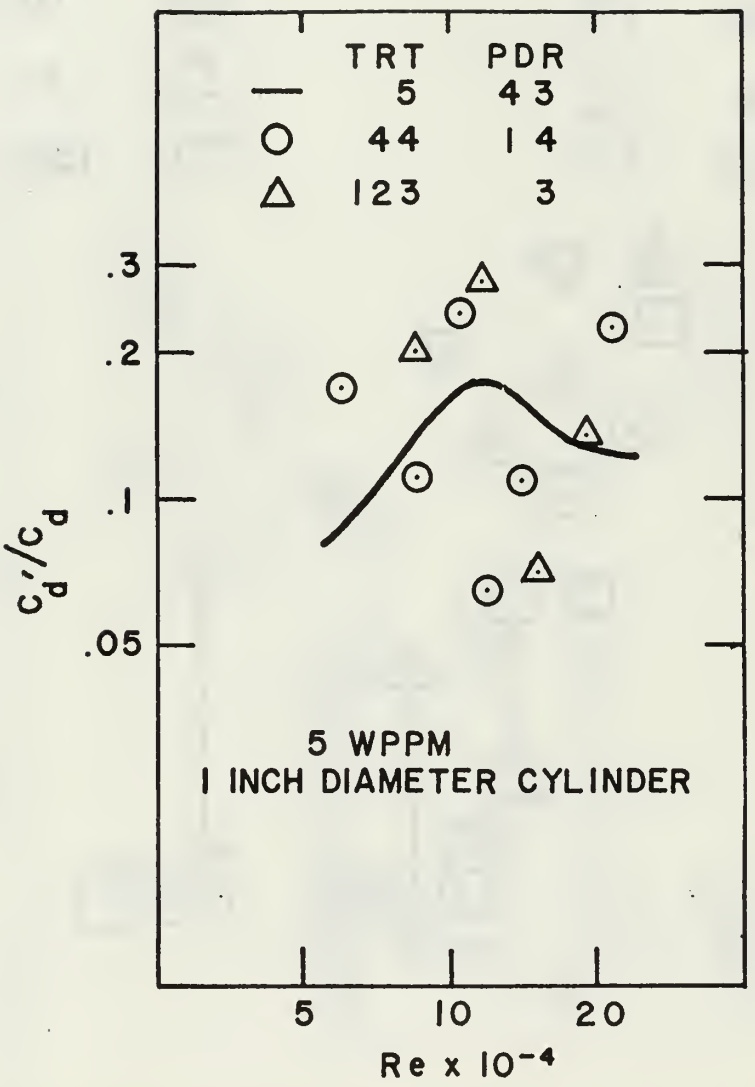

FIG. 32 AMPLITUDE OF DRAG OSCILLATIONS

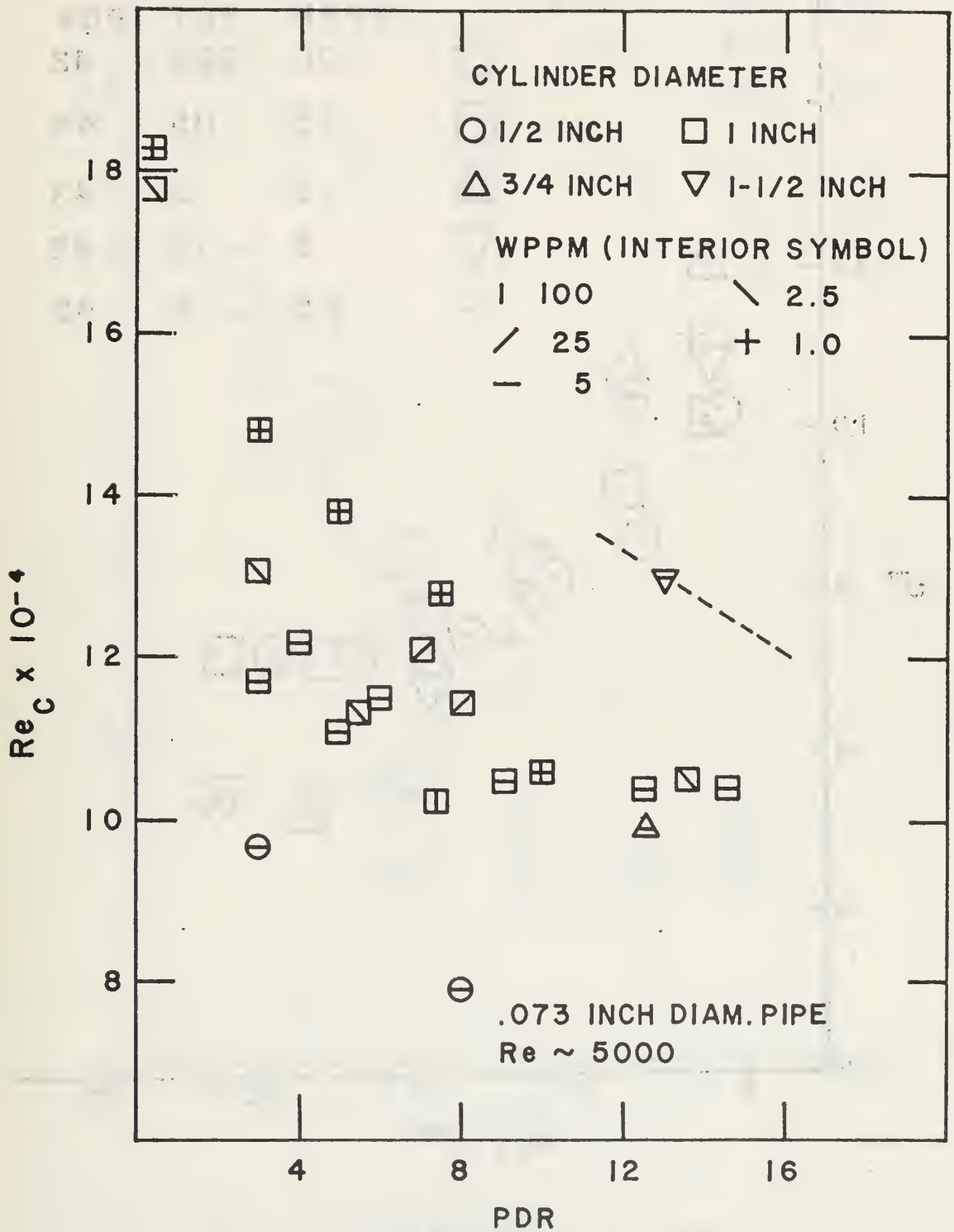

FIG. 33 CRITICAL Re VERSUS PDR

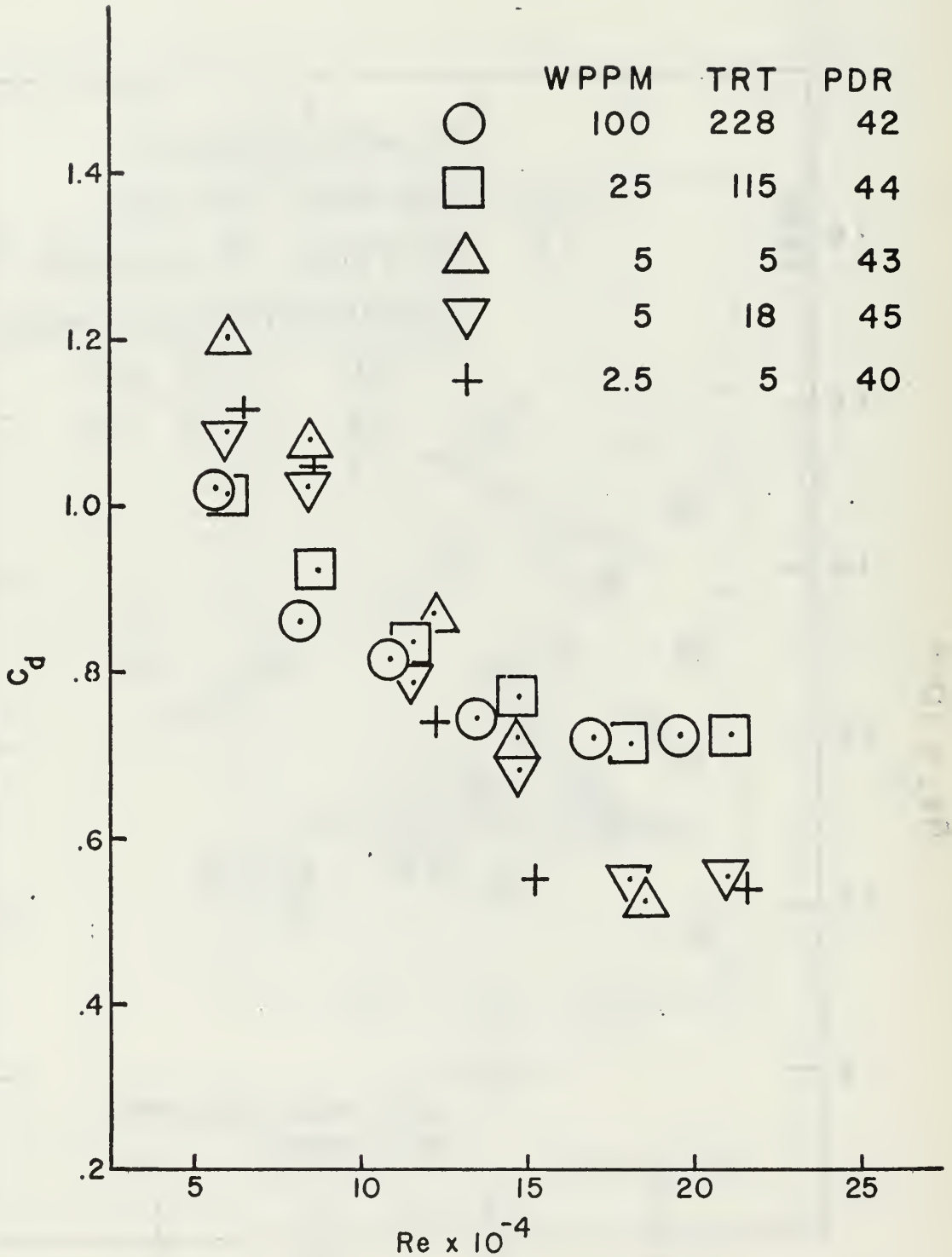

FIG. 34 C_d VERSUS Re
1 in. DIAMETER CYLINDER
(PDR≈45)

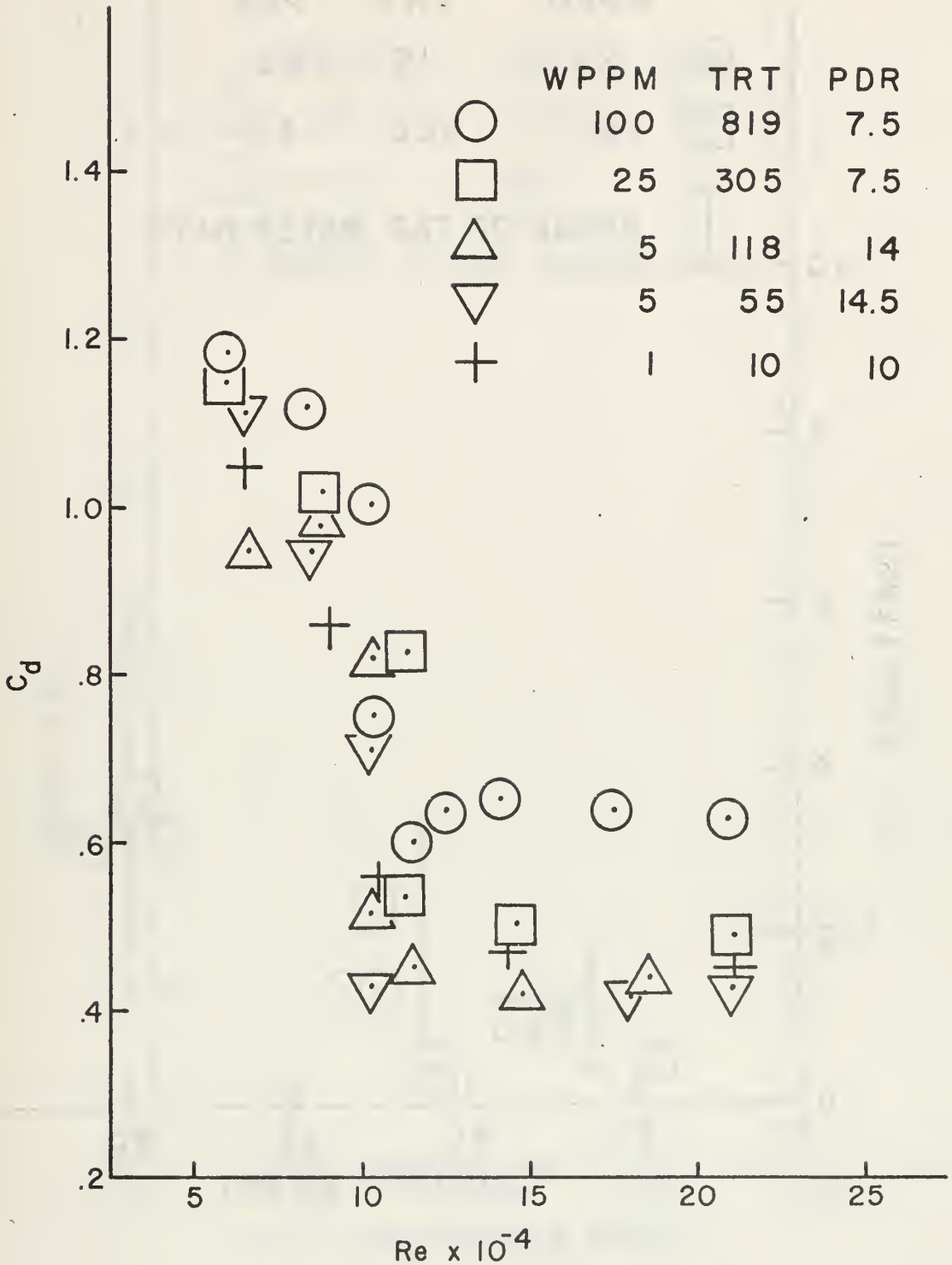

FIG. 35 C_d VERSUS Re

THE FIRST OBSERVATION OF THE CRITICAL REGION WITH 1 in DIAMETER CYLINDER

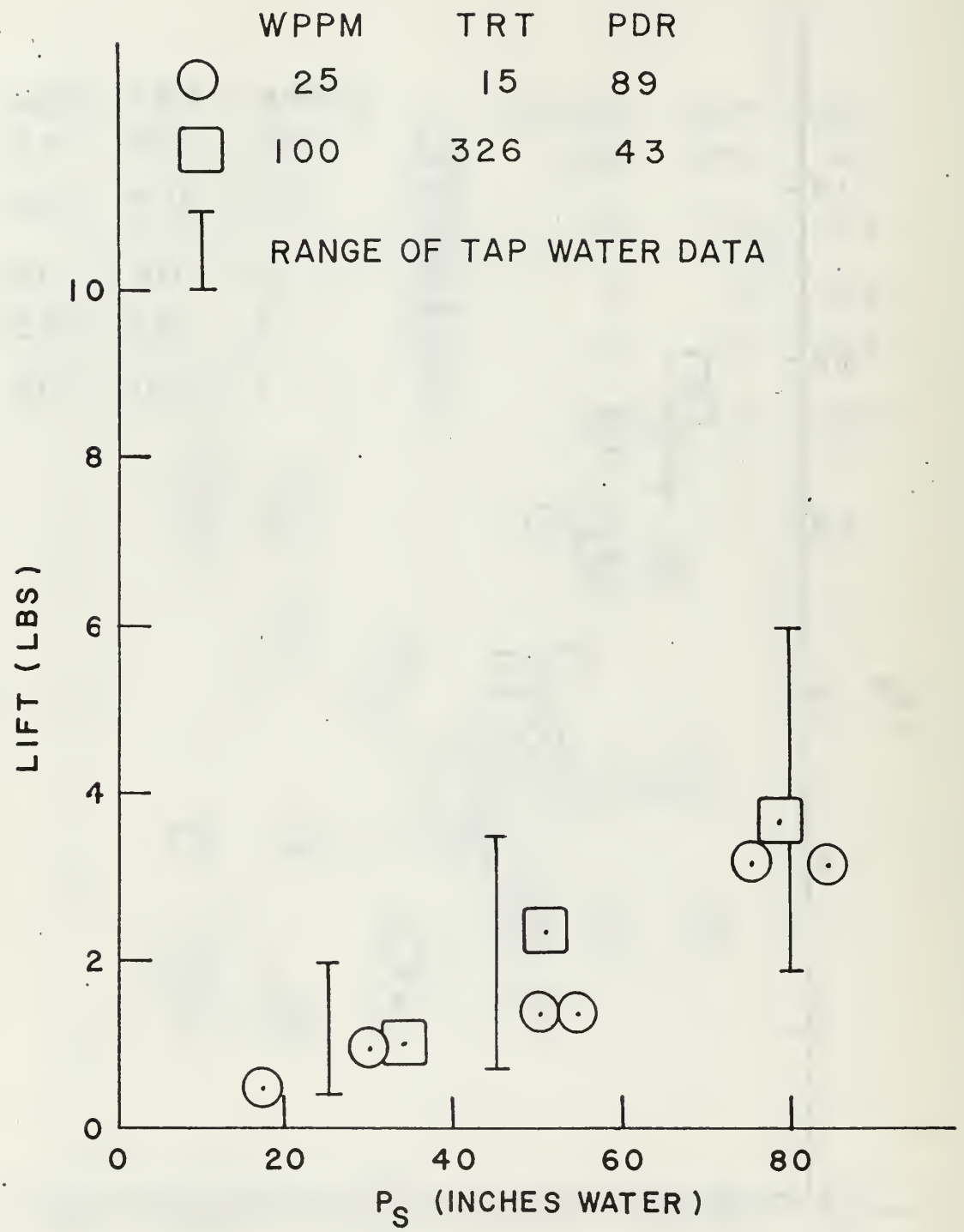

FIG. 36 LIFT VERSUS P_s

α = 0 deg. (Nominal)

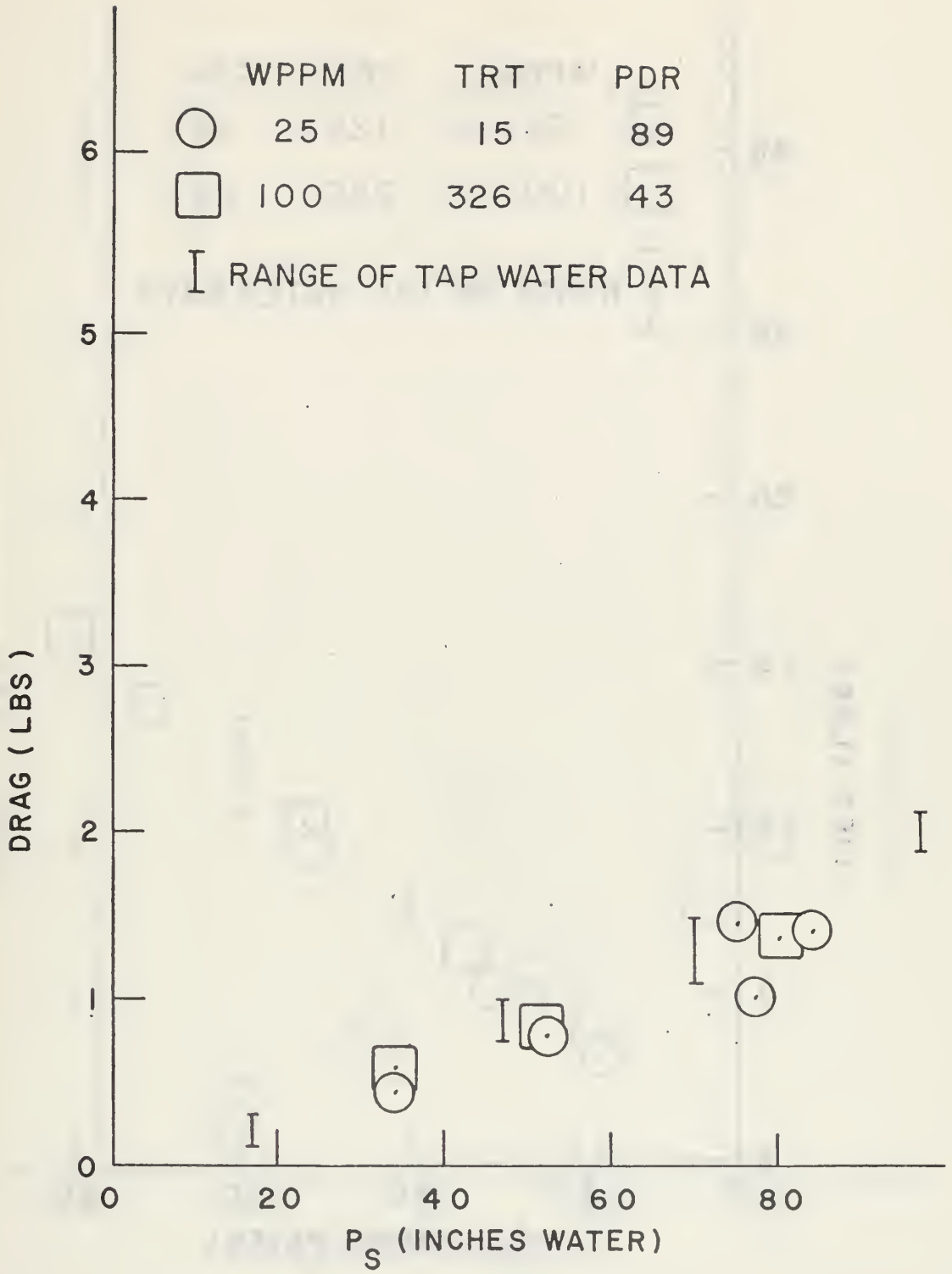

FIG. 37 DRAG VERSUS P_s

α = 0 deg. (Nominal)

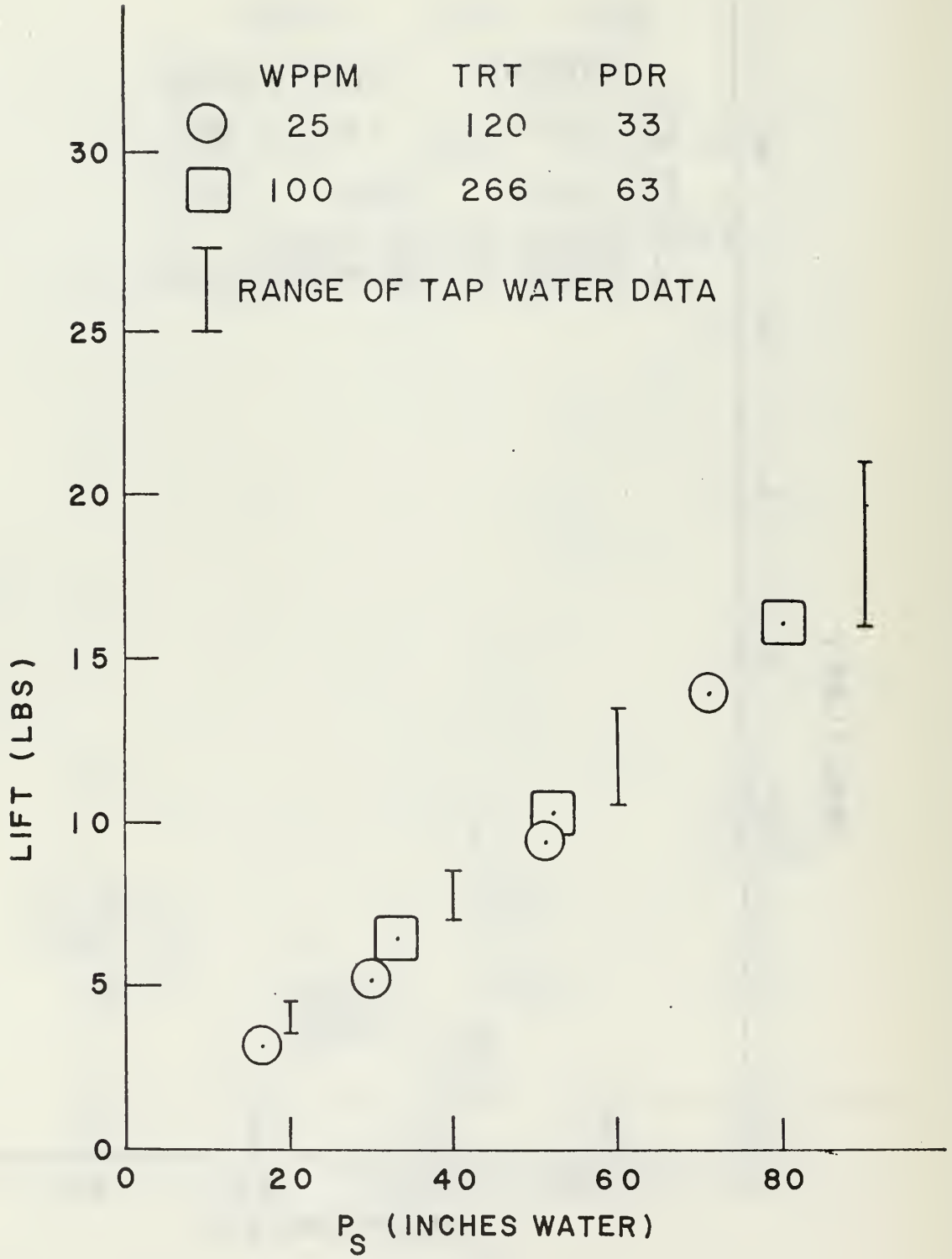

FIG. 38 LIFT VERSUS P_s

α = 3 deg. (Nominal)

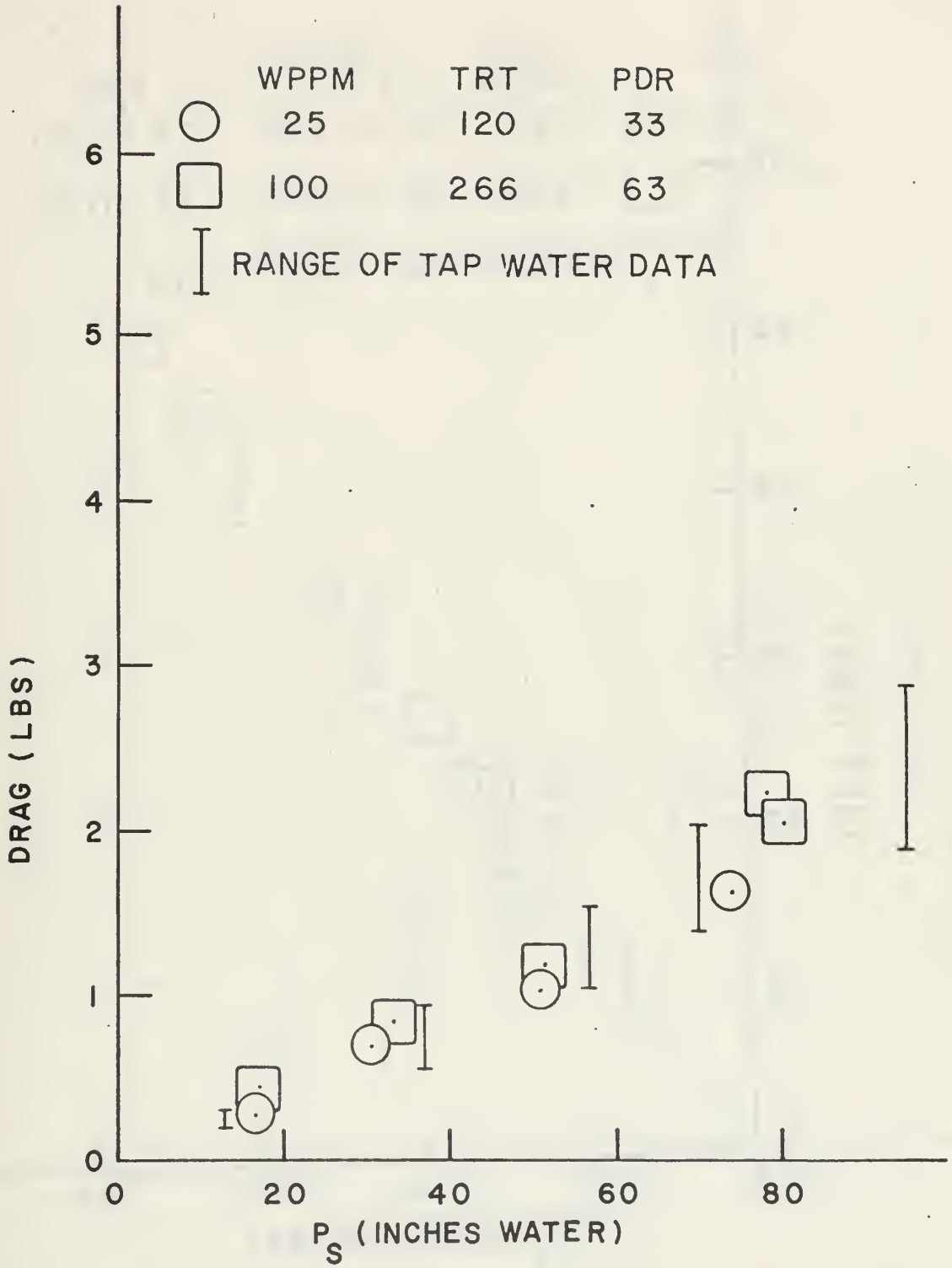

FIG. 39 DRAG VERSUS P_s

α = 3 deg. (Nominal)

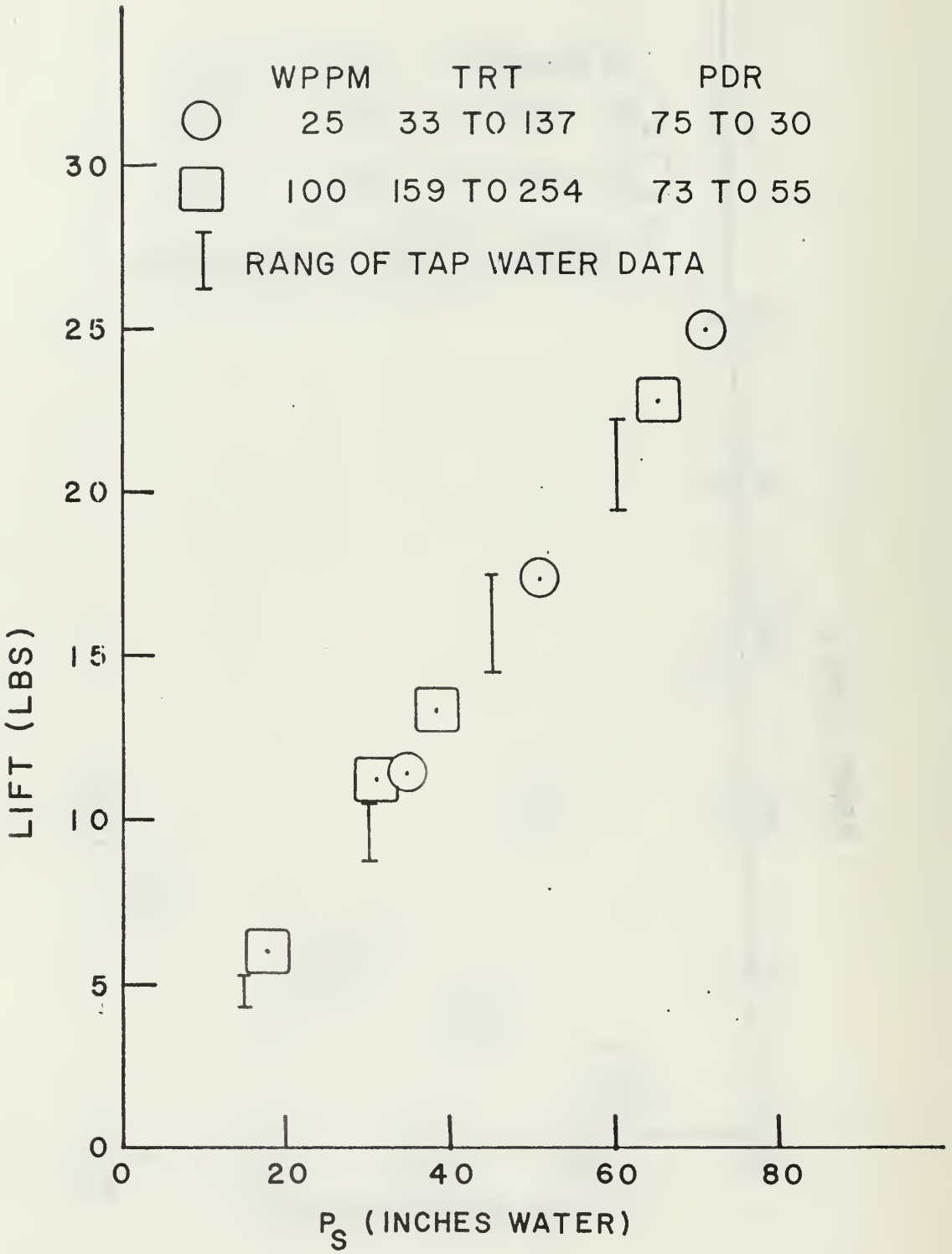

FIG. 40 LIFT VERSUS P_s

α = 6 deg. (Nominal)

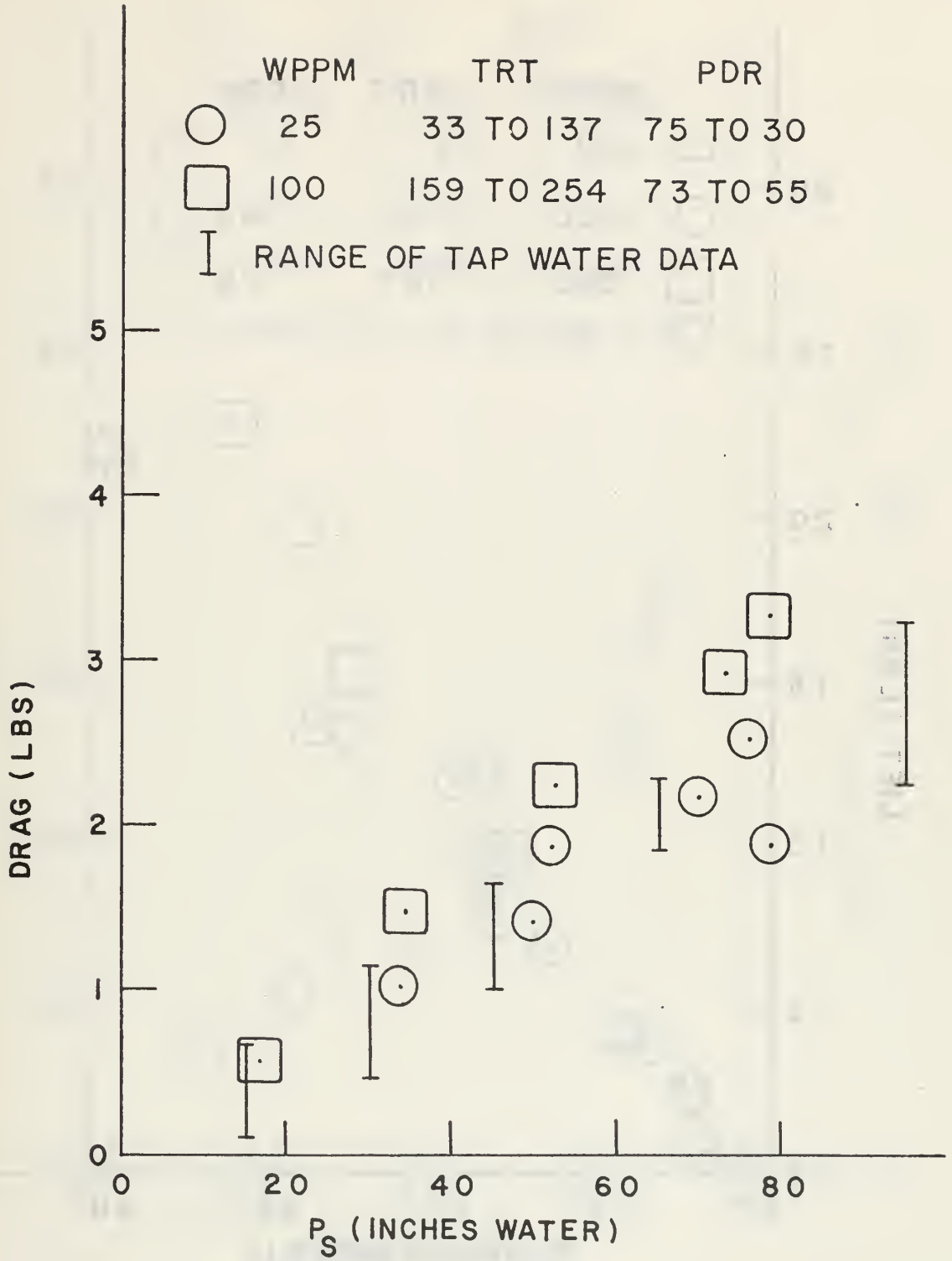

FIG. 41 DRAG VERSUS P_s

α = 6 deg. (Nominal)

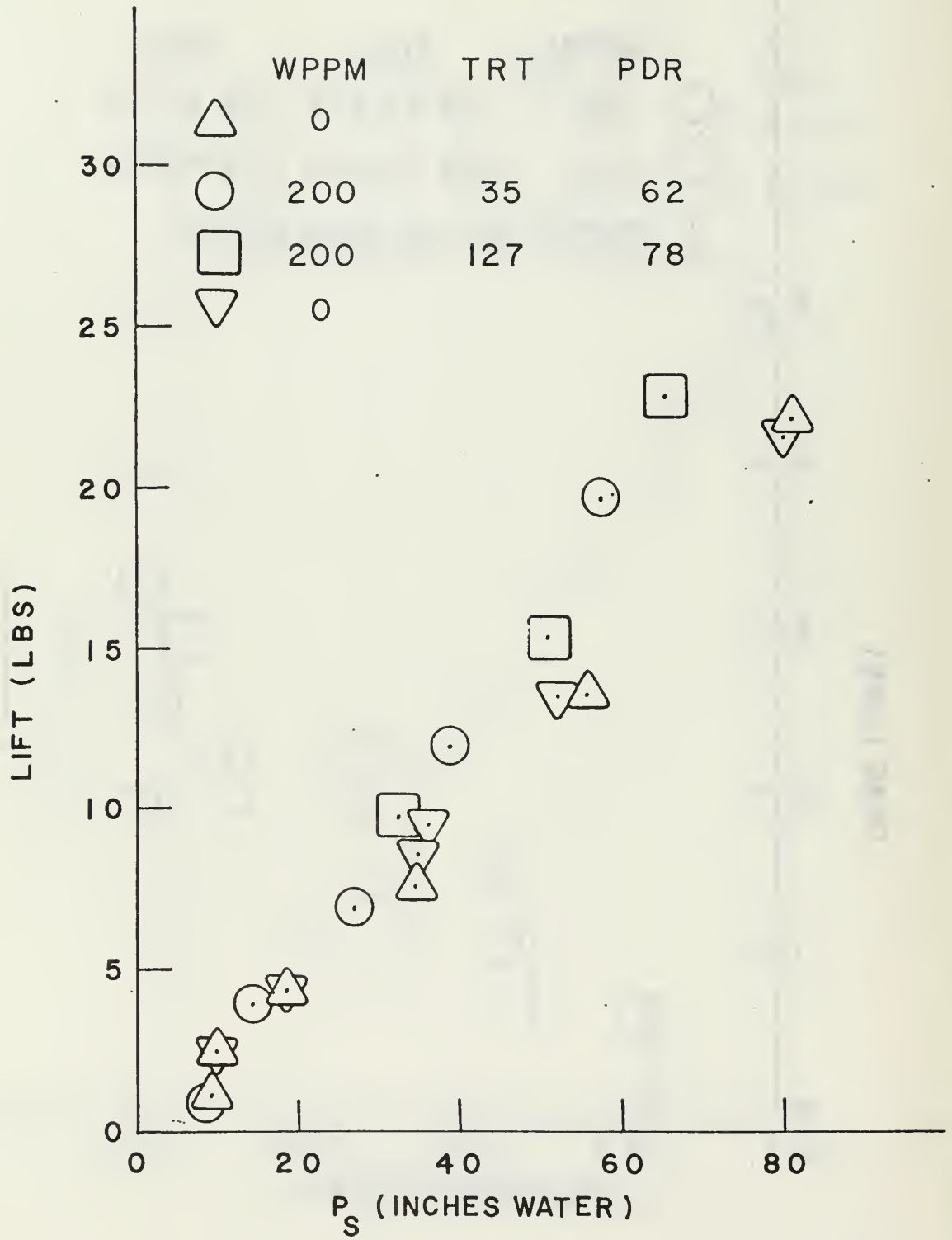

FIG. 42 LIFT VERSUS P_s

α = 4.5 deg. (Measured)

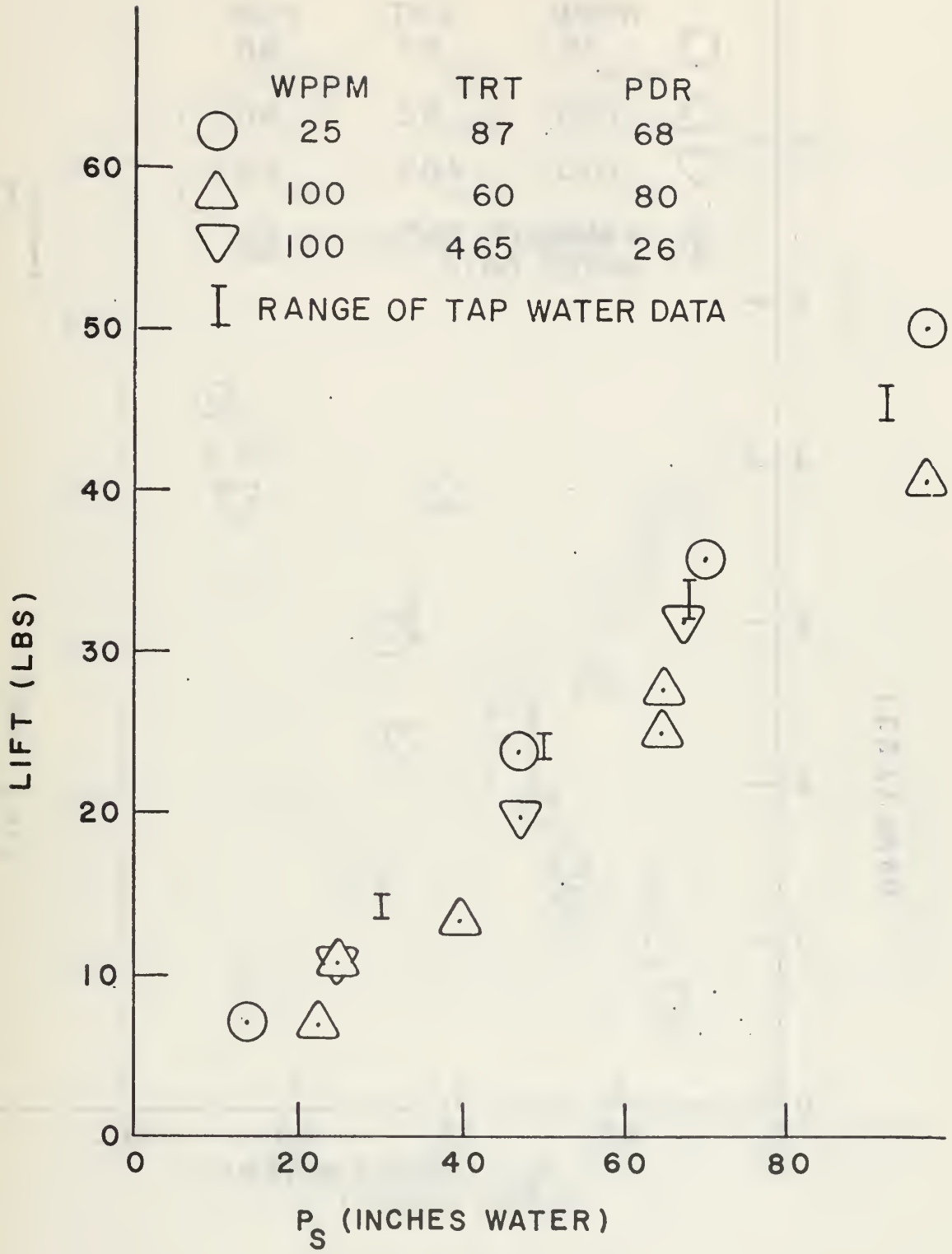

FIG. 43 LIFT VERSUS P_S

α = 9 deg. (Nominal)

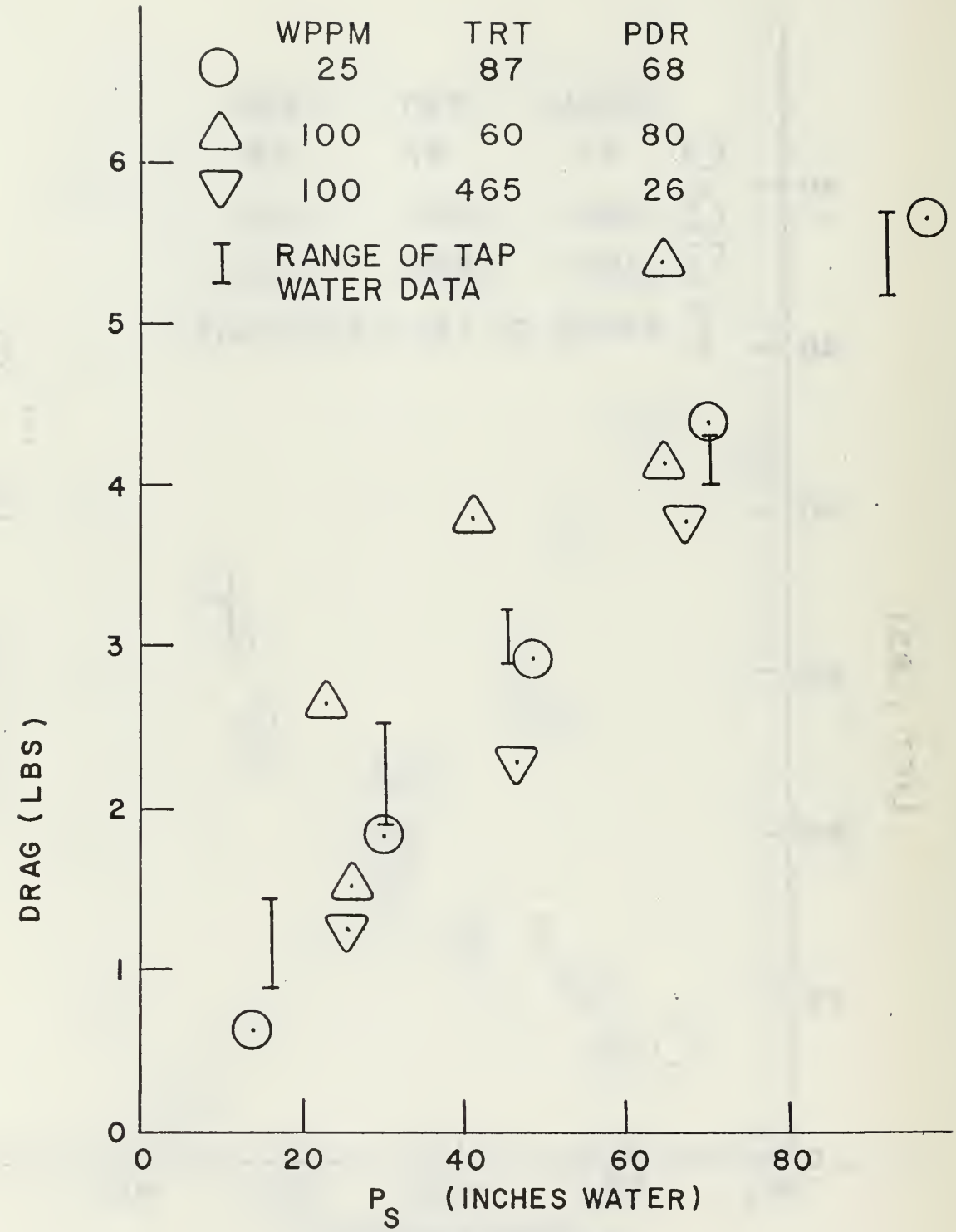

FIG. 44 DRAG VERSUS P_s

α = 9 deg. (Nominal)

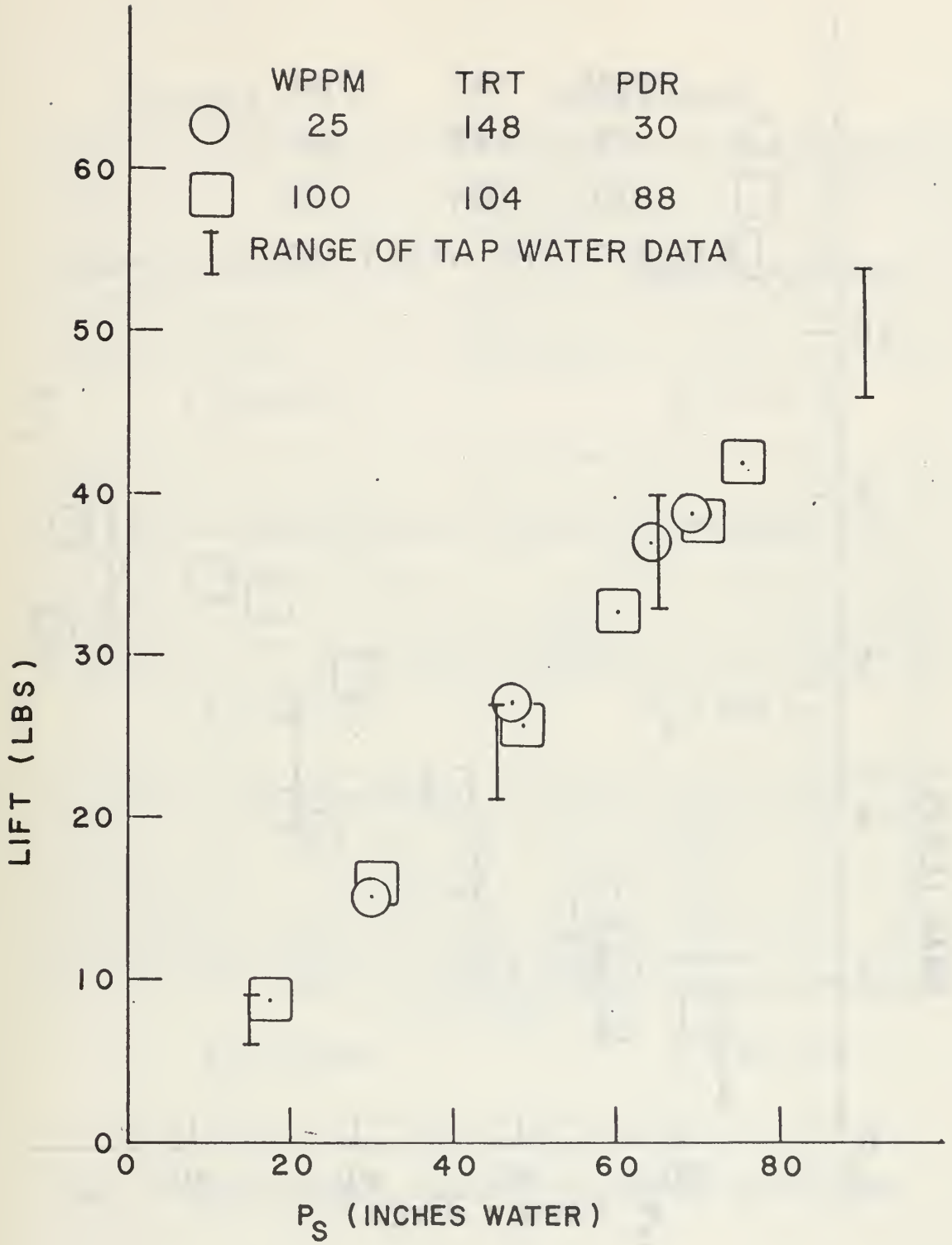

FIG. 45 LIFT VERSUS P_s

α = 12 deg. (Nominal)

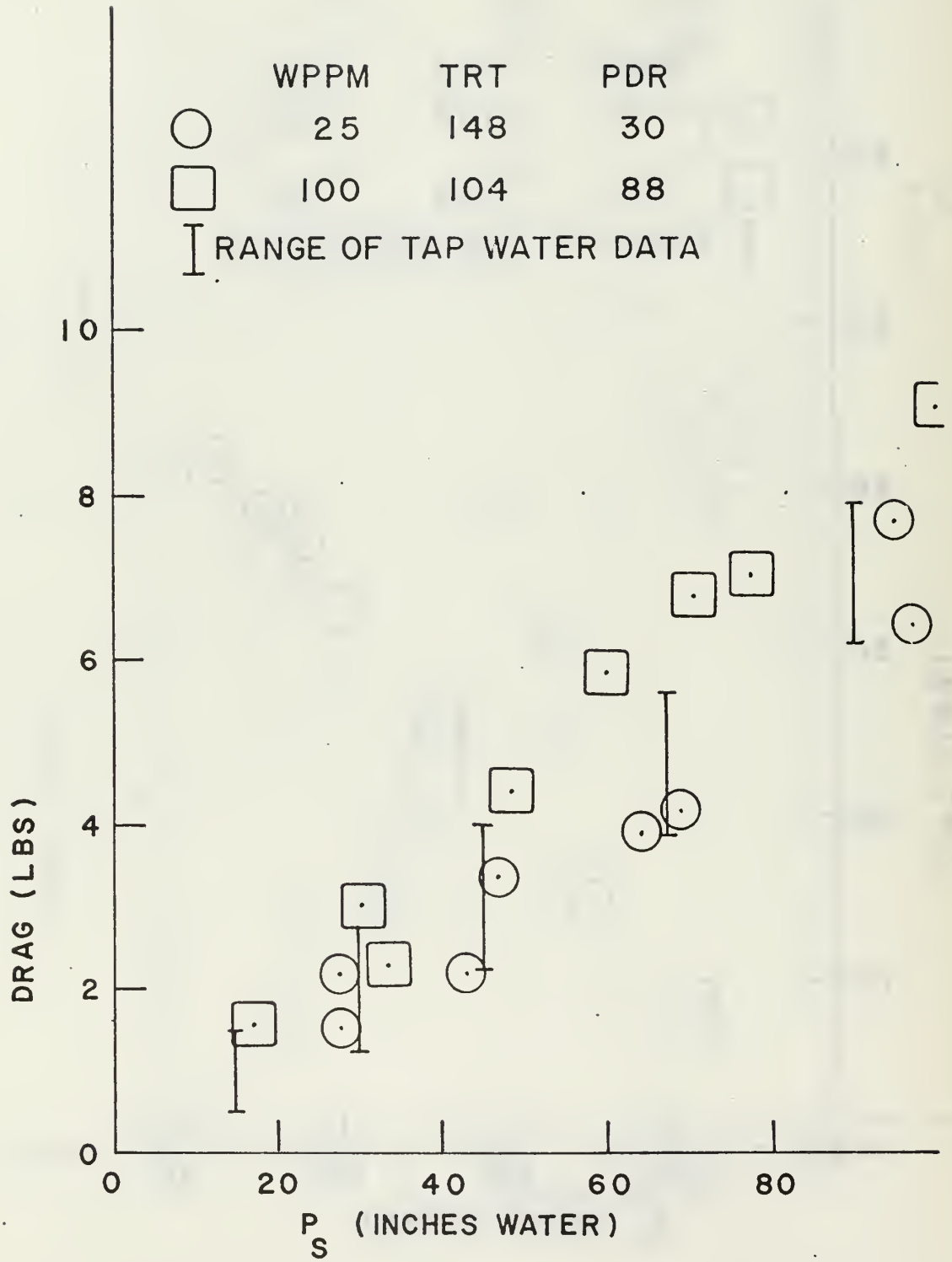

FIG. 46 DRAG VERSUS P_s

α = 12 deg. (Nominal)

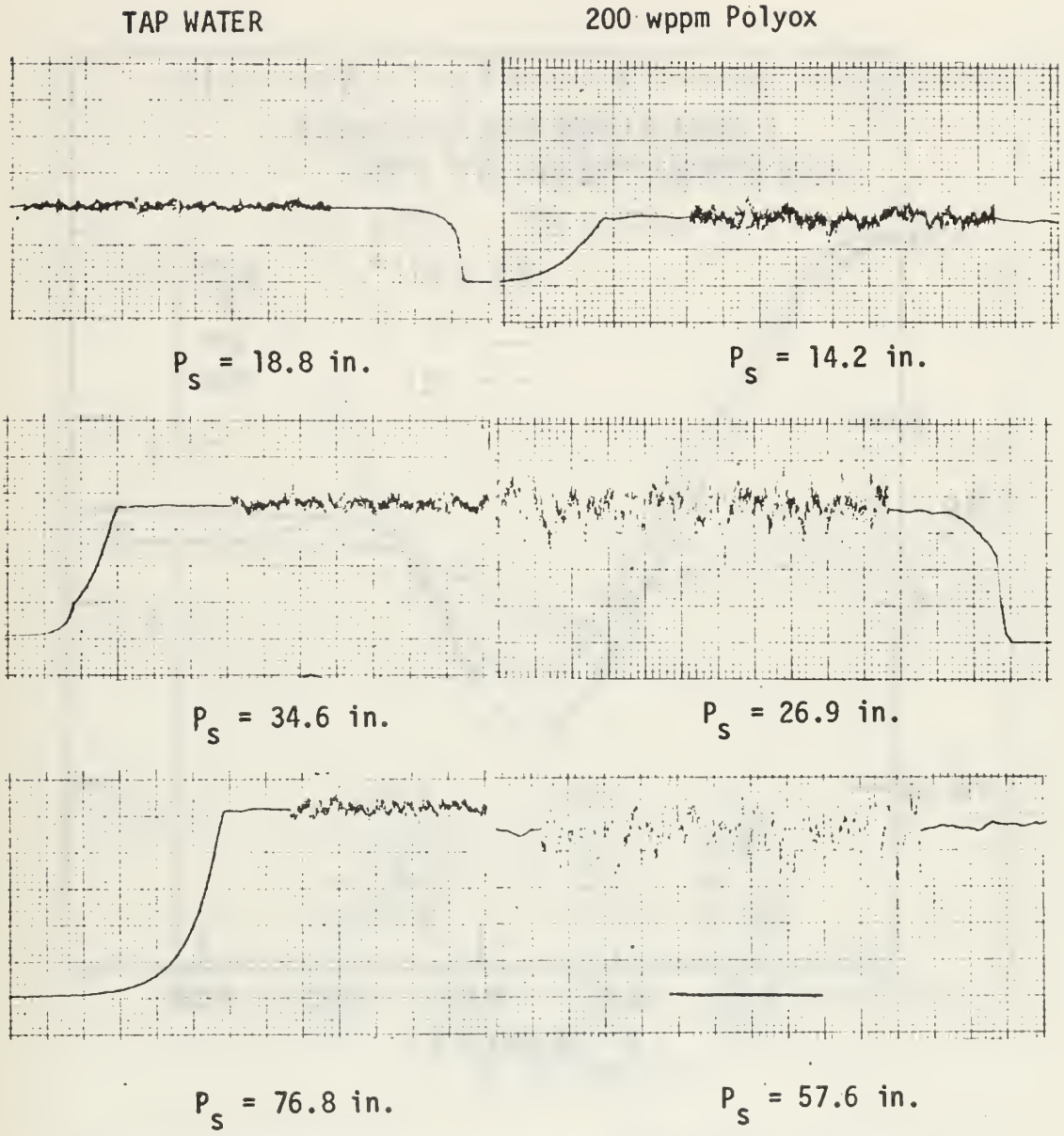

FIG. 47 OSCILLOGRAPH TRACINGS OF DYNAMIC LIFT FORCE

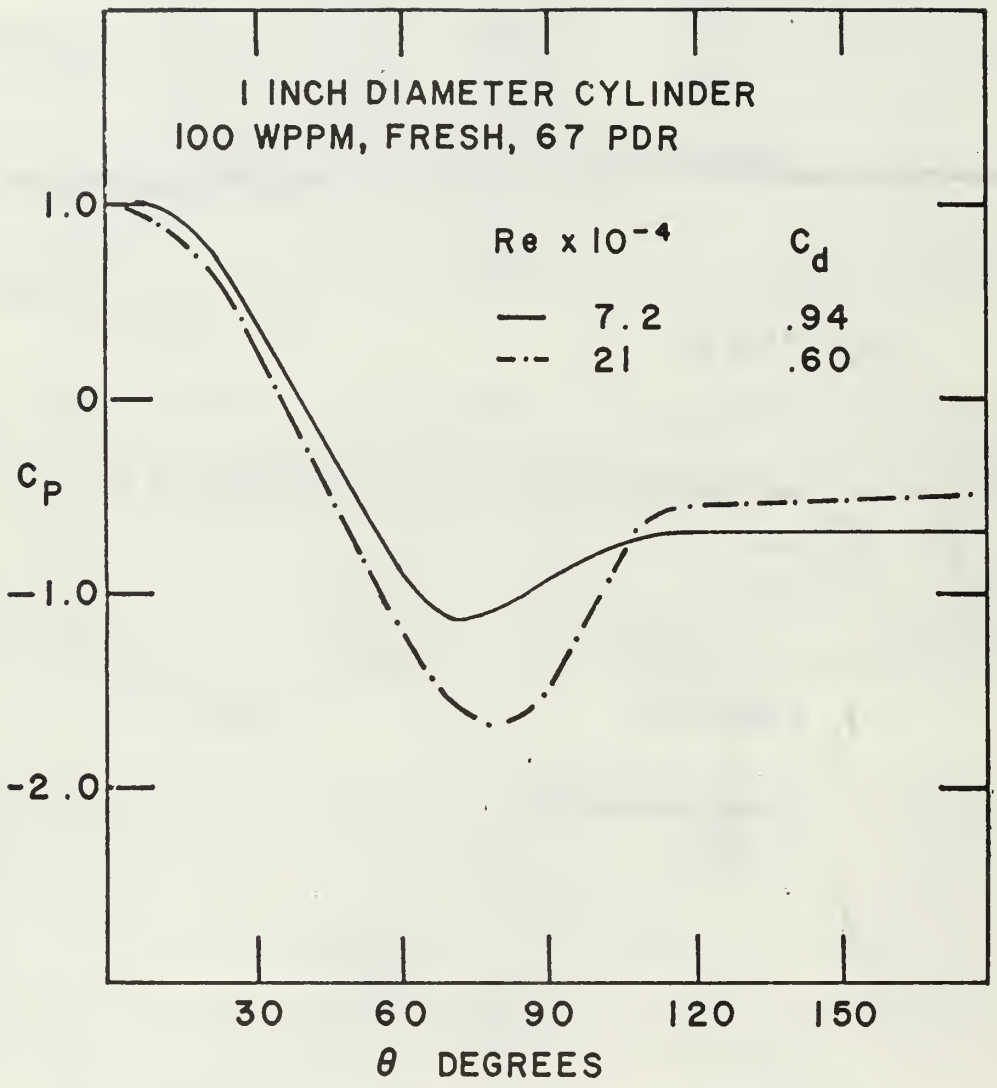

FIG. 48 CHARACTERISTIC PRESSURE DISTRIBUTIONS

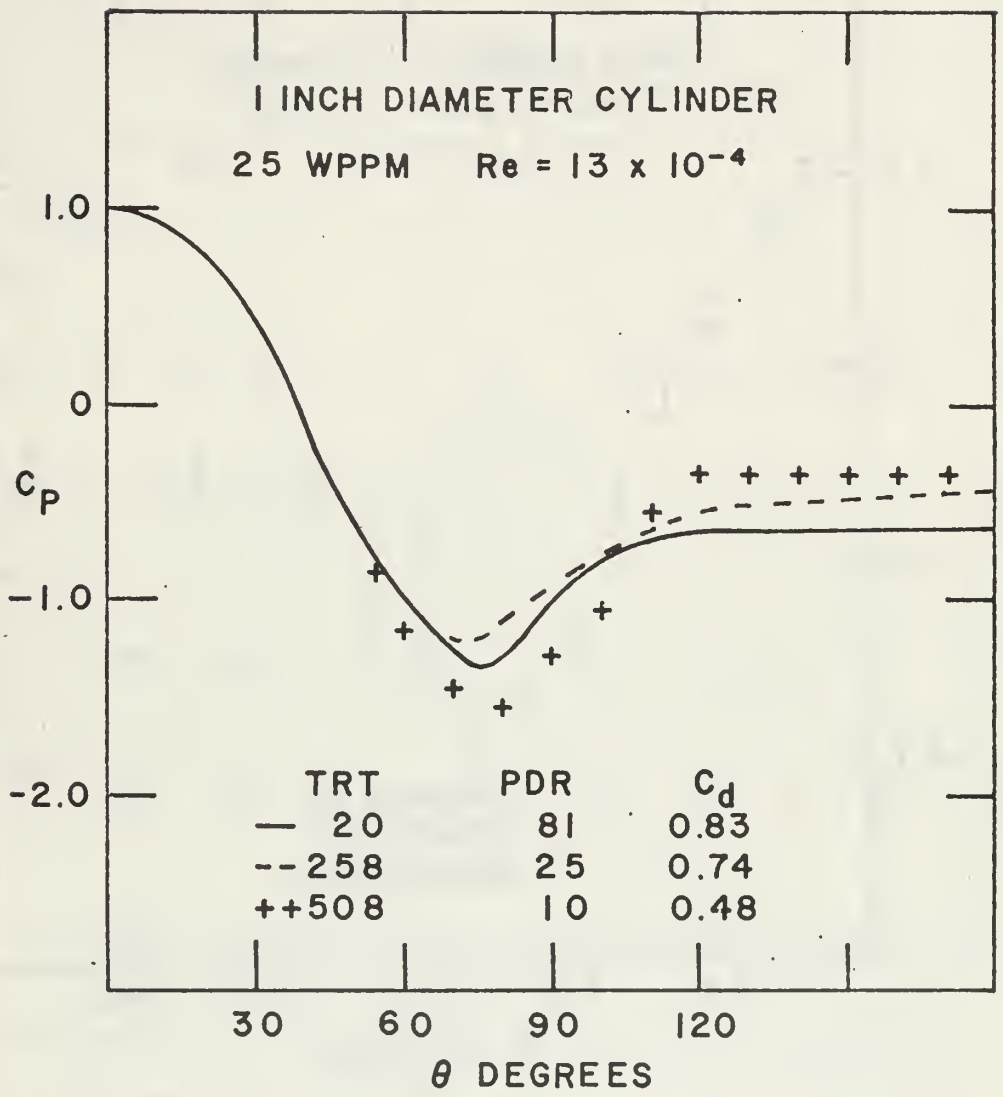

FIG. 49 CHANGE IN PRESSURE DISTRIBUTION AS SOLUTION DEGRADES

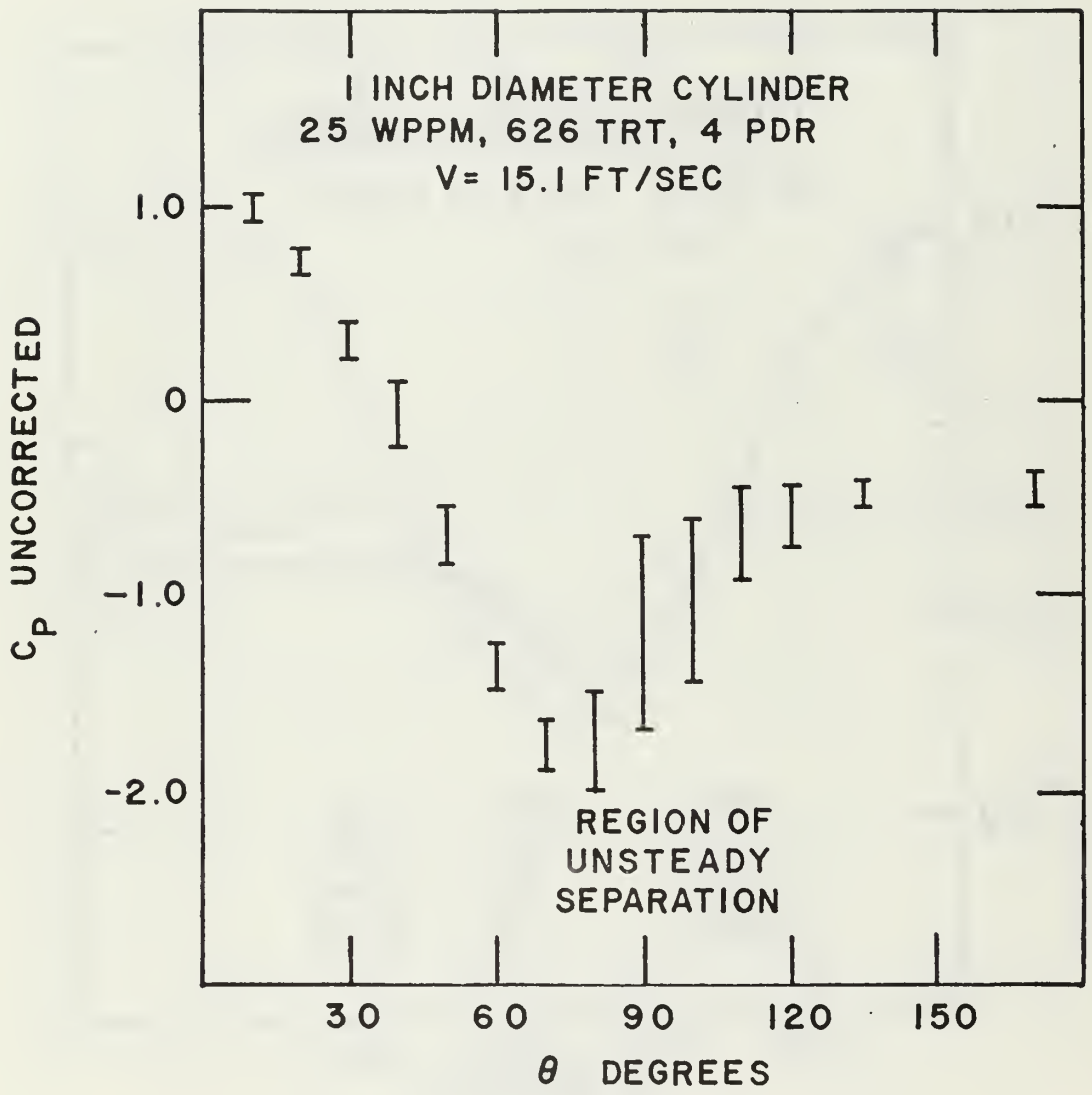

FIG. 50 PRESSURE DISTRIBUTION AT CRITICAL VELOCITY

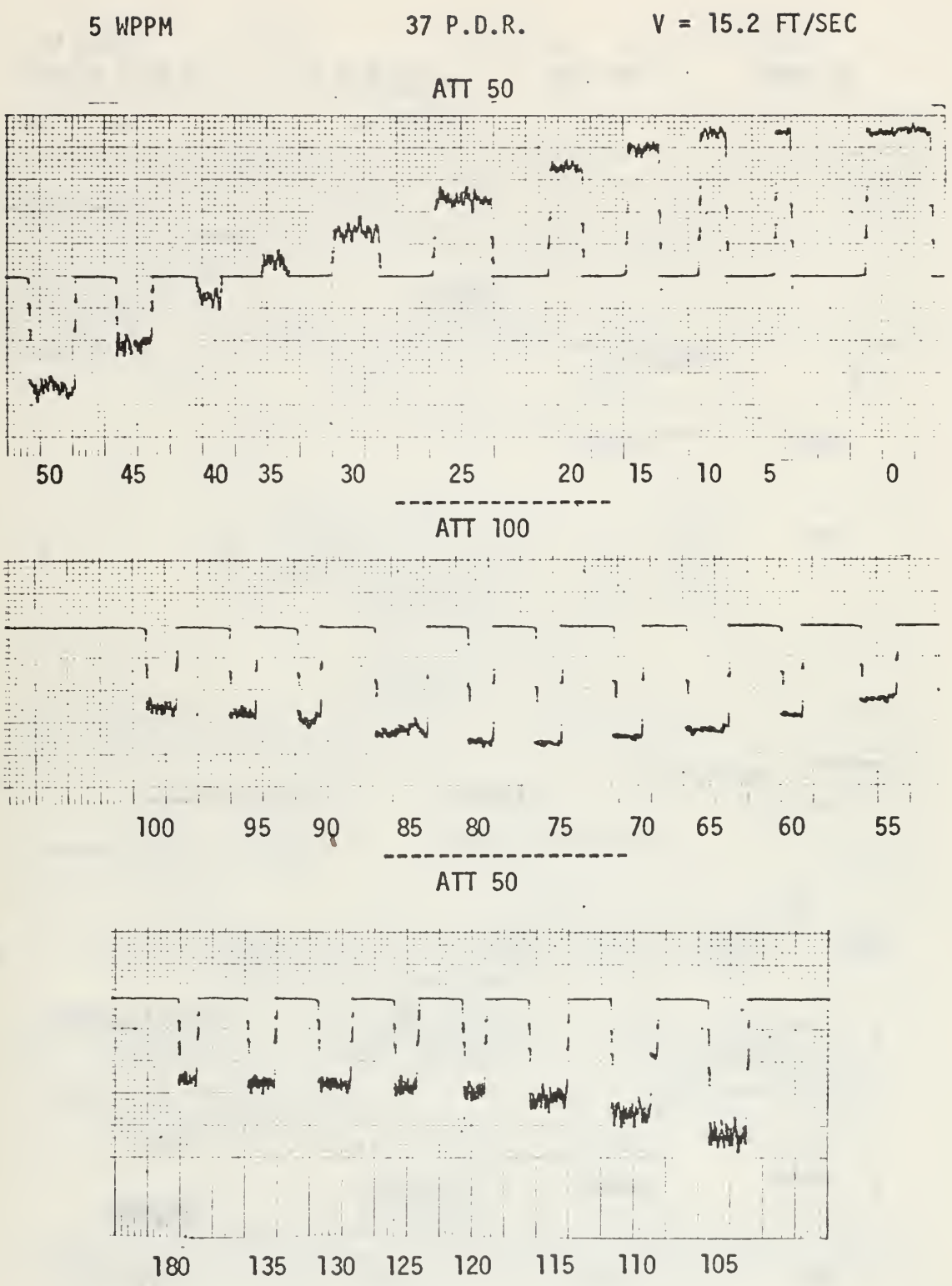

FIG. 51 OSCILLOGRAPH TRACINGS OF DYNAMIC PRESSURE

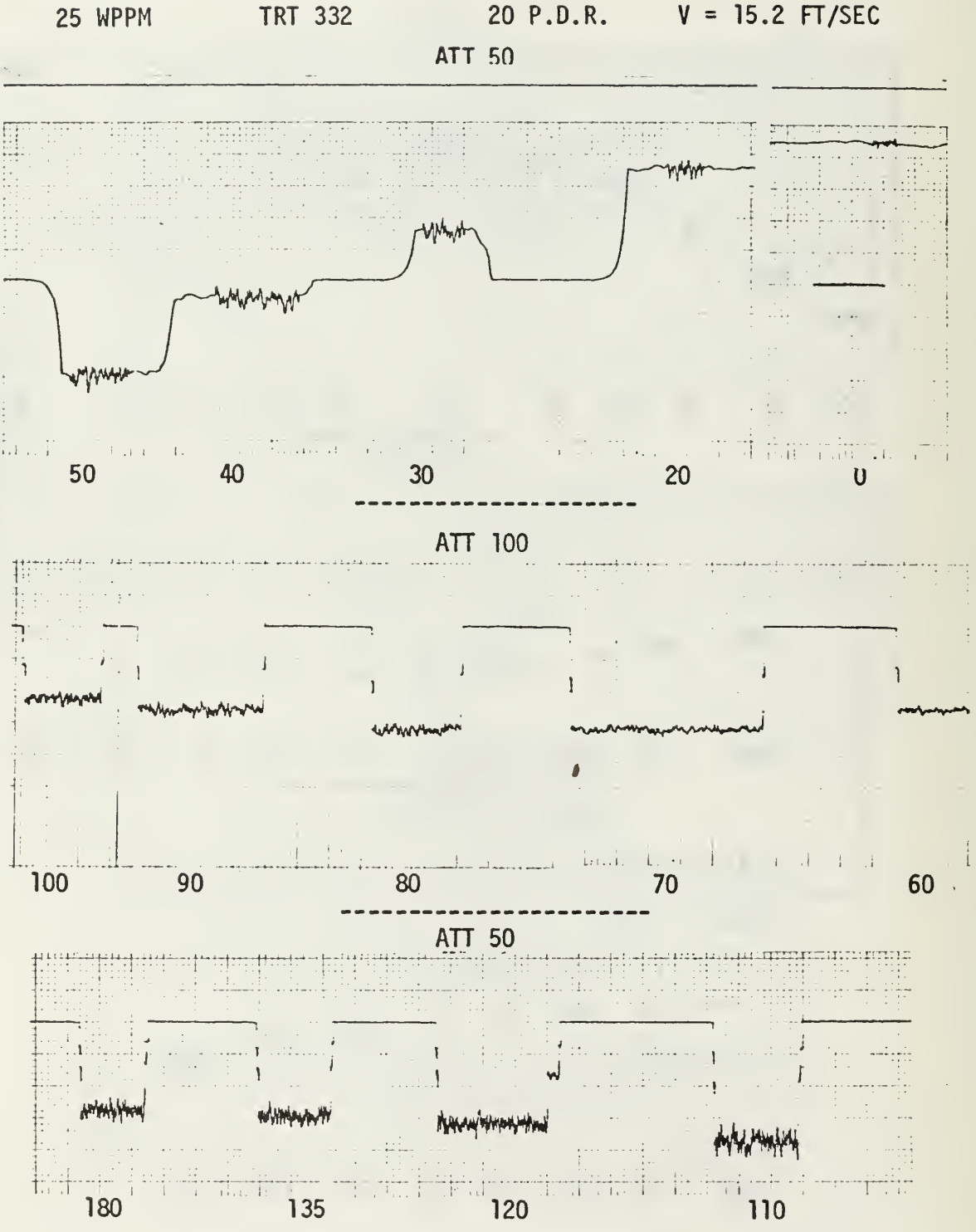

FIG. 52 OSCILLOGRAPH TRACINGS OF DYNAMIC PRESSURE

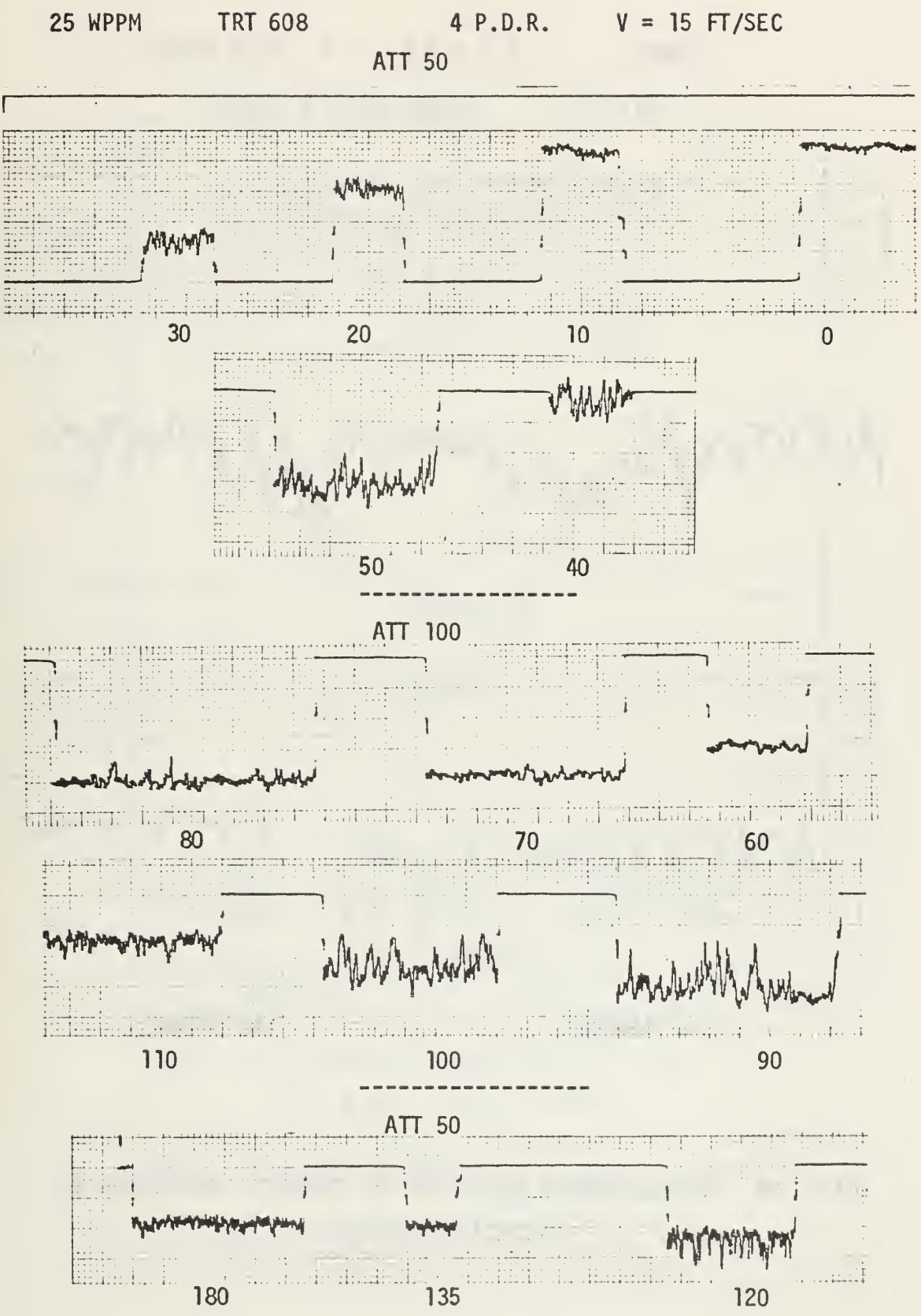

FIG. 53 OSCILLOGRAPH TRACINGS OF DYNAMIC PRESSURE

5 WPPM 9.5 P.D.R. V = 12.8 FT/SEC

ATT 50 CHART SPEED 5 MM/SEC

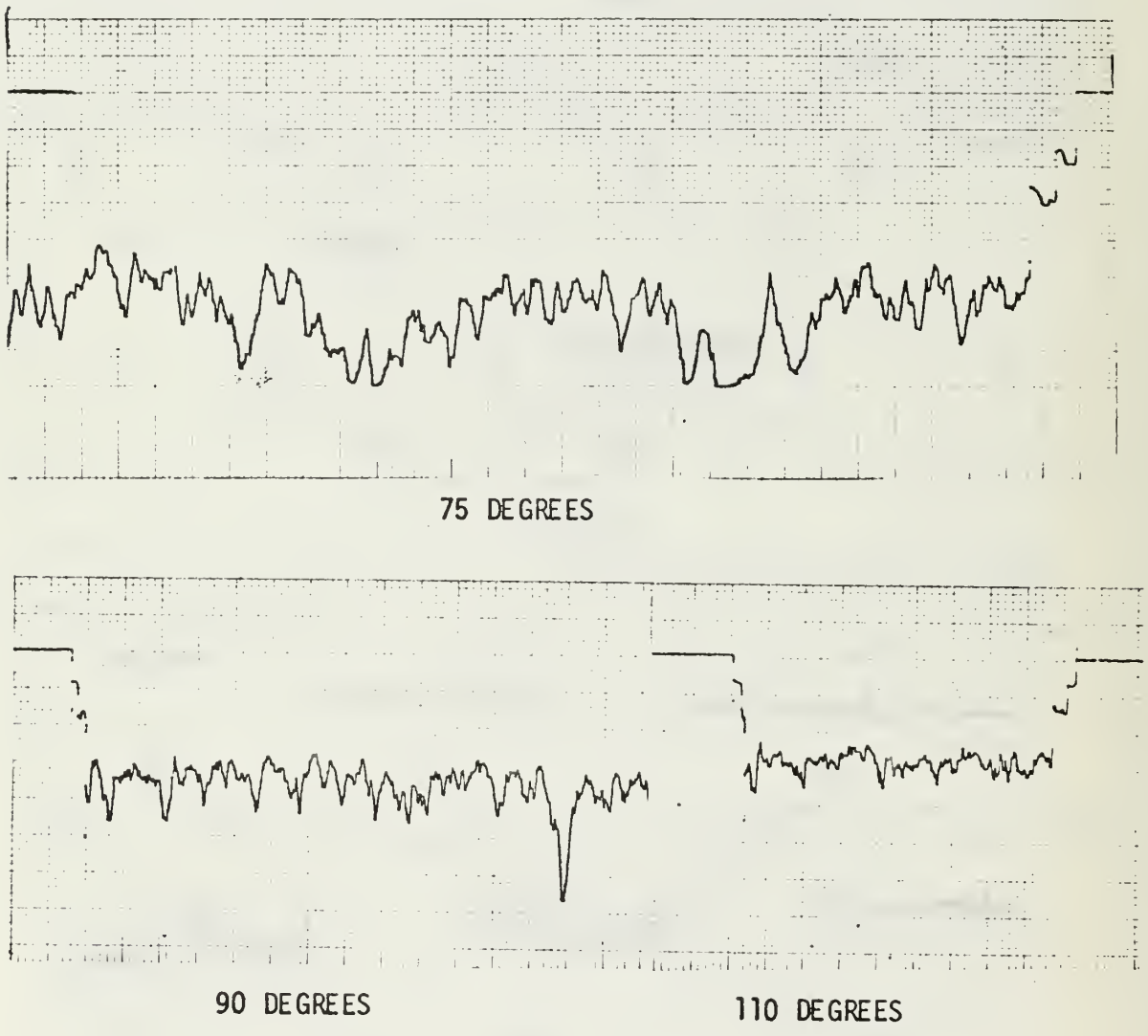

FIG. 54 OSCILLOGRAPH TRACINGS OF DYNAMIC PRESSURE AT CRITICAL VELOCITY

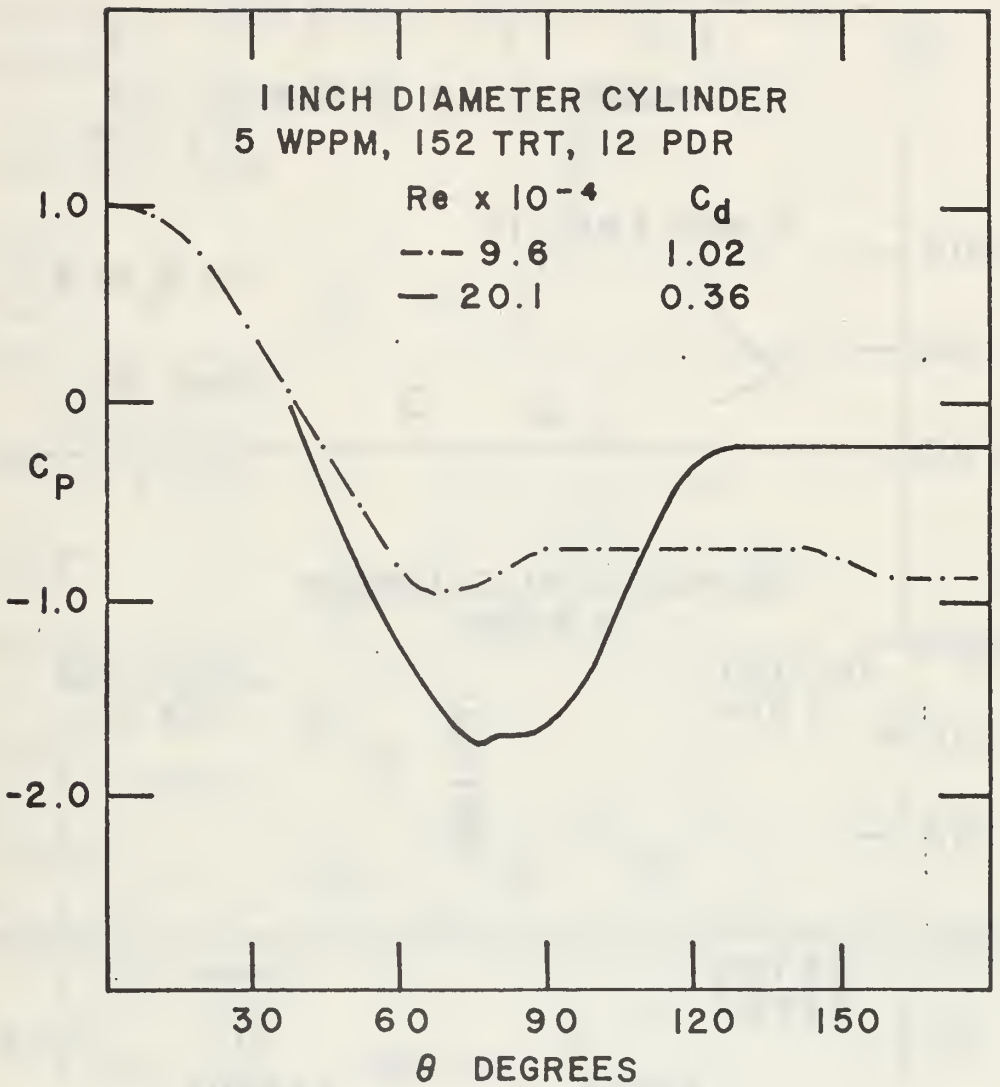

FIG. 55 PRESSURE DISTRIBUTIONS FOR $Re < Re_c$ AND $Re > Re_c$

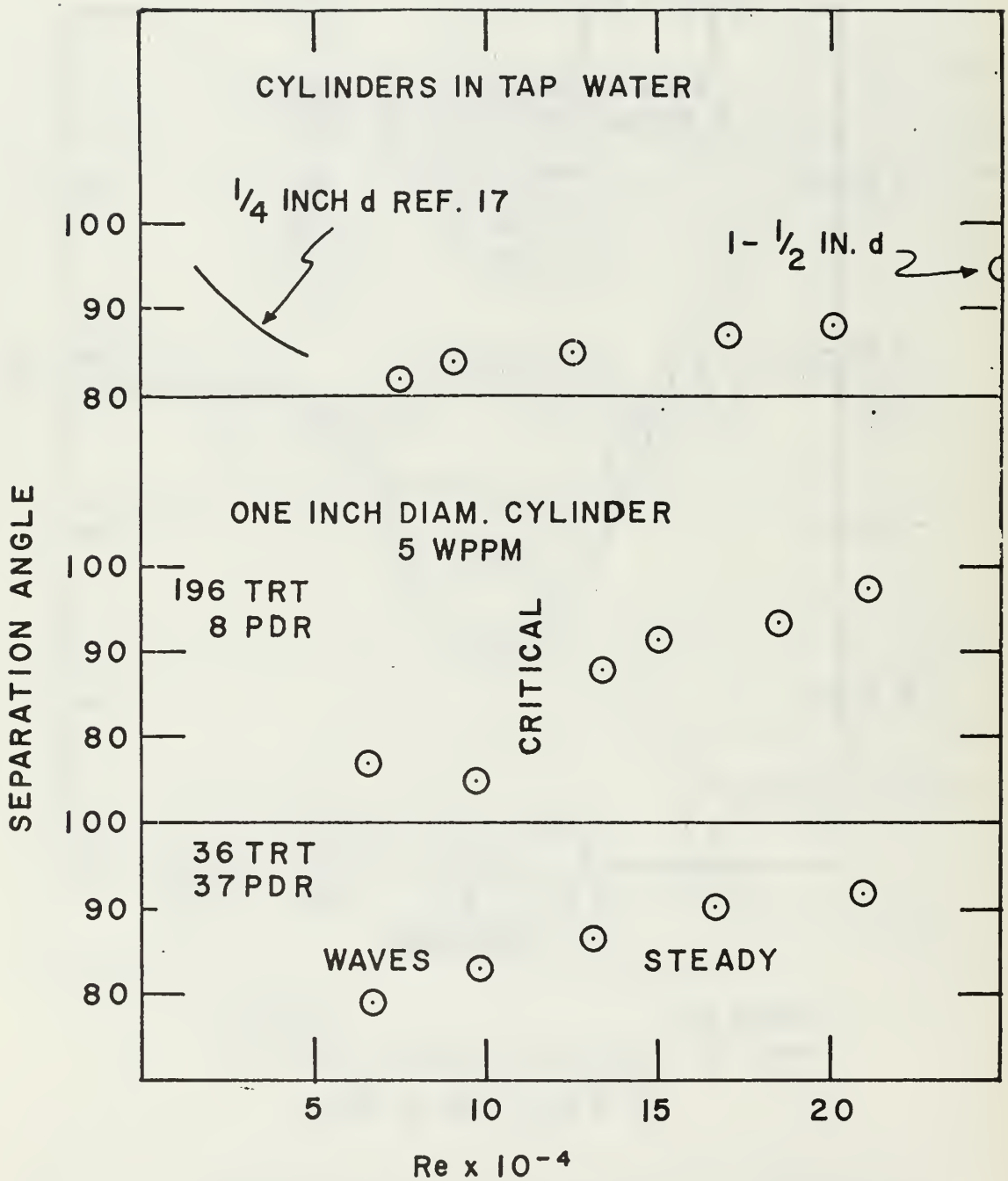

FIG. 56 SEPARATION ANGLE VERSUS Re

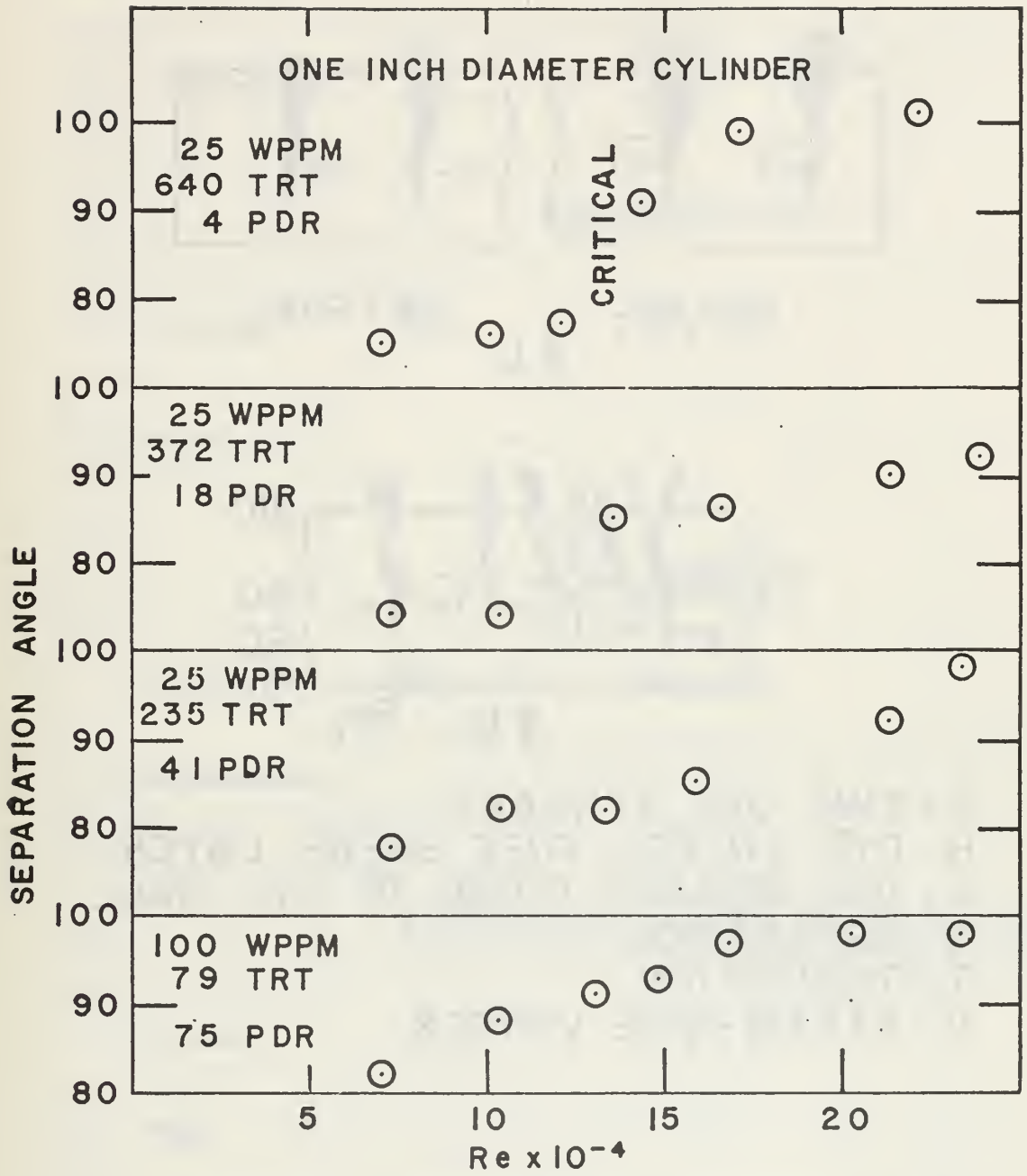

FIG. 57 SEPARATION ANGLE VERSUS Re

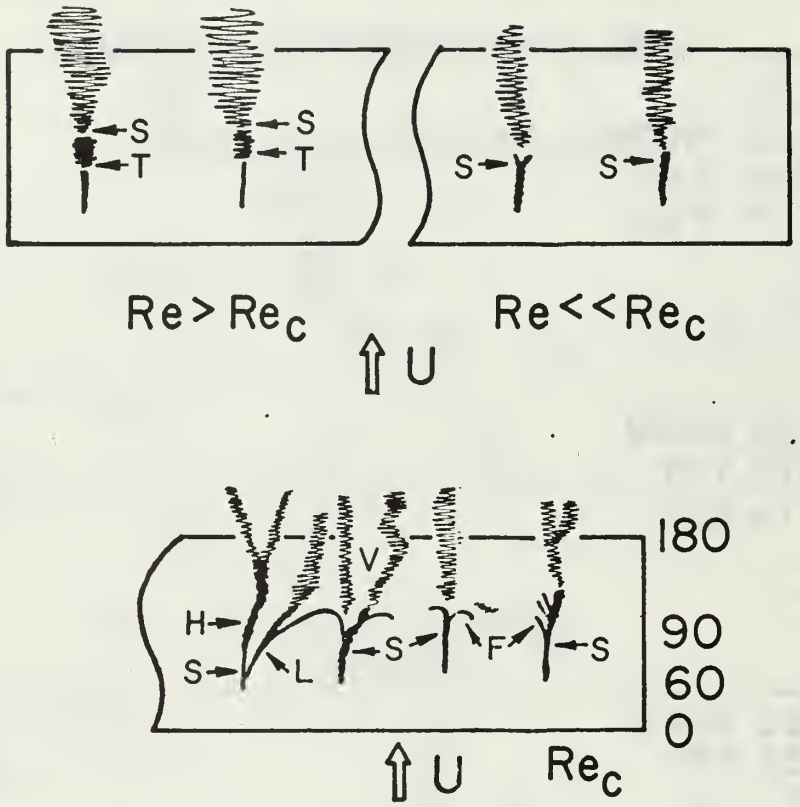

F : FINE DYE STREAKS
H : DYE ENTERS FREE SHEAR LAYER
L : DYE REMAINS CLOSE TO CYL. WALL
S : SEPARATION
T : TRANSITION
V : STEAM-WISE VORTEX

FIG. 58 SEPARATION FLOW PATTERN AT CRITICAL Re

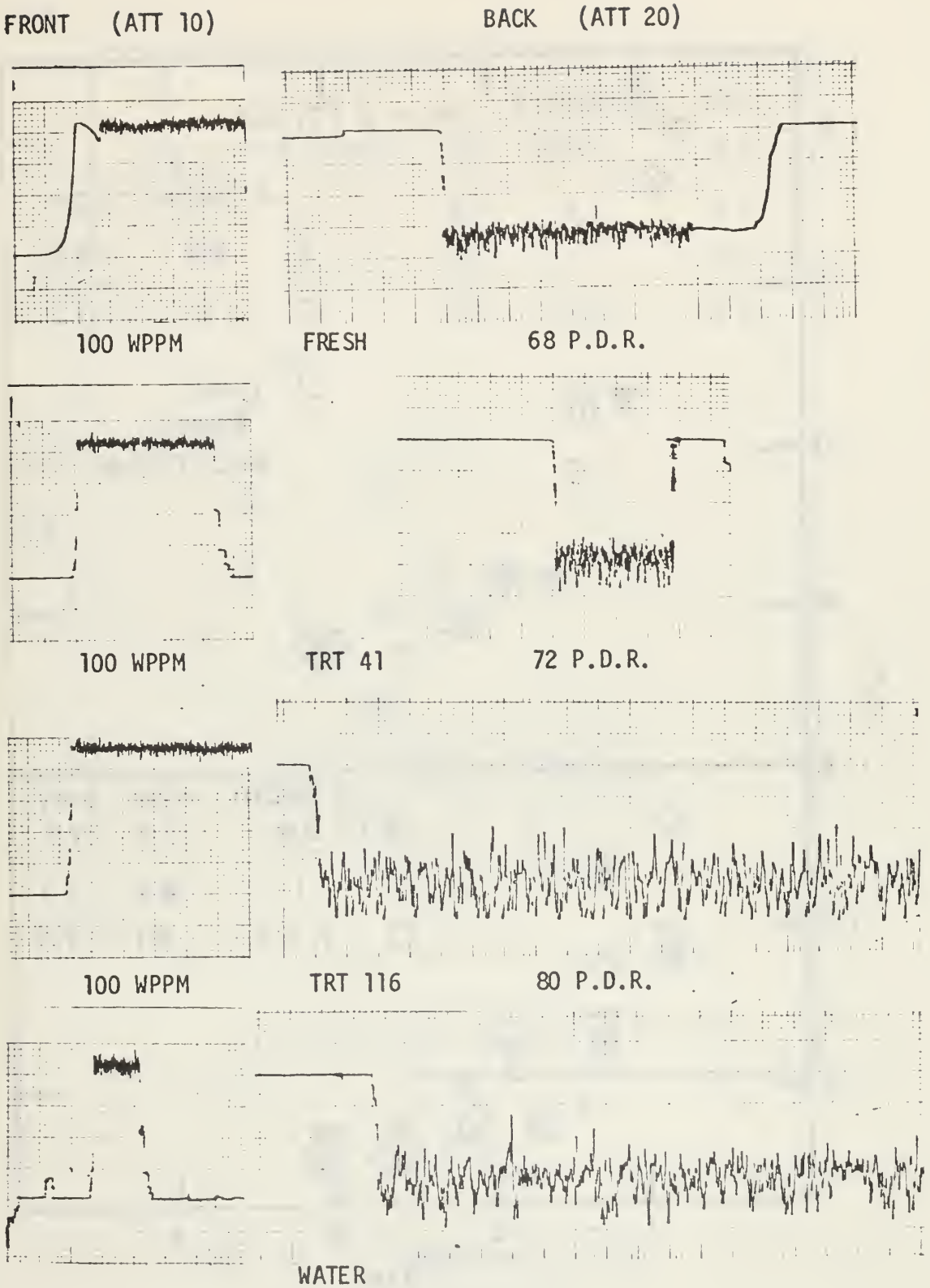

FIG. 59 OSCILLOGRAPH TRACINGS OF THE FRONT AND BACK PRESSURES ON A FLAT PLATE PERPENDICULAR TO THE FLOW

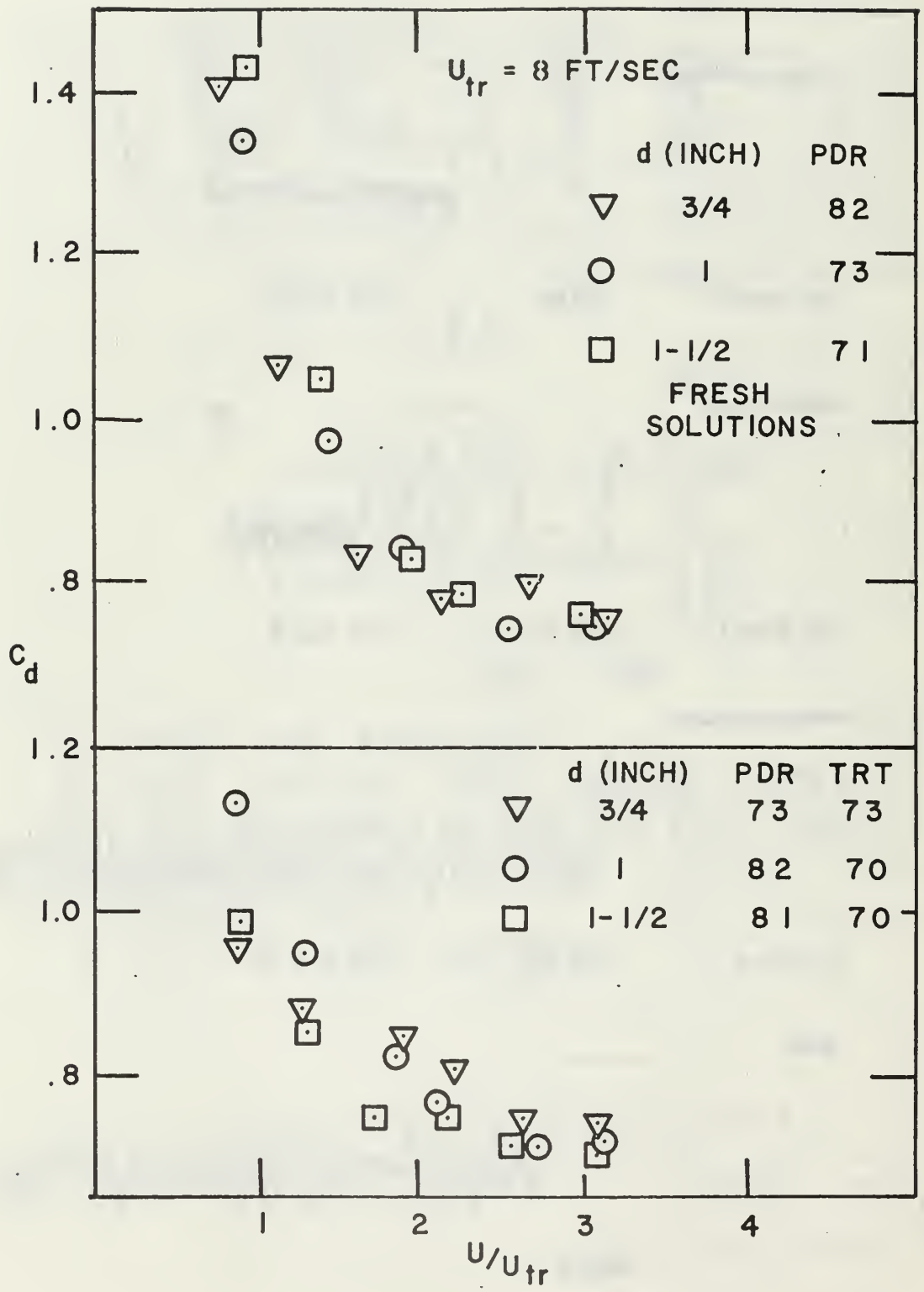

FIG. 60 C_d VERSUS U/U_{tr} FOR
100 WPPM SOLUTIONS

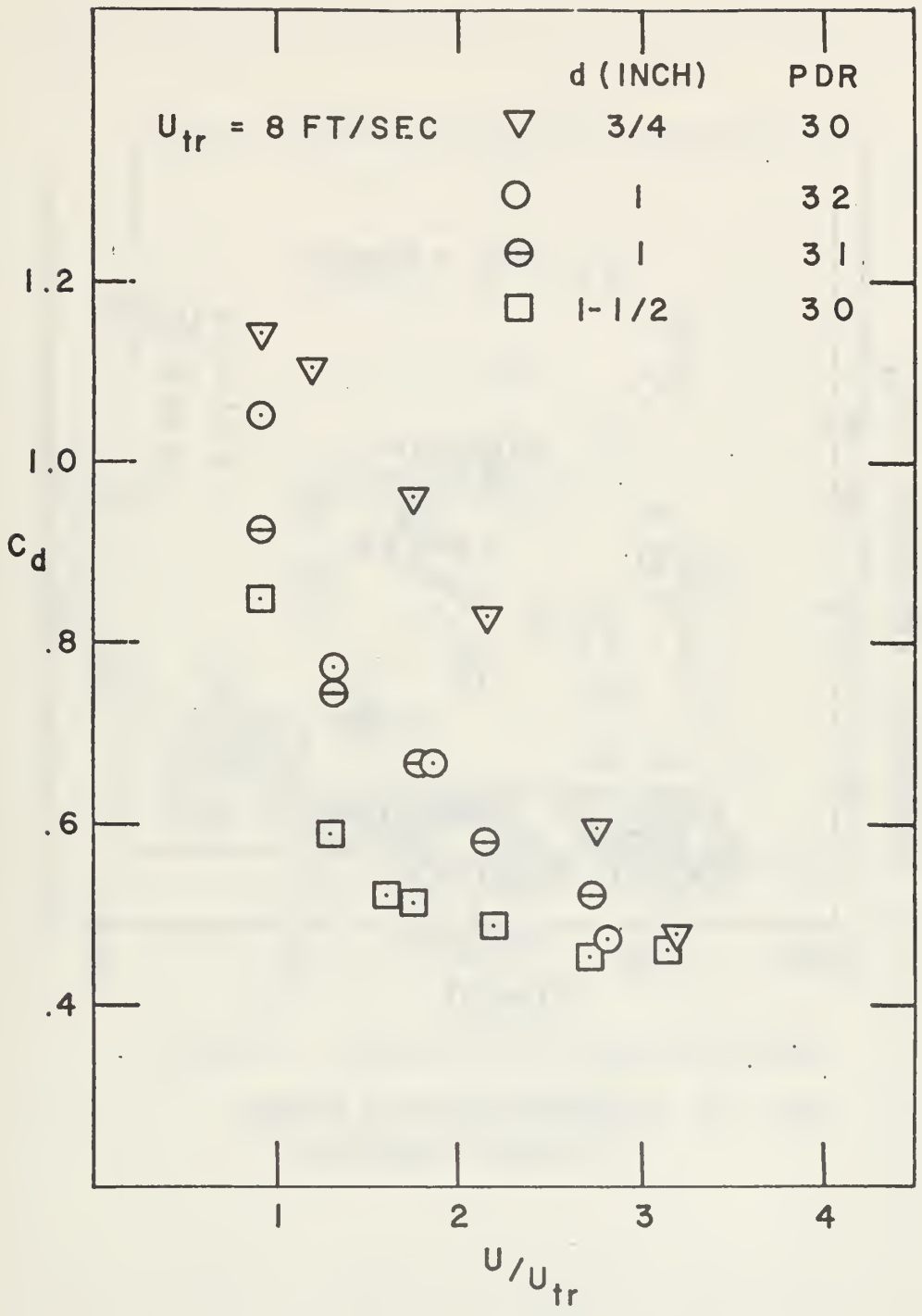

FIG. 61 C_d VERSUS U/U_{tr} FOR
5 WPPM SOLUTIONS

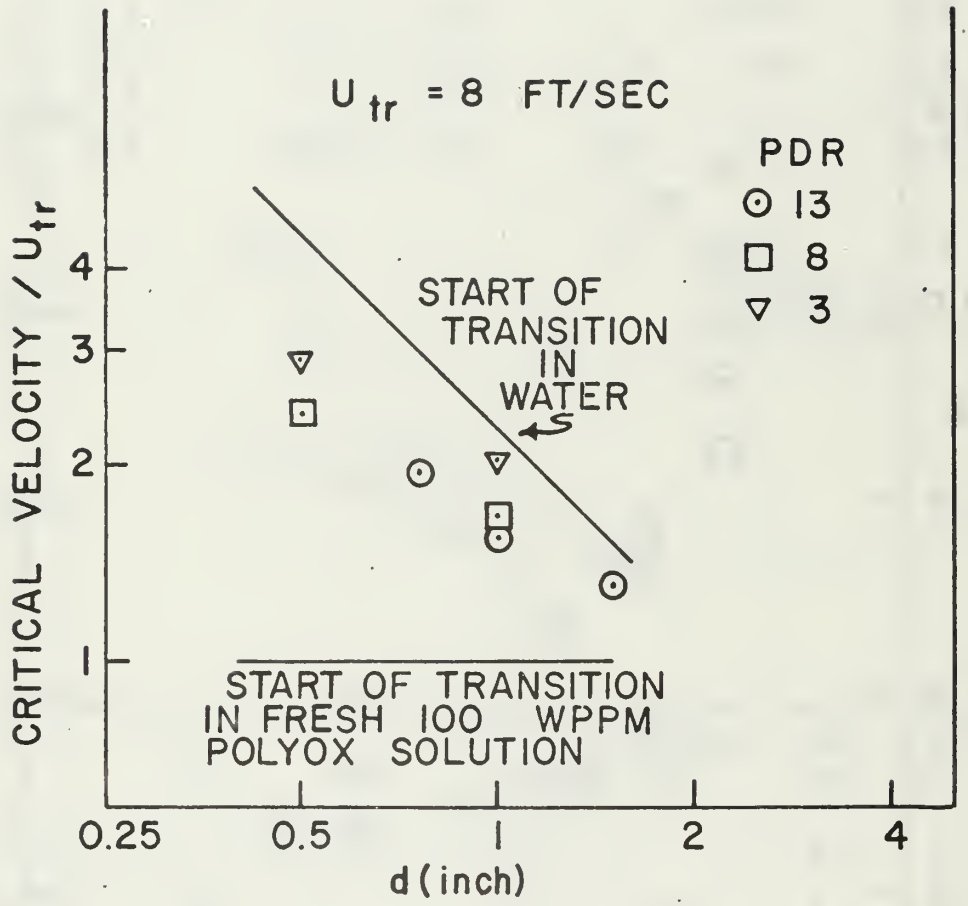

FIG. 62 CRITICAL VELOCITY VERSUS CYLINDER DIAMETER

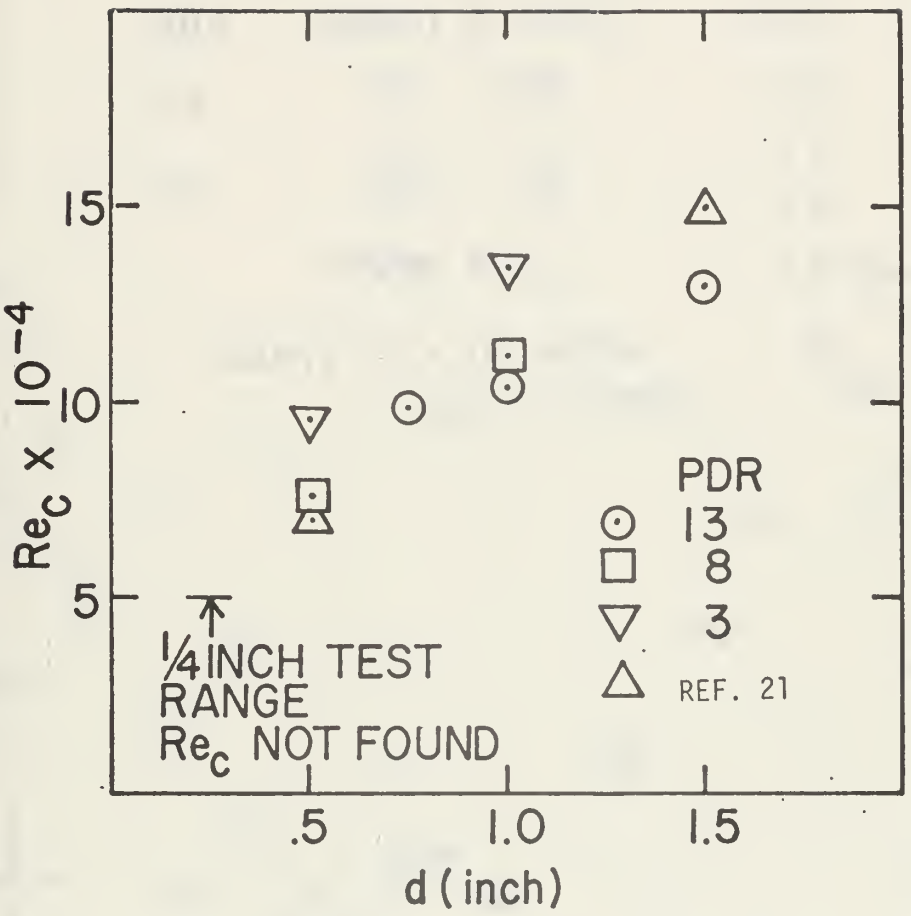

FIG. 63 CRITICAL Re VERSUS CYLINDER DIAMETER

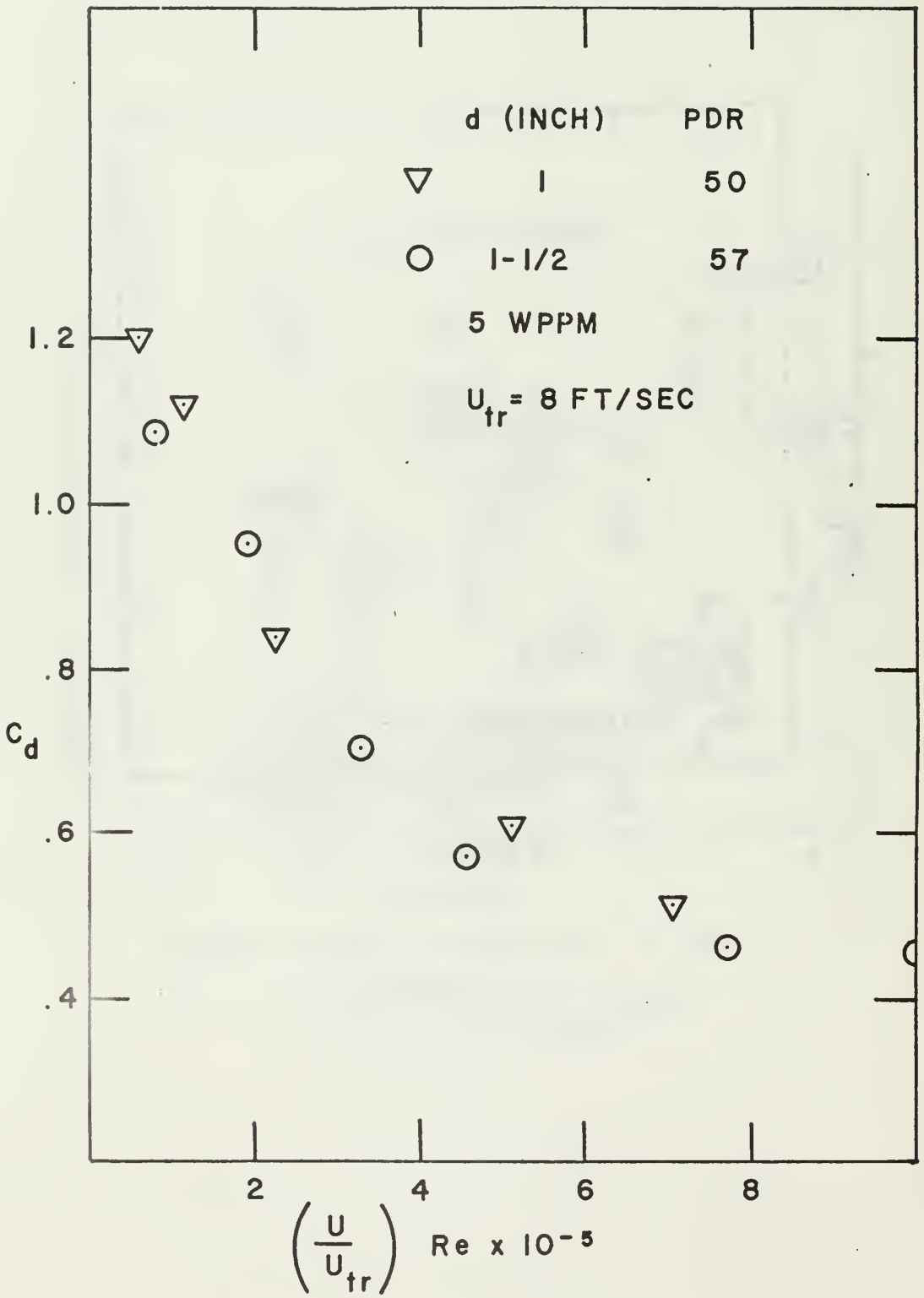

FIG. 64 EVOLUTION OF TRANSITION WITH PDR IN TERMS OF (U/U_{tr})Re.

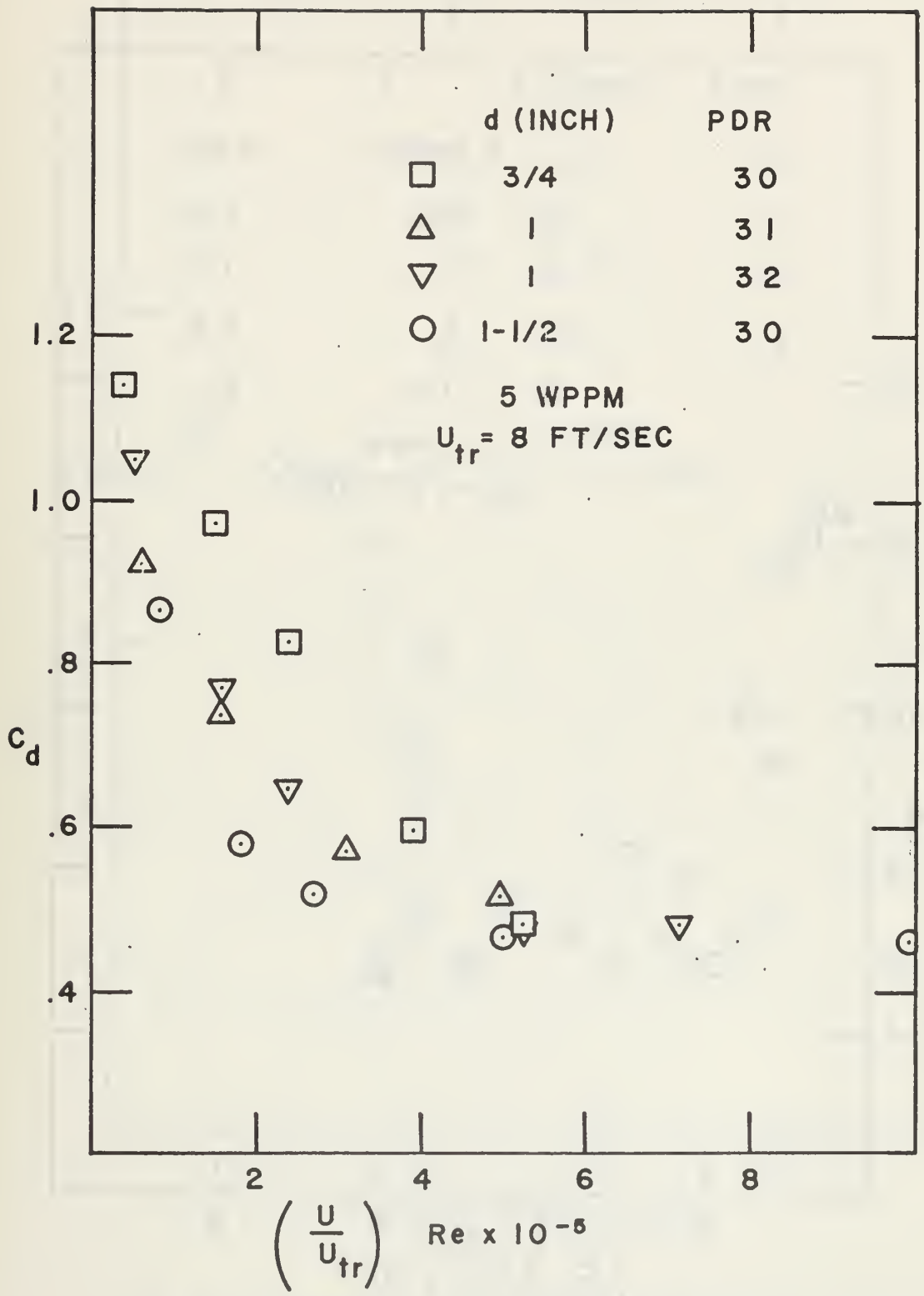

FIG. 65 EVOLUTION OF TRANSITION WITH PDR IN TERMS OF (U/U_{tr})Re.

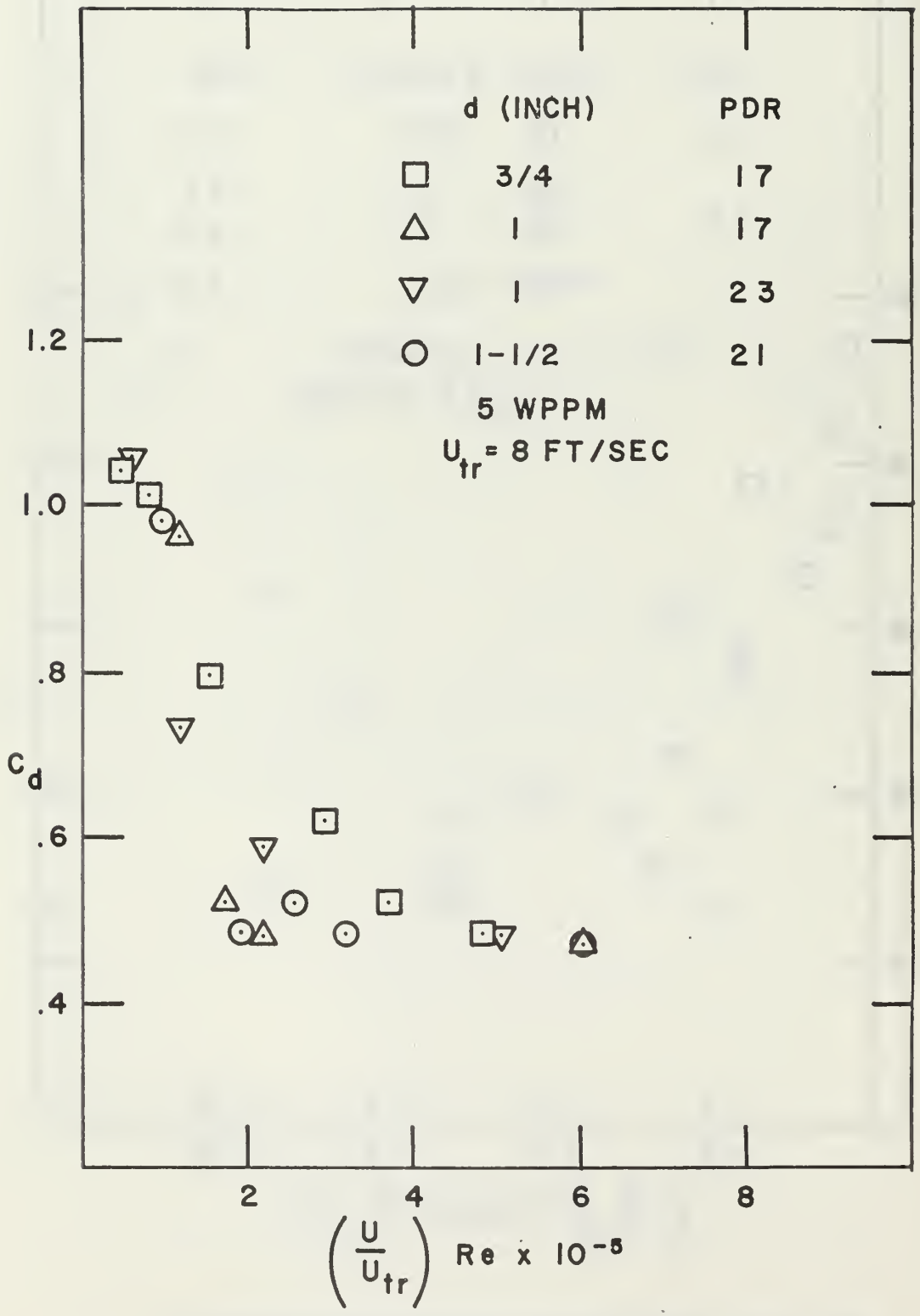

FIG. 66 EVOLUTION OF TRANSITION WITH PDR IN TERMS OF (U/U_{tr})Re.

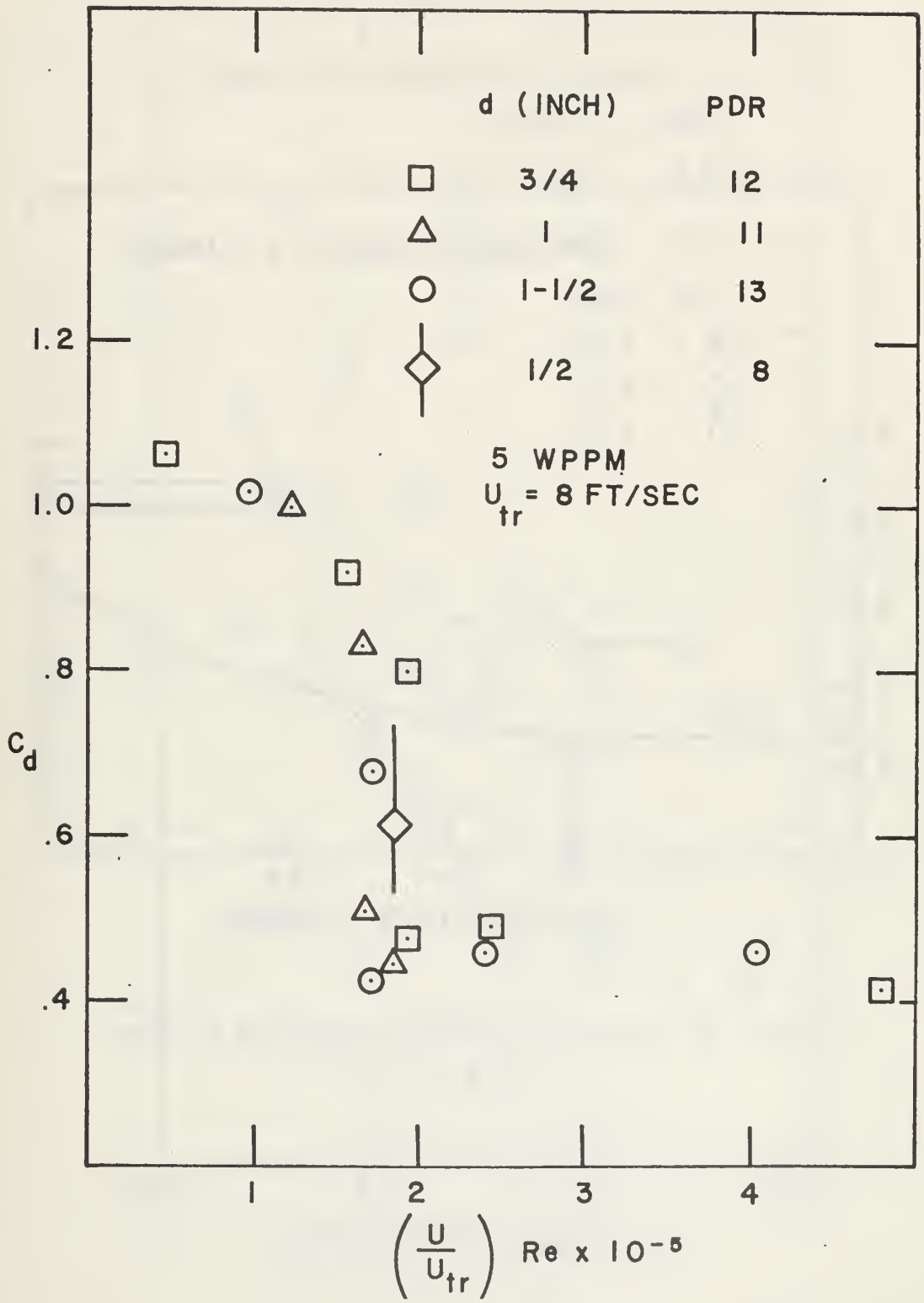

FIG. 67 EVOLUTION OF TRANSITION WITH PDR IN TERMS OF U/U_{tr}.Re. (CRITICAL TRANSITION)

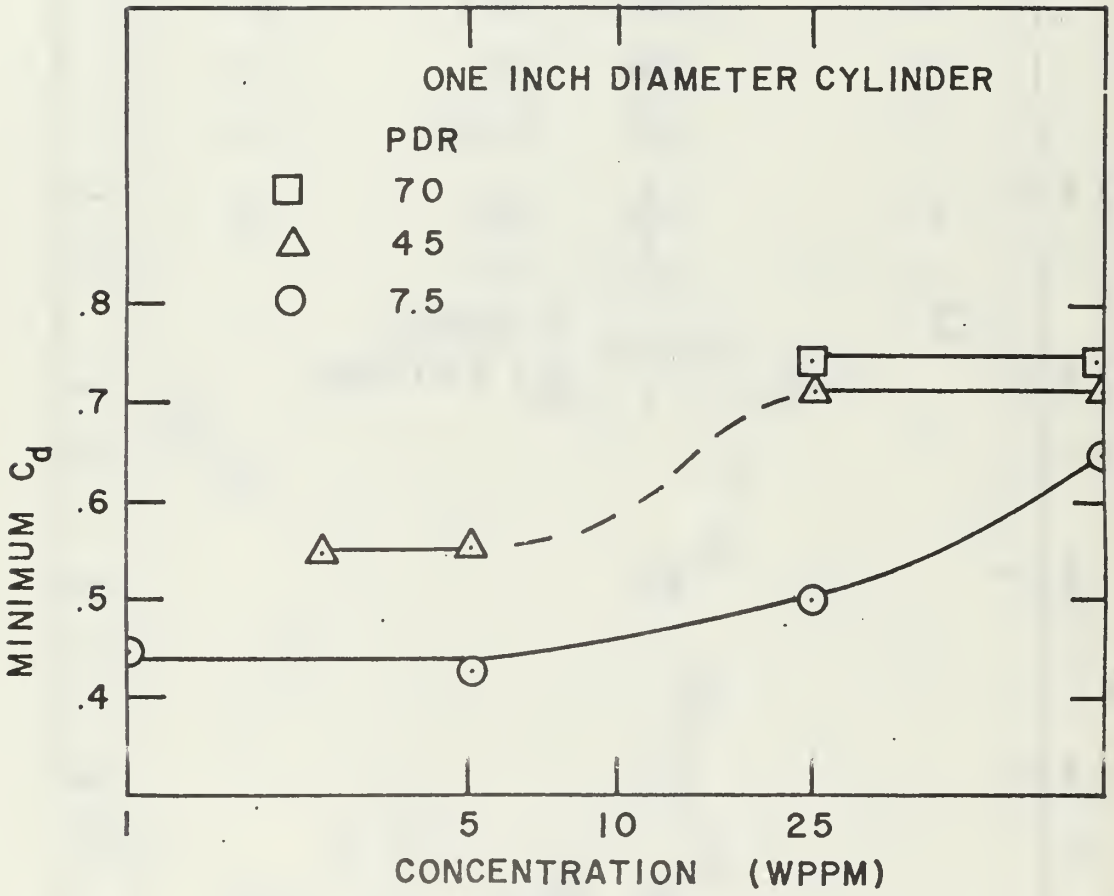

FIG. 68 EFFECT OF CONCENTRATION ON C_d FOR $Re < 3 \times 10^5$

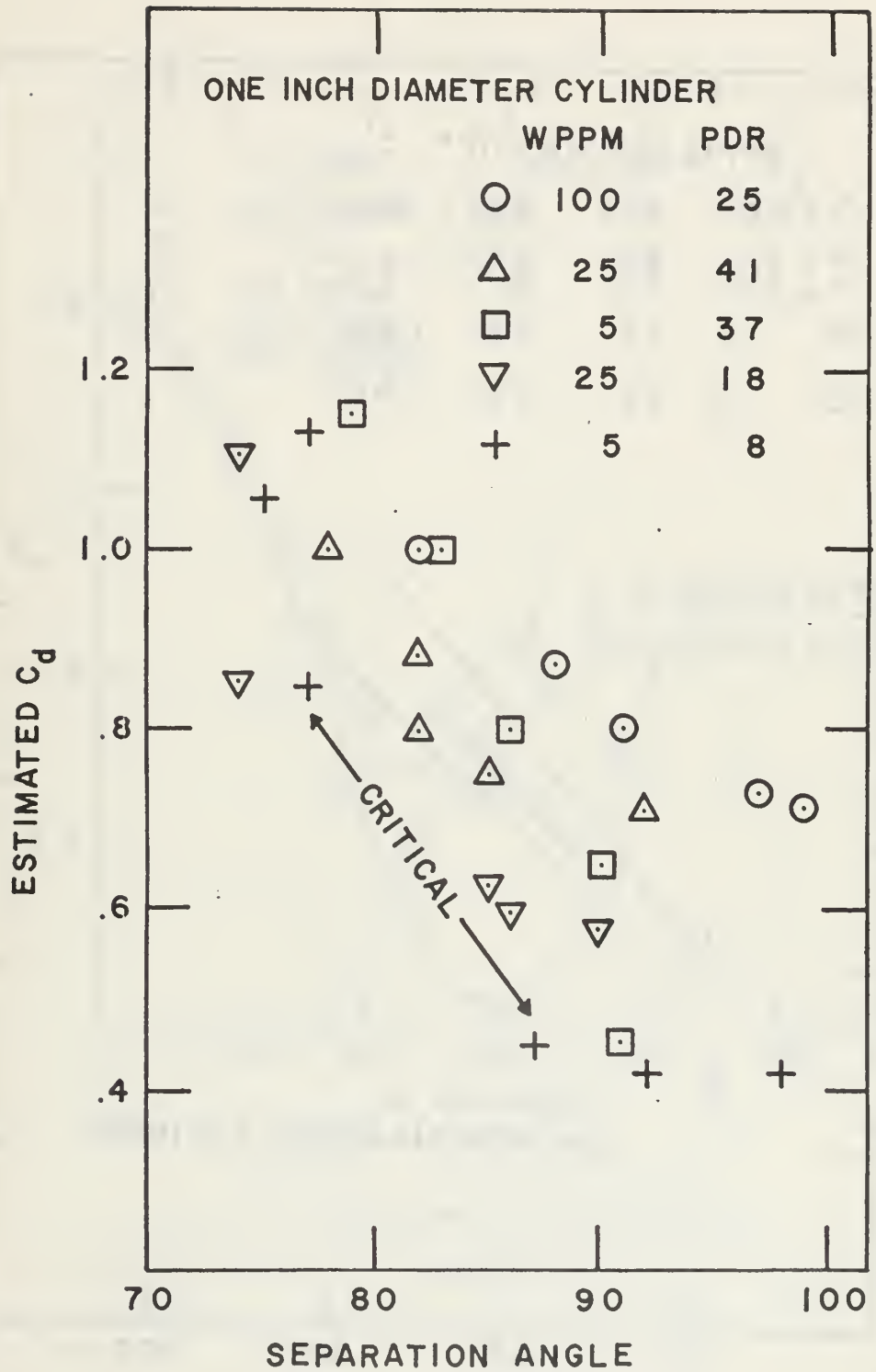

FIG. 69 C_d VERSUS SEPARATION ANGLE

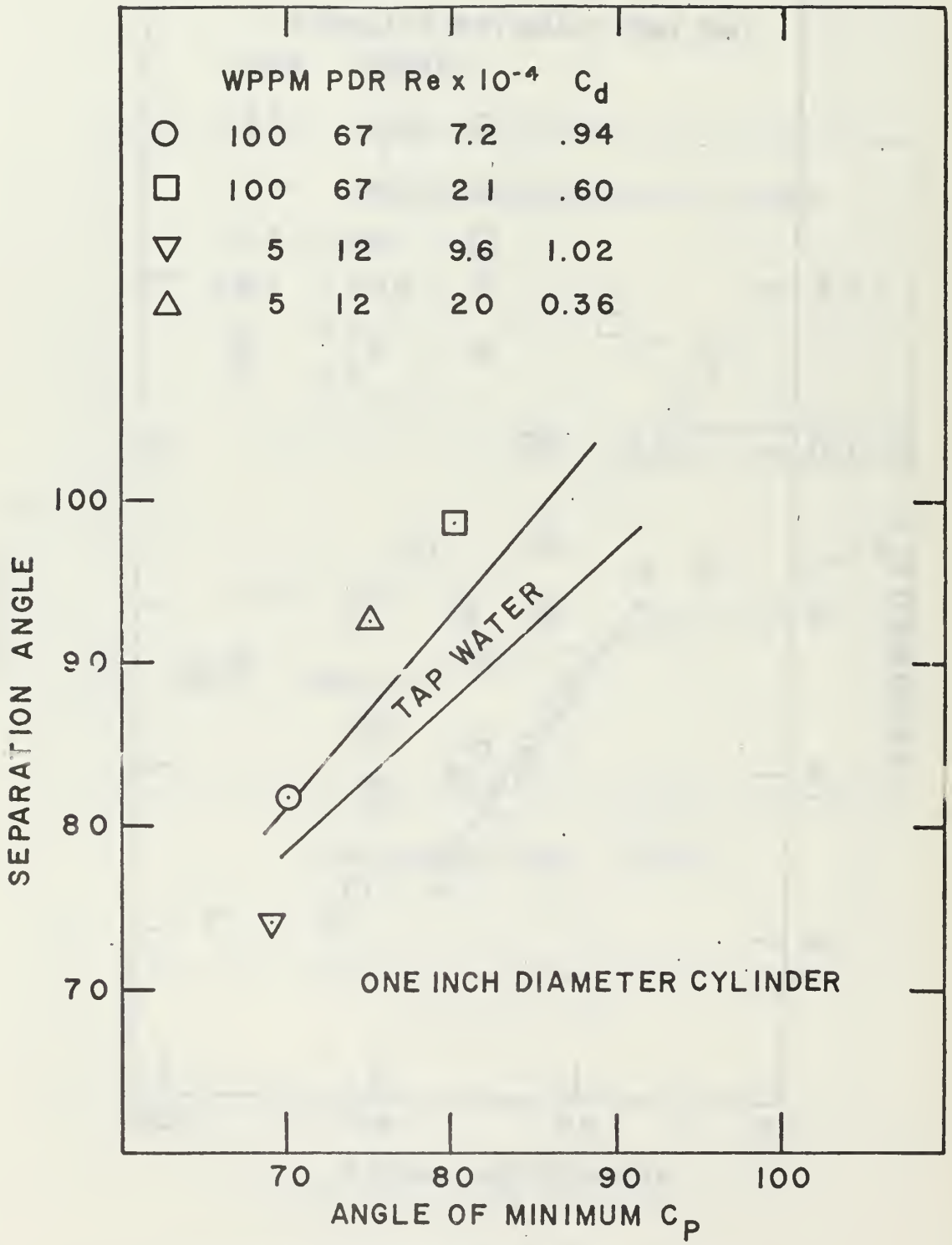

FIG. 70 SEPARATION ANGLE VERSUS THE ANGLE OF MINIMUM C_p

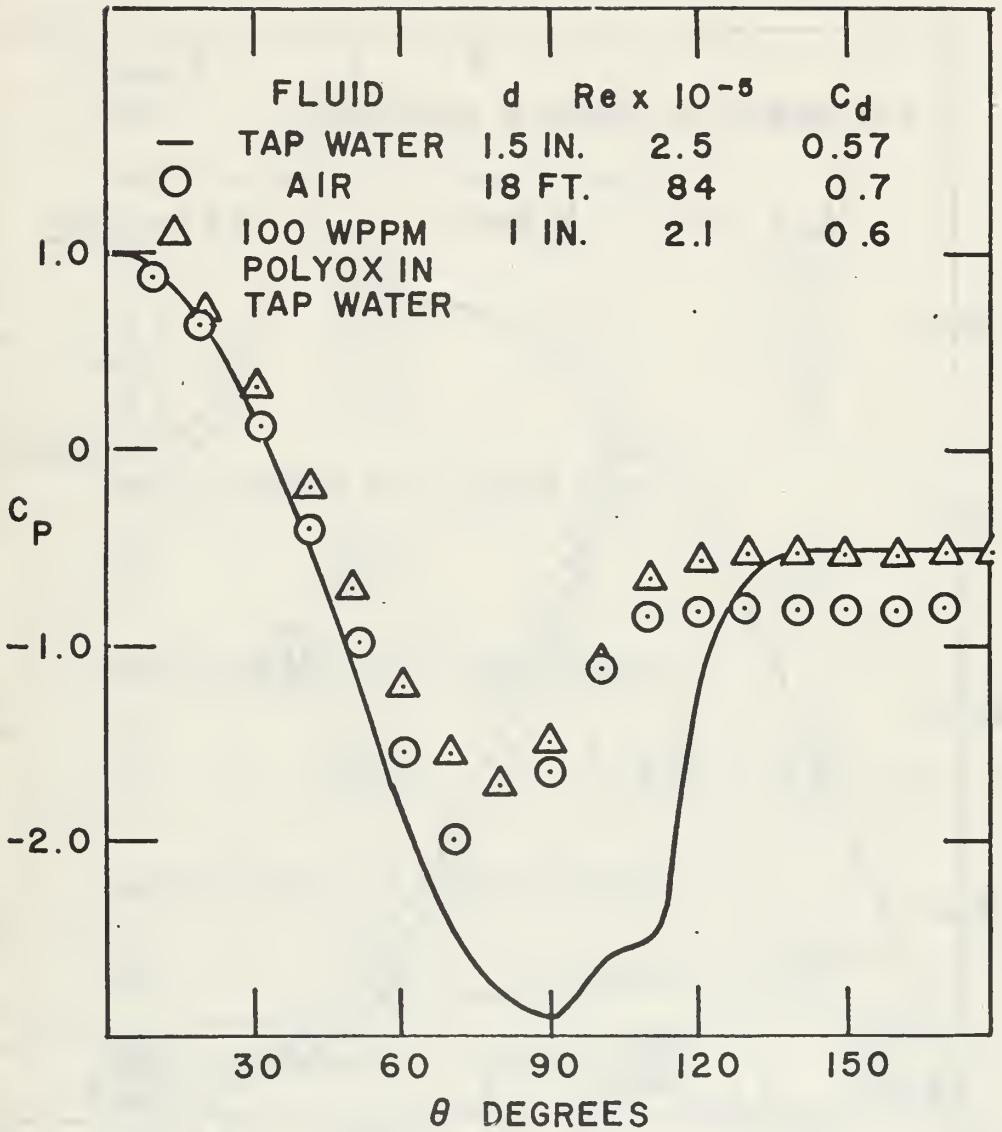

FIG. 71 PRESSURE DISTRIBUTIONS AT $C_d \sim 0.6$

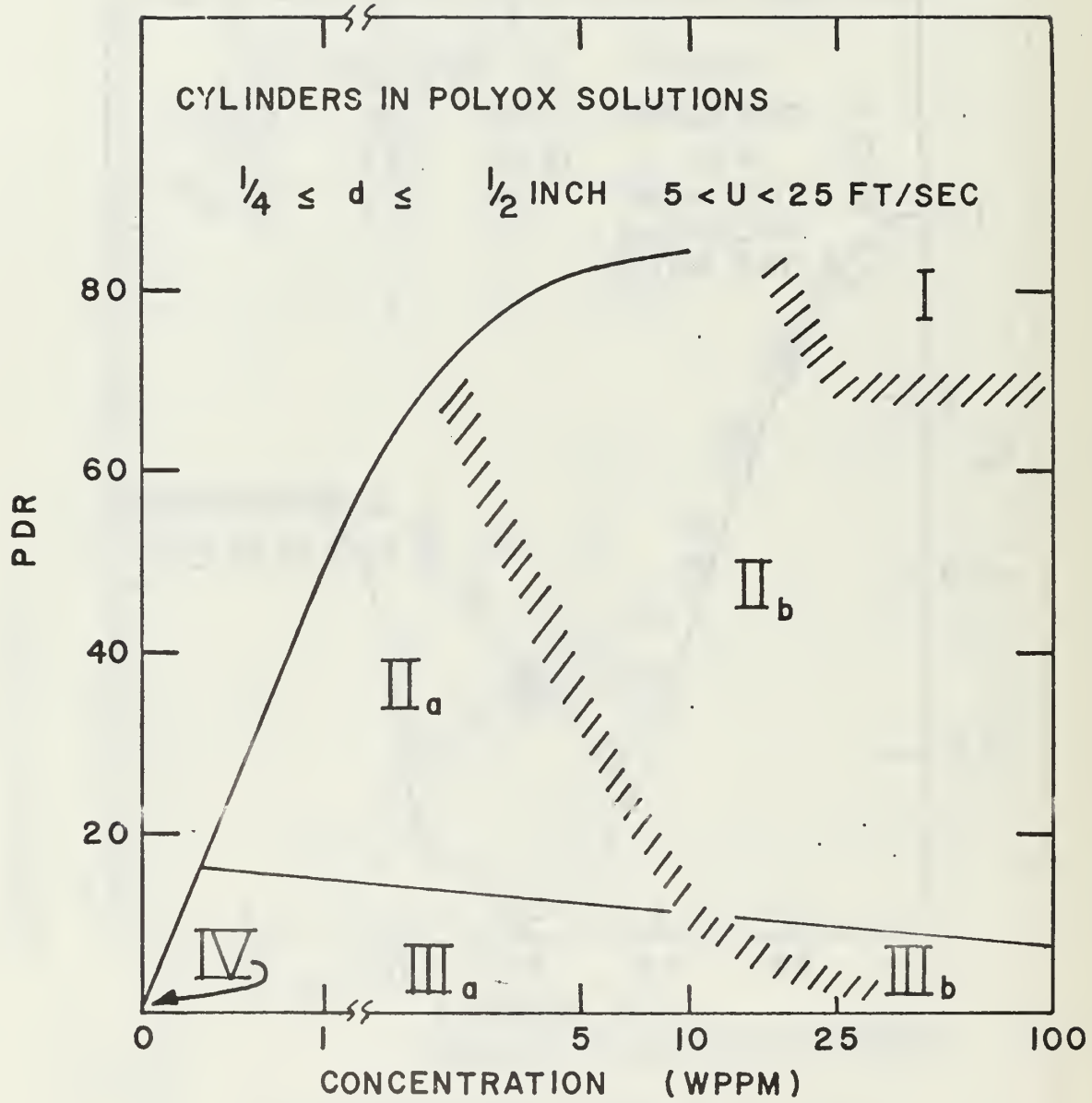

FIG. 72 DELINEATION OF THE DEPENDENCE OF TRANSITION ON VARIOUS FLOW PARAMETERS

TABLE I

Laboratory Sample Polyox WSR-301 Solutions

Conc. wppm	$\overline{P.D.R.}$	N	s.d.
Master solution #1	aged 20 hours		
10	80.0	4	0.0
5	81.4	4	0.8
1	46.8	4	2.3
0.5	24.5	4	3.9
0.2	8.7	4	2.0
0.1	3.2	4	1.9
Master solution #2	aged 36 hours		
10	87.0	4	1.2
5	66.6	4	3.6
Master solution #3	aged 60 hours		
10	82.4	4	1.0
5	88.0	4	0.7
1	38.0	4	4.7
Master Solution #4	aged 24 hours		
10	82.0	2	1.0
0.2	8.7	4	2.5
Master solution #5	aged 18 hours		
10	79.9	4	0.8
0.5	21.4	5	5.9

$\overline{P.D.R.}$ is the mean of N number of data from the rheometer tests and s.d. is the root mean of the sum of the errors squared.

LIST OF REFERENCES

1. Toms, B. A., "Some Observations on the Flow of Linear Polymers through Straight Tubes at Large Reynolds Numbers," Proc. Int'l. Cong. Rheol. Part II, 1949.

2. Hoyt, J. W. and Fabula, A. G., "The Effect of Additives on Fluid Friction," 5th Symposium Naval Hydrodynamics ACR-112, p. 947-974, Sept. 1964.

3. Deavours, C. A., A Critical Survey of Literature Concerning the Toms' Effect, Div. of Applied Mathematics, Brown U. Tech. Report No. 1, Project No. NR062-179/8-2-65, May 1966.

4. Lumley, J. L., "The Toms Phenomenon: Anomalous Effects in Turbulent Flow of Dilute Solutions of High Molecular Weight Linear Polymers," Applied Mechanics Reviews, V. 20, no. 12, p. 1139-49, Dec. 1967.

5. White, A., "Some Observations on the Flow Characteristics of Certain Dilute Macromolecular Solutions," Proceedings of the Symposium on Viscous Drag Reduction, Dallas, Texas, Sept. 1968, p. 107-130, Plenum Press, 1969.

6. Crawford, H. R. and Pruitt, G. T., Symposium Non-Newtonian Fluid Mechanics, 56th Annual Meeting Inst. Chem. Eng., Houston, Texas, Dec. 1963.

7. Ruszczycky, M. A., "Sphere Drop Tests in High-polymer Solutions," Nature, v. 206, p. 614-15, May 1965.

8. White, A., "Effect of Polymer Additives on Boundary Layer Separation and Drag of Submerged Bodies," Nature, v. 211, p. 1390, Sept. 1966.

9. White, A., "Drag of Spheres in High Polymer Solutions," Nature, v. 216, p. 994, Dec. 1967.

10. Brennen, C. and Gadd, G. E., "Aging and Degradation in Dilute Polymer Solutions," Nature, v. 215, p. 1368, 1967.

11. Lang, T. G. and Patrick, H. V. L., Drag of Blunt Bodies in Polymer Solutions, Naval Ordnance Test Station Tech. Report 4379, July, 1967.

12. Hayes, M. F., Drag Coefficients of Spheres Falling in Dilute Aqueous Solutions of Long-Chain Macromolecules, M.S. Thesis, Naval Postgraduate School, Monterey, 1966.

13. Chenard, J. H., Drag of Spheres in Dilute Aqueous Solutions of Poly(ethylene oxide) within the Region of the Critical Reynolds, M.S. Thesis, Naval Postgraduate School, Monterey, 1967.

14. James, D. F., Laminar Flow of Dilute Polymer Solutions Around Circular Cylinders, Ph. D. Thesis, California Institute of Technology, Pasadena, 1967.

15. McClanahan, T. and Ridgely, P. J., Drag of Circular Cylinders in Dilute Solutions of Poly(ethylene oxide) for Flows Characterized by Laminar Boundary Layer Separation, M.S. Thesis, Naval Postgraduate School, Monterey, 1968.

16. Sanders, J. V., "Drag Coefficients of Spheres in Poly(ethylene oxide) Solutions," Int'l. Shipbuilding Progress, v. 14, p. 140-157, Apr. 1967.

17. Brennen, C., "Some Cavitation Experiments with Dilute Polymer Solutions," J. Fluid Mech., v. 44, p. 51-63, 1970.

18. Luikov, A. V., Shul'man, Z. P. and Puris, B. I., "Mass Transfer of a Cylinder in Forced Flow of a Non-Newtonian Viscoelastic Fluid," Heat-Transfer-Soviet Research, v. 1, no. 1, p. 121-32, 1969.

19. Barenblatt, G. I., Bulina, I. G. and Myasnikov, V. P., "Drag Reducing Effect of Solutions of Some High-Molecular Compounds in Turbulent Flow Past Bodies," Zhurnal Prikladnoi Mekh. i Tekhn Fiziki, no. 3, p. 95-6, 1965.

20. Paterson, R. W., Turbulent Flow Drag Reduction and Degradation with Dilute Polymer Solutions, Div. of Eng. and Applied Physics, Eng. Sci. Lab., Harvard University, 1969.

21. Sarpkaya, T., "Flow of Dilute Polymer Solutions About Circular Cylinders," Naval Postgraduate School Report No: NPS-59SL0011B, January 1970.

22. Sarpkaya, T., "Flow of Dilute Polymer Solutions About Bluff Bodies," Proceedings of the Canadian Congress of Applied Mechanics, May 1971; (Presented at the Congress held in Calgary, Alberta, Canada on 17-21 May, 1971).

23. White, W. C. and McEligot, D. M., "Transition of Mixtures of Polymers in a Dilute Aqueous Solution," presented at Winter Annual, ASME, Los Angeles, paper no. 69-WA/FE-20, Nov. 1969.

24. Maskell, E. C., A Theory of the Blockage Effects on Bluff Bodies and Stalled Wings in a Closed Wind Tunnel, A.R.C. R. No. 3400, 1965.

25. Lienhard, J. H., Synopsis of Lift, Drag and Vortex Frequency Data for Rigid Circular Cylinders, College of Eng. Research Div., Washington State University, Bulletin 300, 1966.

26. Fage, A., "The Drag of Circular Cylinders and Spheres at High Values of Reynolds Number," A.R.C. R&M 1370, 1930.

27. Fage, A. and Falkner, V. M., "Further Experiments on the Flow Around a Circular Cylinder," A.R.C. R&M 1369, 1931.

28. Fage, A. and Warsap, A., "The Effects of Turbulence and Surface Roughness on the Drag of a Circular Cylinder," A.R.C. R&M 1283, 1930.

29. Delany, N. K. and Sorensen, N. E., Low Speed Drag of Circular Cylinders of Various Shapes, NACA TN 3038, 1953.

30. Humphreys, J. S., "On a Circular Cylinder in a Steady Wind at Transition Reynolds Numbers," J. Fluid Mech., v. 9, pt. 4, p. 603-12, 1960.

31. White, D. A., "Drag Coefficients for Spheres in High Reynolds Number Flow of Dilute Solutions of High Polymers," Nature, v. 212, p. 277, 1966.

32. Roshko, A., "Experiments on the Flow Past a Circular Cylinder at Very High Reynolds Number," J. Fluid Mech., v. 10, pt. 3, p. 345-56, 1961.

33. Fabula, A. G., An Experimental Study of Grid Turbulence in Dilute High-Polymer Solutions, Ph.D. Thesis, Pennsylvania State U., 1966.

34. Friehe, C. A. and Schwarz, W. H., "Grid-Generated Turbulence in Dilute Polymer Solutions," J. Fluid Mech., v. 44, pt. 1, p. 173-93, 1970.

35. Ultman, J. S. and Denn, M. M., "Anomalous Heat Transfer and a Wave Phenomenon in Dilute Polymer Solutions," Trans. of the Society of Rheology, v. 14, pt. 3, p. 307-17, 1970.

36. Coleman, B. D. and Gurtin, M. E., "On the Stability against Shear Waves of Steady Flows of Non-Linear Visco-Elastic Fluids," J. Fluid Mech., v. 33, pt. 1, p. 165-181, 1968.

37. Tlapa, G. A., Elastic Recovery and the Toms Effect--A Simple Model, Illinois Inst. of Tech., Dept. of Mathematics TR4, July 1968.

38. Sarpkaya, T. and Rainey, P. G., "Stagnation Point Flow of a Second-Order Viscoelastic Fluid," (To appear in Acta Mechanica).

39. White, F. M., "A Theory of Boundary-Layer Flow Noise with Application to Pressure Gradients and Polymer Solutions," J. Hydronautics, v. 3, no. 2, Apr. 1969.

40. Walsh, A. M., On the Turbulent Flow of Dilute Polymer Solutions, Ph.D. Thesis, California Inst. of Tech., Pasadena, 1967.

INITIAL DISTRIBUTION LIST

1. Commander
   Naval Ship Research and Development Center
   Washington, D. C. 20007
   Attn: Code L41 (39)
   Attn: Code 513 (1)

2. Commanding Officer
   Naval Ship Research and Development Lab.
   Annapolis, Maryland 21402
   Attn: Library (2)

3. Commanding Officer
   Naval Ship Research and Development Lab.
   Panama City, Florida 32402
   Attn: Library (2)

4. Commander
   Naval Ship Systems Command
   Department of the Navy
   Washington, D. C. 20360
   Attn: Code 0342 (1) DEF
   Code 037 (1) ADF
   Code 00V (1) F
   Code 2052 (3)
   Code PMS 81 (1) ABCDF
   Code 03412 (1)

5. Director
   Defense Documentation Center
   5010 Duke Street
   Alexandria, Virginia 22314 (20)

6. Chief of Naval Research
   Department of the Navy
   Washington, D. C. 20360
   Attn: Mr. Ralph D. Cooper
   Code 438 (1)

7. Director
   Office of Naval Research Branch Office
   495 Summer Street
   Boston, Massachusetts 02210 (1)

8. Director
Office of Naval Research Branch Office
219 S. Dearborn Street
Chicago, Illinois 60604 (1)

9. Office of Naval Research
Resident Representative
207 West 24th Street
New York, New York 10011 (1)

10. Chief Scientist
Office of Naval Research Branch Office
1030 East Green Street
Pasadena, California 91101 (1)

11. Director
Office of Naval Research Branch Office
1076 Mission Street (1)
San Francisco, California 94103

12. Commanding Officer
Office of Naval Research Branch Office
Box 39, Fleet Post Office
New York 09510 (3)

13. Commander
Naval Facilities Engineering Command
Department of the Navy
Washington, D. C. 20390
Attn: Code 0321 (1) BCDE

14. Commander
Naval Ship Engineering Center
Department of the Navy
Center Building, Prince Georges Center
Hyattsville, Maryland 20782
Attn: Code 6110 (1)
Code 6114D (1)
Code 6120 (1)
Code 6132 (1) AC
Code 6132 (1) CDE
Code 6136 (1)
Code 6140 (1) ADEF

15. Strategic Systems Projects Office
Department of the Navy
Washington, D. C. 20360 (1)
Attn: Dr. John Craven (NSP-001)

16. Commanding Officer
Naval Air Development Center
Johnsville, Warminster, Pa. 18974
Attn: Technical Library (1)

17. Commanding Officer and Director
Naval Applied Science Laboratory
Flushing & Washington Avenues
Brooklyn, New York 11251 (1)

18. Officer-in-Charge
Naval Undersea Warfare Center
3202 E. Foothill Boulevard
Pasadena, California 91107
Attn: Dr. J. Hoyt (1) AD
Dr. A. Fabula (1) AD

19. Commander
Naval Electronics Laboratory Center
San Diego, California 92152
Attn: Library (1) DEF

20. Director (Code 2027)
Naval Research Laboratory
Washington, D. C. 20390 (1)

21. Commanding Officer
Navy Underwater Weapons Research and
Engineering Station
Newport, Rhode Island 02840 (1)

22. Commander
Naval Proving Ground
Dahlgren, Virginia 22448
Attn: Technical Library (1) BDE

23. Commanding Officer and Director
Naval Civil Engineering Laboratory
Port Hueneme, California 93401
Attn: Code L31 (1) DE

24. Commander
Naval Weapons Center (Code 753)
China Lake, California 9355 (1)

25. Commander
Boston Naval Shipyard
Boston, Massachusetts 02129
Attn: Technical Library (1)

26. Commander
Charleston Naval Shipyard
Naval Base
Charleston, South Carolina 29408
Attn: Technical Library (1)

27. Commander
Long Beach Naval Shipyard
Long Beach, California 90802
Attn: Technical Library (1) ABCF

28. Commander
Norfolk Naval Shipyard
Portsmouth, Virginia 23709
Attn: Technical Library (1)

29. Commander
Pearl Harbor Naval Shipyard
Box 400, Fleet Post Office
San Francisco, California 96610
Attn: Code 246-P (1)

30. Commander
Philadelphia Naval Shipyard
Philadelphia, Pennsylvania 19112
Attn: Code 240 (1) ABCF

31. Commander
Portsmouth Naval Shipyard
Portsmouth, N. H. 03801
Attn: Technical Library (1)

32. Commander
Puget Sound Naval Shipyard
Bremerton, Washington 98314
Attn: Engineering Library (1)

33. Commander
San Francisco Bay Naval Shipyard
Vallejo, California 94952
Attn: Technical Library (1)
Code 250 (1)
Code 130L1 (1) BDF

34. AFFDL (FDDS - Mr. J. Olsen)
Wright-Patterson AFB
Dayton, Ohio 45433 (1) BDE

35. NASA Scientific and Technical
Information Facility
P.O. Box 33
College Park, Maryland 20740 (1)

36. AFORSR (SREM)
1400 Wilson Blvd.
Arlington, Virginia 22209 (1) BD

37. Library of Congress
Science and Technology Division
Washington, D. C. 20540 (1)

38. U. S. Coast Guard
1300 E. Street, N.W.
Washington, D. C. 20591
Attn: Division of Merchant Marine
Safety (1)

39. Director
National Bureau of Standards
Washington, D. C. 20234
Attn: Dr. G. B. Schubauer, Chief,
Fluid Mechanics Branch (1) D

40. Director of Research
National Aeronautics and Space
Administration
600 Independence Avenue, S.W.
Washington, D. C. 20546 (1) D

41. Director
Waterways Experiment Station
Box 631
Vicksburg, Mississippi 39180
Attn: Research Center Library(1) BDE

42. Commander
Naval Ordnance Systems Command
Department of the Navy
Washington, D. C. 20360
Attn: Code ORD-035 (1) D

43. Commandant (E)
U. S. Coast Guard (Sta 5-2)
1300 E. Street, N. W.
Washington, D. C. 20591

44. University of Bridgeport
Bridgeport, Connecticut 06602
Attn: Prof. Earl Uram
Mech. Engrg. Dept. (1) ABDE

45. Brown University
Providence, Rhode Island 02912
Attn: Div. Of Applied Math. (1) D

46. Naval Architecture Department
College of Engineering
University of California
Berkeley, Califonia 94720
Attn: Librarian (1)
Prof. J. R. Paulling (1)
Prof. J. V. Wehausen (1)
Dr. H. A. Schade (1)

47. California Institute of Technology
Pasadena, California 91109
Attn: Dr. A. J. Acosta (1) ABDE
Dr. T. Y. Wu (1)
Dr. M. S. Plesset (1) BDE

48. University of Connecticut
Box U-37
Storrs, Connecticut 06268
Attn: Prof. V. Scottron (1) DE
Hydraulic Research Lab.

49. Cornell University
Graduate School of Aerospace Engrg.
Ithaca, New York 14850
Attn: Prof. W. R. Sears (1)

50. Harvard University
2 Divinity Avenue
Cambridge, Massachusetts 02138
Attn: Prof. G. Birkhoff
Dept. of Mathematics (1) DE

51. Pierce Hall
Harvard University
Cambridge, Massachusetts 02138
Attn: Prof. G. F. Carrier (1) D

52. University of Illinois
College of Engineering
Urbana, Illinois 61801
Attn: Dr. J. M. Robertson
Theoretical & Applied
Mechanics Dept. (1) DE

53. University of Iowa
Iowa City, Iowa 52240
Attn: Dr. Hunter Rouse (1)

54. The University of Iowa
Iowa Institute of Hydraulic Research
Iowa City, Iowa 52240
Attn: Dr. L. Landweber (1)
Dr. J. Kennedy (1)

55. The Johns Hopkins University
Mechanics Department
Baltimore, Maryland 21218
Attn: Prof. O. M. Phillips (1) DF

56. Kansas State University
Engineering Experiment Station
Seaton Hall
Manhattan, Kansas 66502
Attn: Prof. D. A. Nesmith (1) DE

57. University of Kansas
Lawrence, Kansas 60644 (1)D
Attn: Chm., Civil Engrg. Dept.

58. Lehigh University (1) DE
Bethlehem, Pennsylvania 18015
Attn: Fritz Laboratory Library

59. Long Island University
Graduate Dept. of Marine Science
40 Merrick Avenue
East Meadow, New York 11554
Attn: Prof. David Price (1)

60. Massachusetts Institute of Technology
Hydrodynamics Laboratory
Cambridge, Massachusetts 02139
Attn: Prof. A. T. Ippen (1) DEF

61. Massachusetts Institute of Technology
Department of Naval Architecture
and Marine Engineering
Cambridge, Massachusetts 02139
Attn: Dr. A. H. Keil (1)
Prof. P. Mandel (1) ADE
Prof. J. R. Kerwin (1)
Prof. P. Leehey (1) DEF
Prof. M. A. Abkowitz (1) ABCDE
Prof. F. M. Lewis (1) D
Prof. J. N. Newman (1) ACD

62. U. S. Merchant Marine Academy
Kings Point, L. I., N. Y. 11024
Attn: Capt. L. S. McCready, Head
Dept. of Engineering (1) AB

63. University of Michigan
Department of Naval Architecture
Ann Arbor, Michigan 48104
Attn: Dr. T. F. Ogilvie (1)
Prof. H. Benford (1)
Dr. F. C. Michelsen (1)

64. U. S. Naval Academy
Annapolis, Maryland 21402
Attn: Library (1)
Dr. Bruce Johnson (1) ADF

65. St. Anthony Falls Hydraulic Lab.
University of Minnesota
Mississippi River at 3rd Ave., S. E.
Minneapolis, Minnesota 55414
Attn: Director (1)
Dr. C. S. Song (1)
Mr. J. M. Killen (1) BDEF
Mr. F. Schiebe (1) DEF
Mr. J. M. Wetzel (1) DE

66. New York University
University Heights
Bronx, New York 10453 (1)
Attn: Prof. W. J. Pierson, Jr.

67. New York University
Courant Institute of Mathematical Sciences
251 Mercier Street
New York, New York 10012
Attn: Prof. A. S. Peters (1)

68. University of Notre Dame
Notre Dame, Indiana 46556
Attn: Dr. A. Strandhagen (1) BDE
Dr. J. Nicolaides (1) BD

69. The Pennsylvania State University
Ordance Research Laboratory
University Park, Pennsylvania 16801
Attn: Director (1) ABDE
Dr. G. Wislicenus (1) ABDEF

70. Colorado State University
Dept. of Civil Engineering
Fort Collins, Colorado 80521
Attn: Prof. M. Albertson (1) BDEF

71. Princeton University
Aerodynamics Laboratory
The James Forrestal Research Center
Princeton, New Jersey 08540
Attn: Prof. G. Mellor (1) DF

72. Scripps Institute of Oceanography
University of California
La Jolla, California 92038
Attn: J. Pollock (1) ABCF
M. Silverman (1)

73. Stanford University
Stanford, California 94305
Attn: Prof. H. Ashley (1) DE
Dept. of Aeronautics and
Astronautics
Prof. R. L. Street (1)
Prof. B. Perry (1)
Dept. of Civil Engrg.

74. University of Texas
Defense Research Laboratory
P. O. Box 8029
Austin, Texas 78712
Attn: Director (1) DF

75. University of Washington
Applied Physics Laboratory
1013 N. E. 40th Street
Seattle, Washington 98105
Attn: Director (1) ABDF

76. Webb Institute of Naval Architecture
Crescent Beach Road
Glen Cove, L.I., N.Y. 11542
Attn: Prof. E. V. Lewis (1)
Prof. L. W. Ward (1)

77. Worcester Polytechnic Institute
Alden Research Laboratories
Worcester, Massachusetts 01609
Attn: Director (1) ADE

78. Aerojet-General Corporation
1100 W. Hollyvale Street
Azusa, California 91702
Attn: Mr. J. Levy (1)
Bldg. 160, Dept. 4223

79. Bethlehem Steel Corporation
Central Technical Division
Sparrows Point Yard
Sparrows Point, Maryland 21219
Attn: Mr. A. Haff, Technical Mgr. (1)

80. Bethlehem Steel Corporation
25 Broadway
New York, New York 10004
Attn: H. deLuce (1) ABC

81. Bolt, Beranek & Newman, Inc.
1501 Wilson Blvd.
Arlington, Virginia 22209
Attn: Dr. F. Jackson (1) DF

82. Bolt, Beranek & Newman, Inc.
50 Moulton Street
Cambridge, Massachusetts 02138
Attn: Dr. N. Brown (1) A

83. Cornell Aeronautical Laboratory
Applied Mechanics Department
P.O. Box 235
Buffalo, New York 14221
Attn: Dr. I. Statler (1) BDE

84. Electric Boat Division
General Dynamics Corporation
Groton, Connecticut 06340
Attn: Mr. V. Boatwright, Jr. (1)

85. Esso International
15 West 51st Street ABCD
New York, New York 10019
Attn: Mr. R. J. Taylor, Manager (1)
R & D Tanker Department (1)

86. General Applied Sciences
Laboratories, Inc. DEF
Merrick & Stewart Avenues
Westbury, L. I., New York 11590
Attn: Dr. F. Lane (1)

87. Gibbs & Cox, Inc.
21 West Street
New York, New York 10006
Attn: Technical Library (1)

88. Grumman Aircraft Engineering Corp.
Bethpage, L. I., New York 11714
Attn: Mr. W. Carl (1)

89. Hudson Laboratories
145 Palisade Street
Dobbs Ferry, New York 10522
Attn: Library D (1)

90. Hydronautics, Inc.
Pendell School Road
Howard County
Laurel, Maryland 20810
Attn: Mr. P. Eisenberg (1)
Mr. M. Tulin (1)

91. Lockheed Missiles & Space Company
P. O. Box 504 AE
Sunnyvale, California 94088
Attn: Mr. R. L. Waid, Facility #1 (1)
Dept. 57-01, Bldg. 150

92. McDonnell Douglas Aircraft Company
Douglas Aircraft Division DE
3855 Lakewood Boulevard
Long Beach, California 90801 (1)

93. Measurement Analysis Corporation
10960 Santa Monica Boulevard DF
Los Angeles, California 90025 (1)

94. National Science Foundation
Engineering Division
1800 G Street, N.W. DE
Washington, D. C. 20550
Attn: Director (1)

95. Newport News Shipbuilding and
Drydock Company
4101 Washington Avenue
Newport News, Virginia 23607
Attn: Technical Library Dept. (1)

96. Oceanics, Incorporated
Technical Industrial Park
Plainview, L. I., New York 11803
Attn: Dr. Paul Kaplan (1)

97. Pennsalt Chemicals Corporation
900 First Avenue D
King of Prussia, Pennsylvania 19406
Attn: Mr. W. M. Lee, Director
Contracts Res. Dept. (1)

98. Robert Taggart, Inc.
3930 Walnut Street
Fairfax, Virginia 22030
Attn: Mr. R. Taggart (1)

99. Sperry-Piedmont Company
Charlottesville, Virginia 22901
Attn: Mr. T. Noble (1)

100. Society of Naval Architects and
Marine Engineers
74 Trinity Place
New York, New York 10006 (1)

101. Southwest Research Institute
8500 Culebra Road BCDEF
San Antonio, Texas 78206
Attn: Dr. H. Abramson (1)
Applied Mechanics Review (1)

102. Sun Shipbuilding & Dry Dock Co.
Chester, Pennsylvania 18013
Attn: Mr. F. Pavlik ABC (1)
Chief Naval Architect

103. Tracor Incorporated
6500 Tracor Lane
Austin, Texas 78721 (1) BDF

104. Tracor Incorporated
627 Loftstrand Lane
Rockville, Maryland 20850 (1) BDF

105. Woods Hole Oceanographic Institute
Woods Hole, Massachusetts 02543
Attn: Reference Room (1) ABCDF

106. TRG/A Division of Control Data Corp.
535 Broad Hollow Road (Rt. 110)
Melville, L.I., N.Y. 11746 (1)

107. Prof. Jerome Lurye
Department of Mathematics
St. John's University
Jamaica, New York 11432 (1) ABCDE

108. Mr. B. H. Ujihara
North American Aviation, Inc.
Space and Information Systems Div.
12214 Lakewood Boulevard
Downey, California 90241 (1) BD

109. Stanford Research Institute
Menlo Park, California 94025
Attn: Library (1)

110. Cambridge Acoustical Associates, Inc.
129 Mount Auburn Street
Cambridge, Massachusetts 02138
Attn: Dr. M. C. Junger (1) ABDF

111. Dr. Roland W. Jeppson
College of Engineering
Utah State University
Logan, Utah 84321 (1) BDE

112. Stevens Institute of Technology
Davidson Laboratory
711 Hudson Street
Hoboken, New Jersey 07030
Attn: Dr. J. Breslin (3)

113. Naval Postgraduate School
Monterey, California 93940
Attn: Code 02 (1)
Code 023 (2)
Code 59S1(T. Sarpkaya) (20)
Code 59 (2)
Code 0212 (2)

DOCUMENT CONTROL DATA - R & D

(Security classification of title, body of abstract and indexing annotation must be entered when the overall report is classified)

1. ORIGINATING ACTIVITY (Corporate author)
Naval Postgraduate School
Monterey, California 93940

2a. REPORT SECURITY CLASSIFICATION
Unclassified

2b. GROUP

3. REPORT TITLE
FLOW OF DILUTE POLYMER SOLUTIONS ABOUT CIRCULAR CYLINDERS

4. DESCRIPTIVE NOTES (Type of report and inclusive dates)

5. AUTHOR(S) (First name, middle initial, last name)
TURGUT SARPKAYA, Professor & Chairman, Department of Mechanical Engineering, Naval Postgraduate School, Monterey, California 93940, LT P. G. RAINEY, USN

6. REPORT DATE
26 February 1971

7a. TOTAL NO. OF PAGES
146

7b. NO. OF REFS
40

8a. CONTRACT OR GRANT NO.
WR-0-7008 (NAVAL SHIP RESEARCH AND DEVELOPMENT CENTER).

b. PROJECT NO.

c.

d.

9a. ORIGINATOR'S REPORT NUMBER(S)
NPS-59SL1021A

9b. OTHER REPORT NO(S) (Any other numbers that may be assigned this report)

10. DISTRIBUTION STATEMENT
This document has been approved for public release and sale; its distribution is unlimited.

11. SUPPLEMENTARY NOTES

12. SPONSORING MILITARY ACTIVITY

13. ABSTRACT

Flow of aqueous solutions of Polyox WSR-301, with concentrations of 1.0 to 200 wppm, past circular cylinders was investigated in the drag-transition region of Reynolds numbers. Drag force, pressure distribution, and separation angle were measured on cylinders with diameters from 1/4 to 1-1/2 inch. Lift and drag forces acting on a NACA-0024 hydrofoil-model were also measured.

The polymer additive was found to alter only those force coefficients which have a Reynolds-number transition region. Two distinct types of cylinder drag transition were observed: (1) At high concentrations, transition from sub-critical to a transcritical flow occurred at the same free-stream velocity independent of body diameter; and (2) at low concentrations and/or molecular weights, tripping from a sub-critical to a super-critical flow occurred at a well defined flow condition which was a function of free-stream velocity, body diameter, and turbulent pipe-flow friction reduction. In all cases, transition occurred earlier than that in the pure solvent. The polymer had a de-stabilizing effect on the boundary-layer flow.

14 KEY WORDS	LINK A		LINK B		LINK C	
	ROLE	WT	ROLE	WT	ROLE	WT
Polymer Flow						
Bluff Body						
Circular Cylinders in Polymer Flow						
Drag Reduction with Polyox						